DNAPL SOURCE CONTROL BY REDUCTIVE DECHLORINATION

WITH IRON-BASED DEGRADATIVE SOLIDIFICATION/STABILIZATION

A Dissertation

by

SI HYUN DO

Submitted to the Office of Graduate Studies of
Texas A&M University
in partial fulfillment of the requirements for the degree of

DOCTOR OF PHILOSOPHY

December 2007

Major Subject: Civil Engineering

DNAPL SOURCE CONTROL BY REDUCTIVE DECHLORINATION

WITH IRON-BASED DEGRADATIVE SOLIDIFICATION/STABILIZATION

A Dissertation

by

SI HYUN DO

Submitted to the Office of Graduate Studies of
Texas A&M University
in partial fulfillment of the requirements for the degree of

DOCTOR OF PHILOSOPHY

Approved by:

Chair of Committee,	Bill Batchelor
Committee Members,	Kung-Hui Chu
	Bruce Herbert
	Jennifer McGuire
Head of Department,	David V. Rosowsky

December 2007

Major Subject: Civil Engineering

ABSTRACT

DNAPL Source Control by Reductive Dechlorination with Iron-based Degradative Solidification/Stabilization. (December 2007)

Si Hyun Do, B.S., Soong Sil University; M.S., Han Yang University

Chair of Advisory Committee: Dr. Bill Batchelor

Iron-based degradative solidification/stabilization (Fe(II)-DS/S) is a treatment method that could be economically applied to smaller DNAPL-contaminated sites and to those sites with impermeable soils. Reductive dechlorination is achieved by compounds that are formed by reaction of ferrous iron with components of Portland cement or with defined chemicals ($FeCl_3$ + $Ca(OH)_2$). These dechlorinating agents can effectively degrade chlorinated hydrocarbons (PCE, TCE, and 1,1,1-TCA) that are dissolved in aqueous solution. This research investigated the application of Fe(II)-DS/S to remove chlorinated hydrocarbons that are present as DNAPLs in source zones and to compared the reactivity of ferrous iron in different mixtures, including the conventional mixture with cement (Fe(II)+C) and an iron-solid mixture (ISM) that was synthesized without the addition of cement.

The modified first-order model, which the rate was proportional to the concentration of target in the aqueous phase and it was also nearly constant when DNAPL was present, was developed to describe dechlorination kinetics. The modified second-order model assumed that the rate was proportional to the product of the

concentration of target in the aqueous phase and the concentration of reductive capacity of the solid reductant. The modified first-order model was used to describe degradation of target compounds with ISM, and the modified second-order model was used to describe removals for TCE and 1,1,1-TCA with Fe(II)+C. Results of experiments on PCE dechlorination with ISM indicated that the increase of Fe(II) in ISM increased rate constants and decreased the solubility of targets. The half-life was increased with increasing total PCE concentration. The product analysis implied that degradation of PCE with ISM was via a combination of the hydrogenolysis and β-elimination pathways. A comparison of the types of targets and reductants indicated that Fe(II)+C had better reactivity for chlorinated ethenes (PCE and TCE) than ISM. However, ISM could dechlorinate a chlorinated ethane (1,1,1-TCA) as rapidly as Fe(II)+10%C. The ratio of $[RC]^o/[Fe(II)]^o$ implied that Fe(II) in Fe(II)+C was more involved in reducing chlorinated ethenes than was Fe(II) in ISM. Dechlorination of a DNAPL mixture followed the same order of reactivity as with individual DNAPLs with both reductants.

TABLE OF CONTENTS

CHAPTER Page

CHAPTER Page

LIST OF FIGURES

Page

Page

LIST OF TABLES

Page

CHAPTER I

INTRODUCTION

Perchloroethylene (PCE), trichloroethylene (TCE) and 1,1,1-trichloroethane (1,1,1-TCA) have been used as cleaning and degreasing solvents in the U.S.A. for several decades. PCE has been generally used for dry-cleaning and TCE has been used for degreasing. Use of 1,1,1-TCA as a replacement for PCE, TCE and CT has gradually increased, because it has excellent solvency and is less toxic than the replaced chemicals (*1,2*).

Even though the characteristics of these solvents satisfy industrial needs, TCE has been noticed as an important contaminant from the middle of 1960's. It and other chlorinated solvents (PCE and 1,1,1-TCA) are of concern because of their impacts to the environment and human health (*1,2*). Toxicology of PCE and 1,1,1-TCA show that the neurological damage is the main effect of exposure to PCE and 1,1,1-TCA in the working environment where they are generally transferred to the human body by inhalation. TCE is a carcinogen and it is also known for its effects on the nervous system, heart, liver, and kidneys. A toxicological profile of interactions of PCE, TCE, and 1,1,1-TCA published by the Agency for Toxic Substance and Disease Registry (ATSDR) proposes that ternary mixtures generally demonstrate toxicity greater than single or binary combinations. In addition, the major media for contamination of these

---

This dissertation follows the style of *Environmental Science and Technology*.

compounds are water, soil and air, sequentially (*3-5*).

PCE, TCE, and 1,1,1-TCA have been of great interest to environmental engineers because they have been reported to exist in the subsurface as dense non-aqueous phase liquid's (DNAPL). Presence of a contaminant at a site as a DNAPL causes an extended-time for remediation, because the DNAPL can continuously dissolve and disperse throughout the groundwater. Therefore, elimination of DNAPL as a source of contamination is a factor that must be resolved to insure effective cleanup of contaminated sites. Moreover, residual compounds that are adsorbed on or trapped in soils with low permeability have the potential to cause future contamination (*6-9*).

A conventional technology for remediation of contamination by chlorinated hydrocarbons is 'pump-and-treat', in which the groundwater is extracted and treated above ground to remove contamination. However, it does not successfully remove all of the contaminants in a source zone that are entrapped in pores of soil as NAPLs and can dissolve slowly into the groundwater. As a result of incomplete removal of NAPLs, the concentration of contaminants rebounds once the extraction wells are shut down. This phenomenon is called 'tail-and-rebound' and it has been shown to make cleanup of DNAPL-contaminated sites by 'pump-and-treat' technology to be ineffective and expensive (*10*).

A number of alternative technologies have been developed to cleanup DNAPL-contaminated sites and some have been categorized as 'promising technologies'. These include permeable reactive barriers (PRB), thermal removal, soil washing, and solidification/stabilization (S/S). Permeable reactive barriers use zero valent iron (ZVI)

in a passive, in-situ treatment technology. They convert chlorinated compounds to non-chlorinated products under abiotic conditions and they are cost-effective alternatives to conventional "pump-and-treat" technology (*11,12*). However, PRBs have negative aspects, such as being susceptible to plugging and blocking of reactive sites on iron surfaces by formation of mineral precipitates. This can be a major problem, because good long-term performance is needed, unless the source of contaminants is eliminated. Furthermore, dechlorination in PRBs can be inhibited by competition with several ions such as nitrate, chromate, and silicate that commonly existed in subsurface (*11-13*). Thermal and soil washing technologies can remove DNAPL, but they need to be applied with other technologies in order to achieve mandated cleanup standards (*14*).

Degradative solidification/stabilization (DS/S) is a modification of conventional S/S. Conventional S/S encapsulates contaminants and reduces their mobility, toxicity, and solubility without destroying them. However, DS/S adds contaminant destruction to the treatment mechanisms of conventional S/S and offers the potential to treat materials containing both organic and inorganic contaminants, including soils contaminated with DNAPLs (*14-16*). The primary DS/S technology is based on the addition of ferrous iron (Fe(II)) and is called iron-based degradative solidification and stabilization (Fe-DS/S).

The degradation reaction in Fe(II)-DS/S is reductive dechlorination and it can occur through the hydrogenolysis or beta-elimination pathways, or a combination of the two (*17-20*). Degradation of chlorinated ethenes (e.g. PCE and TCE) has been observed to occur mainly by beta-elimination, which completely converts PCE or TCE to non-chlorinated compounds. Degradation of chlorinated methanes (e.g. carbon tetrachloride

(CT) and chloroform (CF)) has been observed to proceed primarily through the hydrogenolysis pathway (*18-20*). However, it is suspected that the degradation of chlorinated methanes follows a complex pathway that includes hydrogenolysis, reductive hydrolysis, and radical coupling (*20*). The degradation of chlorinated ethanes (e.g. 1,1,1-TCA) has been reported to proceed through the hydrogenolysis pathway in Fe(II)-DS/S (*21*). Overall, it appears that chlorinated alkenes primarily degrade through beta-elimination and chlorinated alkanes primarily degrade through hydrogenolysis. However, other more complex pathways are also possible in Fe(II)-DS/S.

Kinetic models to describe reductive dechlorination of chlorinated hydrocarbons have been developed and successfully used to interpreted data from systems with reductants using Fe(II). First-order models are most commonly used and they often include a partitioning factor that describes equilibrium among the gas, solid, and aqueous phases. These models have described results from Fe(II)-DS/S systems reasonably well (*17,18*). On the other hand, a modified Langmuir-Hinshelwood model (L-H model) has been applied to describe the kinetics of reductive dechlorination by iron-bearing minerals (pyrite, magnetite, green rust, and iron-bearing phyllosilicates). This model assumes that the minerals have a finite reductive capacity that is depleted as the chlorinated organics are reduced (*22-24*). This model also assumes that the reactive sites do not react with any degradative intermediates or final products. Because of the presence of DNAPL means that there will be a high concentration of chlorinated hydrocarbons that could exceed the reductive capacity available, a modified L-H model may be needed to describe the kinetics of DNAPL dechlorination.

Investigations to identify the chemical form of the reductants responsible for reductive dechlorination of chlorinated hydrocarbons have been conducted. Recent research shows that reductants formed from ferrous iron at high pH, but without Portland cement, are able to degrade chlorinated compounds (*22-27*). The reductants formed in this system may be a type of green rust or a related compound with similar structure. They appear to have the ability to degrade chlorinated hydrocarbons at concentrations below their solubility.

In this research, the reductive dechlorination of three chlorinated hydrocarbons (PCE, TCE, 1,1,1-TCA) was examined at concentrations above their solubilities using two reductants formed from Fe(II). One reductant was an iron solid mixture (ISM) prepared with ferrous iron and lime. The other was a mixture of ferrous iron with Portland cement (Fe+C). The effectiveness of these reductants was verified in experiments with suspensions in a batch slurry reactor without soils. Moreover, because the experimental system was developed to deal with high concentrations of chlorinated hydrocarbons, it evaluated the suitability of DS/S as a technology for source removal of individual DNAPL and mixtures of DNAPLs.

The goal of this research was to evaluate the applicability of Fe-based DS/S as a source removal technology at sites contaminated with DNAPLs. To achieve this goal, three objectives were pursued, primarily by conducting kinetic experiments in which the concentrations of the target compounds and their chlorinated and non-chlorinated products were determined as functions of time. Moreover, before conducting kinetic experiments, well-planed preliminary tests were conducted to obtain data to better

design the kinetic experiments. Three tasks were performed to achieve project objectives. First, the effective experimental and analytical procedures were designed and modified because of the existence of DNAPLs. The ability of mixtures of Fe(II) without Portland cement to dechlorinate PCE DNAPL was determined. Second, experiments were conducted to determine the kinetics of reduction of three chlorinated hydrocarbons (PCE, TCE, and 1,1,1-TCA) as DNAPLs by three types of reductants (ISM, ISM+C, and Fe+C). The effect of the dose of Portland cement was also evaluated. Finally, the availability of Fe-based DS/S to reduce DNAPL mixtures was evaluated.

CHAPTER II

BACKGROUND

2.1 Degradative Solidification/Stabilization of Chlorinated Hydrocarbons DNAPLs

2.1.1 Problems and Resolutions of DNAPL Contamination

Chlorinated hydrocarbons are one of the main sources of sub-surface organic contamination in the world. These compounds have received increased attention from environmental scientists and engineer, especially when they are present as dense non-aqueous phase liquids (DNAPL). It has been estimated that in the U.S. up to 60% of sites on the National Priorities List are contaminated with DNAPLs (*28*). The presence of DNAPL results in extended times for remediation, because the DNAPL continuously dissolves and contaminates large volumes of groundwater. Therefore, effective remediation of a contaminated aquifer usually requires removal of DNAPL in order to remove the source of groundwater contamination.

A number of technologies remove chlorinated hydrocarbons present as DNAPLs by promoting contaminant transport through addition of air (soil vapor extraction and air sparging), steam (steam flooding), solvents (alcohols and surfactants) or heating (electrical heating) (*14,29*). All of these technologies are limited by relatively impermeable and heterogeneous soils and some are expensive, particularly for small sites. This can be overcome by applying Fe(II)-based degradative

solidification/stabilization (Fe(II)-DS/S), which utilizes the mechanism of abiotic reductive dechlorination

Fe(II)-DS/S uses the combination of a conventional solidification/stabilization reagent (Portland cement) to reduce permeability and a reductant (ferrous iron or iron mixture) to promote degradation. Hydraulic conductivities for wastes treated by conventional S/S can be as low as 10^{-8} cm/s (*30,31*), which is typical of materials used as landfill liners. Therefore, the groundwater is protected from contamination, while the chlorinated solvents are being destroyed. This removes the need for rapid remediation and provides the time required for abiotic dechlorination to occur. Furthermore, Fe(II)-based DS/S is applicable to treatment of chlorinated organics in source zones, whether inorganic contaminants are present or not, and patents have been granted for this use (*15,16*).

2.1.2 The Ability of Fe(II)-DS/S to Degrade Chlorinated Hydrocarbons

A number of studies have shown that Fe(II)-DS/S is able to degrade chlorinated hydrocarbons such as tetrachloroethylene (PCE), trichloroethylene (TCE), 1,1-dichloroethylene (1,1,-DCE), vinyl chloride (VC), carbon tetrachloride (CT), chloroform, 1,1,1-trichloroethane (1,1,1-TCA), 1,1,2,2-tetrachloroethane, and 1,2-dichloroethane (*17-19,21*). These investigations have focused on characterizing the kinetics of degradation in slurries that contain target compounds in the aqueous phase and hydration products of Portland cement in the solid phase. Degradation of PCE and TCE has been shown generally to follow a beta elimination pathway that results in complete degradation to non-chlorinated products (*18,20*). Limited experiments with

soils have demonstrated the ability of Fe(II)-DS/S to degrade PCE at low concentrations (*17*).

Research has been conducted to identify the iron-containing compounds that are responsible for dechlorination by Fe(II)-DS/S; however, it is complicated by the chemical complexity of systems containing Portland cement (*25*). Most evidence points to the active agents being what are called AFm phases in cement literature. These compounds are part of a group called layered double hydroxides (LDH), which includes green rusts. Green rusts contain Fe(II) and have been found to be effective reductants for a number of compounds including chlorinated organics (*23,32,33*). Moreover, this suggests the possibility that the dechlorination agent that is formed by reaction of ferrous iron at high pH without the presence of Portland cement could also be an LDH and possibly green rust.

2.2 Cement Hydration Products and Layered Double Hydroxides (LDHs)

2.2.1 Cement Hydration Products

Portland cement mainly consists of four components, which are tricalcium silicate ($(CaO)_3SiO_2$, alite), dicalcium silicate ($(CaO)_2SiO_2$, belite), tricalcium aluminate ($(CaO)_3Al_2O_3$, aluminate), and tetracalcium aluminoferrite ($(CaO)_4\ Al_2O_3\ Fe_2O_3$, ferrite) (*25,34-36*).

When these four components are mixed with water, a diverse group of hydration products are formed. The well-known cement hydration products that form by reaction of calcium silicate phases (both tricalcium silicate and dicalcium silicate) are amorphous

or semi-crystalline calcium silicate hydrate (usually expressed by C-S-H) and Portlandite ($Ca(OH)_2$). C-S-H is the predominant hydration product and has a high specific surface area. Portlandite affords a high pH for pore water in hydrated solids. The cement hydration products of tricalcium aluminate and tetracalcium aluminoferrite are mostly aluminite-ferrite-tri (Aft phase) and aluminate-ferrite-mono (AFm phase). Moreover, the reaction of gypsum ($CaSO_4 \cdot 2H_2O$) with tricalcium aluminate produces ettringite ($((CaO)_3Al_2O_3\ (CaSO_4)_3 \cdot 32H_2O$, Aft phase), and the reaction of ettringite and tricalcium aluminate forms monosulfate ($((CaO)_3Al_2O_3\ CaSO_4 \cdot 12H_2O$, AFm phase). Hydrogarnet ($((CaO)_3Al_2O_3\ \cdot 6H_2O$) also forms from a conversion of hexagonal plate crystals such as tetracalcium aluminate or dicalcium aluminate (*25,34,36*).

Mechanisms of the cement hydration have been developed that focus on development of strength. They are generally described as either an immediate dissolution-precipitation mechanism or a grain coating mechanism followed by a solid state reaction mechanism. In the dissolution-precipitation mechanism, some elements of anhydrous cement pastes dissolve into solution at the early stages of cement hydration, and then, these ions precipitate to form mainly amorphous C-S-H and calcium hydroxide, which occupies 80 % of total produced solid volume. On the other hand, it is also reported by several researchers that the growth of hydration products starts almost immediately after contact with water to produce cement grain coatings of gelatinous hydrates. It is uncertain whether the steps of dissolution-precipitation and cement grain coating are one continuous process or two distinguishable processes. In the later stages of hydration, reactions occur on the surface of solids. The morphology of hydration

products, especially C-S-H depend on water/cement ratio and age of cement sample (*34*). While C-S-H has been considered mainly to provide the strength of cement, other minor hydration products have been studied.

Hydration products of tricalcium aluminate and tetracalcium aluminoferrite are mainly AFt and AFm phases, which include various amorphous aluminum and iron hydroxides. They are known to be difficult subjects for analysis because 1) their composition depends on the surrounding chemical environment, which lead variations in composition and 2) their low crystallinity, which lead ambiguous identification (*37-39*). The general formula for theses phases is $[Ca(Al, Fe)(OH)_6]\cdot X_a \cdot xH_2O$, where X denotes an anion with single or double charge and with a=1 for AFm and a=3 for AFt (*36*). AFt phases are generally found as needles and AFm phases are found in layers (*40*).

The layered structure of AFm phases commonly incorporates water as well as various anions such as hydroxyl, chloride, carbonate, sulfate, and silicate. Figure 2.1 shows the relationship among AFm phase materials with arrows showing the direction of increased component activity. This figure also shows compositions of AFm phases under iron-free conditions. Dashed lines indicate thermodynamically unstable phases at 25 ºC, and solid dots represent individual phases (*39*).

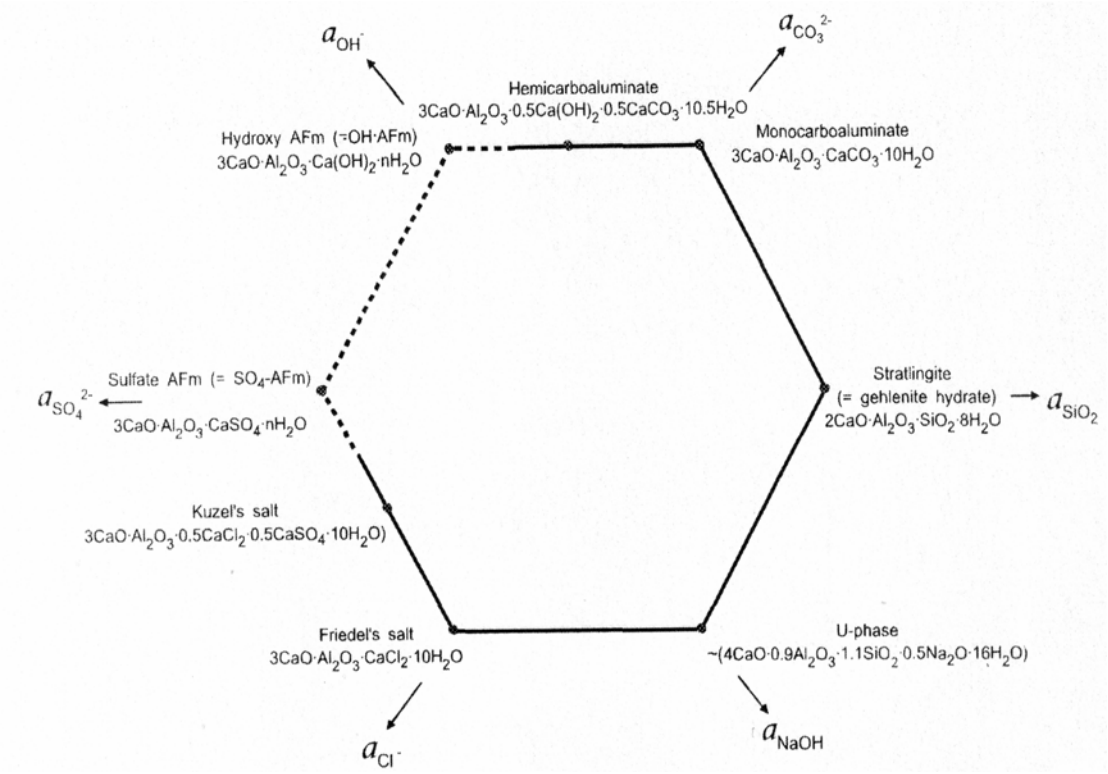

Figure 2.1 The AFm family in cement chemistry (*39*).

2.2.2 Layered Double Hydroxides (LDHs)

Layered double hydroxides (LDHs) can either be found naturally, e.g. hydrotalcite, or they can be synthesized in laboratory. Synthesis occurs through several processes, which include simple hydration, coprecipitation, anion exchanges, aerial oxidation, and steel corrosion (*41-43*). The general formula for a LDH has been reported as $[M^{II}_{1-x}M^{III}_x(OH)_2]^{x+}[A^{n-}_{x/n} \bullet mH_2O]^{x-}$, where M^{II} and M^{III} can be any divalent and trivalent metal ions, A^{n-} can be compensating anions such as OH^-, Cl^-, SO_4^{2-}, and CO_3^{2-}, m is the amount of water in interlamellar region, and x is the ratio $M^{3+}/(M^{2+} + M^{3+})$ (*44,45*). The identification of LDHs is complicated because they can have various

compositions that are affected by the surrounding conditions. The applications of LDHs are wide, and examples include use as catalysts, ceramic precursors, anion exchangers, even gene carriers (*44,45*).

In cement chemistry, several hydration products of C_3A and C_4AF, especially the AFm phases, are parts of the LDH family (*44*). In addition, green rusts are LDHs. They contain ferrous and ferric iron and have hydrotalcite-like or pyroaurite-like structures. They have been known by environmental engineers as the pollutant-reducing agents (*42,43,46,47*).

2.2.2.1 Friedel's Salts

The interaction between cement hydration products (i.e. C-S-H, complex calcium oxychloride, calcium chloroaluminates, chloroferrites, etc.) and the chloride ion is complex. Friedel's salts are examples of compounds in the AFm family that contain chloride ion. It is formed from the hydration of C_3A and has the general formula $(CaO)_3Al_2O_3 \cdot CaCl_2 \cdot H_{10}$ ($C_3A \cdot CaCl_2 \cdot H_{10}$). It is known to be stable in basic solutions (pH > 12), but it is unstable at lower pH (*37,48*).

Friedel's salt is proposed to be formed by two mechanisms; adsorption of chloride ion into the interlayer of an AFm phase and anion-exchange with OH^- ion in other parts of the AFm phase (*49*). Moreover, the composition of Friedel's salt is diverse, like that of other AFm phases, and it depends on the local chemical environment, particularly the concentrations of metal ions, hydroxide, chloride, and sulfate. The relationship between Al^{+3} and Fe^{+3} and the substitution of Cl^{-1} for OH^{-1} in AFm phases is not clearly understood (*37,39,40,48-53*).

Identification of metal ions in AFm phases is difficult, even though well developed analytical methods such as Mossbauer spectrometry have been used. Some researchers found the existence of $Fe(OH)_3$, and others found $Al(OH)_3$ when C_4AF is hydrated (*37,52*). In iron-rich environments, it has been reported that iron can fully substitute to form $[Ca_2Fe(OH)_6]_2$ $[Fe(OH)_4]_2 \cdot$ nH_2O. The hydration products were also found to partly contain aluminum-ferric-AFm phases such as $[Ca_2(Al_{0.9}Fe_{0.1})(OH)_6]_2(OH)_2 \cdot nH_2O$, $[Ca_2(Al_{0.3}Fe_{0.7})(OH)_6]_2[(Al_{0.3}Fe_{0.7})(OH)_4]_2 \cdot nH_2O$, and $Ca(Al_{0.1}Fe_{3.9})O_7 \cdot nH_2O$ (*40*). Other researchers concluded that aluminum was partly or fully replaced by iron oxide in hydration of aluminoferrites, and the transformation rates of metastable to stable phases was slowed with iron-containing hydrates (*37*). It has been suggested that the substitution of iron in Friedel's salts might possibly form $(CaO)_3Fe_2O_3 \cdot CaCl_2 \cdot H_{10}$ ($C_3F \cdot CaCl_2 \cdot H_{10}$) and aluminum-iron containing Friedel's salts $(CaO)_3/Fe,Al/ \cdot CaCl_2 \cdot H_{10}$ ($C_3/A,F/ \cdot CaCl_2 \cdot H_{10}$) have been independently detected (*37*). However, it was emphasized that AFm phases such as C_3AH_6 (mainly containing aluminum), C_3FH_6 (mainly containing iron), and their solid solution ($C_3/A,F/H_6$) could not be distinguished by the methods applied (thermal analysis and XRD) (*37*).

Because of experimental difficulty and the disordered nature of hydroxy AFm phases, the relationship between Friedel's salts and hydroxy AFm phases is complicated (*39,50*). Even though hydroxy AFm has been known to be thermodynamically metastable and contain various water contents, it is recognized that half of the sulfate content of AFm phases can be substituted by OH^- (*39*). Moreover, it has been reported that hydroxy- and sulfate-AFm phases could be replaced by chloride or chloride-sulfate

(*39*). However, the relationship between hydroxy AFm phases and Friedel's salts is still ambiguous. It has been reported that Cl^- could incorporate in hydroxy AFm phases when the aqueous chloride concentration is about 2 mM, and the formation of Friedel's salts was completed at chloride contents of about 14 mM (*50*).

2.2.2.2 Green Rust

Green rusts (GRs) are metastable mixed Fe(II)-Fe(III) hydroxides that can be prepared either by oxidation of aqueous suspensions of $Fe(OH)_2(s)$ or by direct precipitation from solutions containing NaOH, ferrous iron, and ferric iron (*54,55*). The general formula of GR is $[Fe^{II}_{1-x}Fe^{III}_{x}(OH)_2]^{x+}[A^{n-}_{x/n} \bullet mH_2O]^{x-}$, where x is the ratio Fe(III)/[Fe(II)+Fe(III)], A^{n-} is anions in interlayer, and m is amount of water molecule (*56*). According to XRD patterns, GRs are categorized by the ways that anions are incorporated between iron hydroxide sheets. GR1 incorporates planar anions like Cl^- and CO_3^{2-}, while GR2 incorporates 3-dimensional anions like SO_4^{2-} (*56*).

Some researchers have concluded that the preparation methods do not affect the ratio Fe(II)/Fe(III), suggested parameter in GR(CO_3^{2-}) and GR(SO_4^{2-}), which most frequently has a value of 2 (*55*). On the other hand, it has been found that the ratio Fe(II)/Fe(III) varies in GR(Cl^-) under certain conditions (*54*). When the concentrations of Fe(III) and Cl^- were increased, the ratio Fe(II)/Fe(III) in GR(Cl^-) decreased from 2.57 to 1.78 (*56*). However, the ratio Fe(II)/Fe(III) in GR(Cl^-) has a generally accepted value of 3 (*54*). The structure of GR(Cl^-) is shown in Figure 2.2.

The existence of GR(OH^-) has been proposed and it is assumed to have a structure that is similar to that of GR(Cl^-) with a suggested formula of

$[Fe^{II}_{1-x}Fe^{III}_{x}(OH)_2]^{x+}[\,OH^{-}_{x} \bullet mH_2O]^{x-}$, where m is $1 - x$, and values of x range from 0.33 to 0.66, and are equal to 0.5 in soil solution (*56,57*). Figure 2.3 shows the proposed structure of GR(OH^-) (*56*).

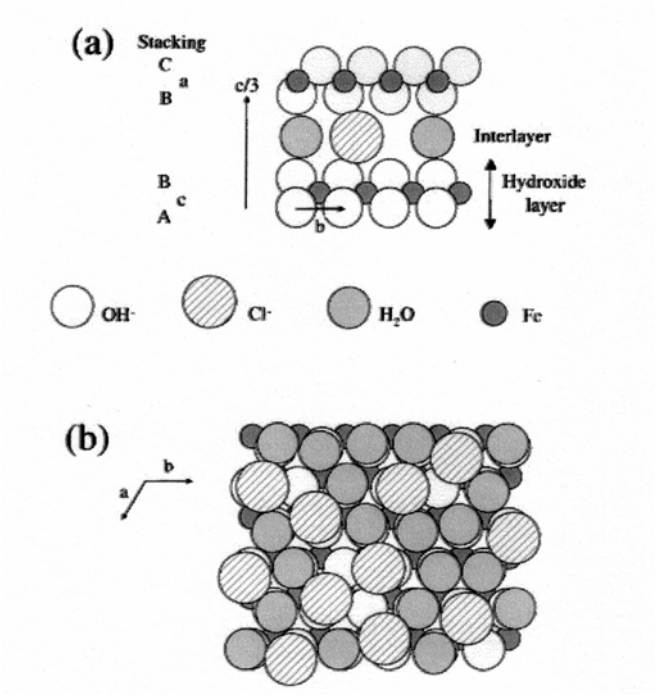

Figure 2.2 A structure of GR(Cl^-); (a) Stacking sequence. (b) Position of water molecules and chloride ions in an interlayer (*56*).

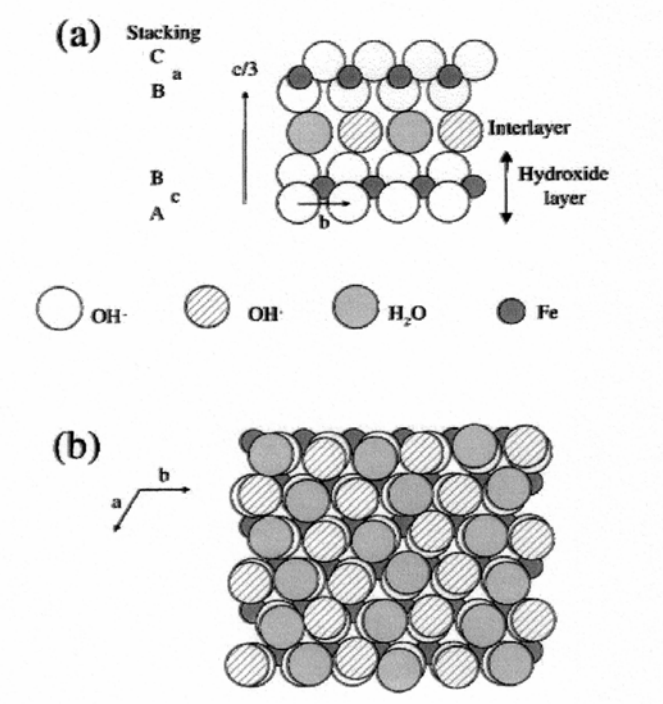

Figure 2.3 A structure of GR(OH^-); (a) Stacking sequence. (b) Position of water molecules and chloride ions in an interlayer (*56*).

Some researcher reported that either GR(Cl^-) or GR(OH^-) was formed directly when NaOH was added to a solution of ferrous and ferric iron (*58,59*). In addition, *β*-$Fe_2(OH)_3Cl$ could be the first compound that is synthesized in the presence of a large excess of ferrous chloride and its oxidation leads to formation of GR(Cl^-) followed by *γ*-FeOOH (*60*).

Various products have been reported to be formed when GRs are oxidized, including ferrihydrite, goethite (α-FeOOH), akaganeite (β-FeOOH), lepidocrocite (γ-FeOOH), δ-FeOOH, maghemite (γ-Fe_2O_3), or magnetite (Fe_3O_4) depending on pH, solution composition, oxidants, etc (*61*).

In addition to the ratio Fe(II)/Fe(III), other variables can be used to categorize GRs, including *x*, which is the ferric iron molar fraction ($x = n_{Fe(III)}/[n_{Fe(II)} + n_{Fe(III)}]$), and *R*, which is the molar ratio of hydroxide to total iron ($R = n_{OH}/[n_{Fe(II)} + n_{Fe(III)}]$) (*58*).

Green rust mediates abiotic redox reactions that remove inorganics (e.g. Se^{VI}, Cr^{VI}, NO_3^-, Ag^I, Au^{III}, Cu^{II}, and Hg^{II}), organics (e.g. HCB (hexachlorobiphenyl), PCE, TCE, 1,1,1-TCA, 1,1,2-TCA, and carbon tetrachloride), and radionuclides (e.g. U^{VI} and possibly Tc^{VII}) and these reactions have been used in subsurface treatment technologies (*26,32,33,62-68*). Moreover, some metals including Ag^I, Au^{III}, and Cu^{II} were reported to act as catalysts with GRs to increase rates of reduction of chlorinated organic contaminants (*61,64,65*).

2.3 Transformation of Chlorinated Hydrocarbons

The transformation reactions of chlorinated hydrocarbons are categorized according to whether or not an external electron transfer occurs. The transformation in which an electron transfer occurs is called reductive dechlorination and it includes several reaction pathways, such as hydrogenolysis, reductive α-elimination, reductive β-elimination, hydrogenation, and coupling. The mechanisms of reactions without electron transfer are nucleophilic substitution (hydrolysis) and hydrodehalogenation (elimination) (*69-71*).

2.3.1 Transformation by Non-Electron Transfer

Nucleophilic substitution (hydrolysis) and hydrodehalogenation (hydrodechlorination) are non-electron transfer reactions that are especially important to

biologically mediated processes and heterogeneously catalyzed reactions (*72*). Hydrolysis may occur via either homogeneous or heterogeneous reactions in both surface and subsurface aqueous environments (*73*).

Hydrolysis is the process in which a water molecule (or hydroxide ion) substitutes in an organic compound for a leaving group such as chlorine. It is an important example of a nucleophilic substitution reaction (*69*) and it is usually faster at high pH. Increased levels of chlorination in an organic compound lead to longer half-lives for substitution, because steric hindrances by chlorine atoms increase as the degree of chlorination increases (*70,71*).

Hydrodechlorination, which is also known as elimination, is a process that consists of removing chlorine from one carbon atom and removing a hydrogen atom from either the same or an adjacent carbon (*70*). Generally, polychlorinated alkanes follow a hydrodechlorination pathway both at neutral and extremely basic conditions (*70*). The rate of hydrodechlorination is faster when more chlorine substituents are attached to a carbon atom (*70*).

PCE can not undergo hydrodechlorination because it does not have hydrogen, and the possible explanation for other chlorinated ethenes, which it needs electron to reduce and hydrodechlorination is not electron transfer mechanism, could be the structural and thermodynamic effects, which mostly explained by π orbital effects (the π bond between carbons give relative high energy to the carbon-chlorine bond). The high heat of formation (> 250 kj/mol) was observed for chlorinated ethenes, while the low or

negative heat of formation was reported for chlorinated ethanes, which it rarely and possibly undergoes via hydrodechlorination (*74*).

It was reported that the half-life of alkaline hydrolysis for PCE at 25 ^{o}C was 9.63 x 10^{8} years. There was no hydrolysis observed at neutral condition for PCE (*72,75*). If the hydrolysis rate of PCE is proportional to hydroxide ion concentration, a half-life of 9.63 x 10^{3} years can be calculated for pH 12 at 25 ^{o}C (*75*). A recent research showed that the hydrolysis rate constants for TCE at neutral and alkaline conditions were 4.74 x 10^{-9} and 6.48 x 10^{-9} $days^{-1}$, respectively. A half-life, which was calculated from an addition of these two rate constants, was 1.7 x 10^{5} years (*76*). If alkaline hydrolysis rate of TCE is proportional to the hydroxide ion concentration, a half-life for TCE at pH 12 would be 1.7 years.

Chloroacetylene has been detected as a product of degradation of 1,1-dichloroethene at pH 13 (*72*), and chlorinated ethenes at extreme basic conditions could be reduced through hydrolysis via homogeneous or heterogeneous reactions (*72,73*).
The half-life of homogeneous hydrolysis for 1,1,1-TCA was reported as 1.1 year under the pH of 2 to 13. This implies that there were not significant levels of hydrolysis associated with hydroxide or hydrogen ions (*72,75,77*). It has been reported that trace amounts of 1,1-dichloroethene, which is the product of hydrodechlorination, is detected at pH 8.5 when a granular iron in presence of silica is reacted with 1,1,1-TCA (*78*). Moreover, it is reported that up to 60 % of 1,1,1-TCA can be transformed to 1,1-DCE using microbially reduced ferruginous smectite (*79*). Principle mechanisms of hydrolysis and hydrodechlorination for polyhalogenated alkanes are depicted in Figure 2.4. Figure

2.4 shows that S_N1 and E_1 are unimolecular, which explains the fact that they are usually pH-independent reactions, and other three (S_N2, E_2, and E_{1CB}) are bimolecular. The hydrodechlorination of 1,1,1-TCA generally accepted to be a unimolecular mechanism (*79,80*).

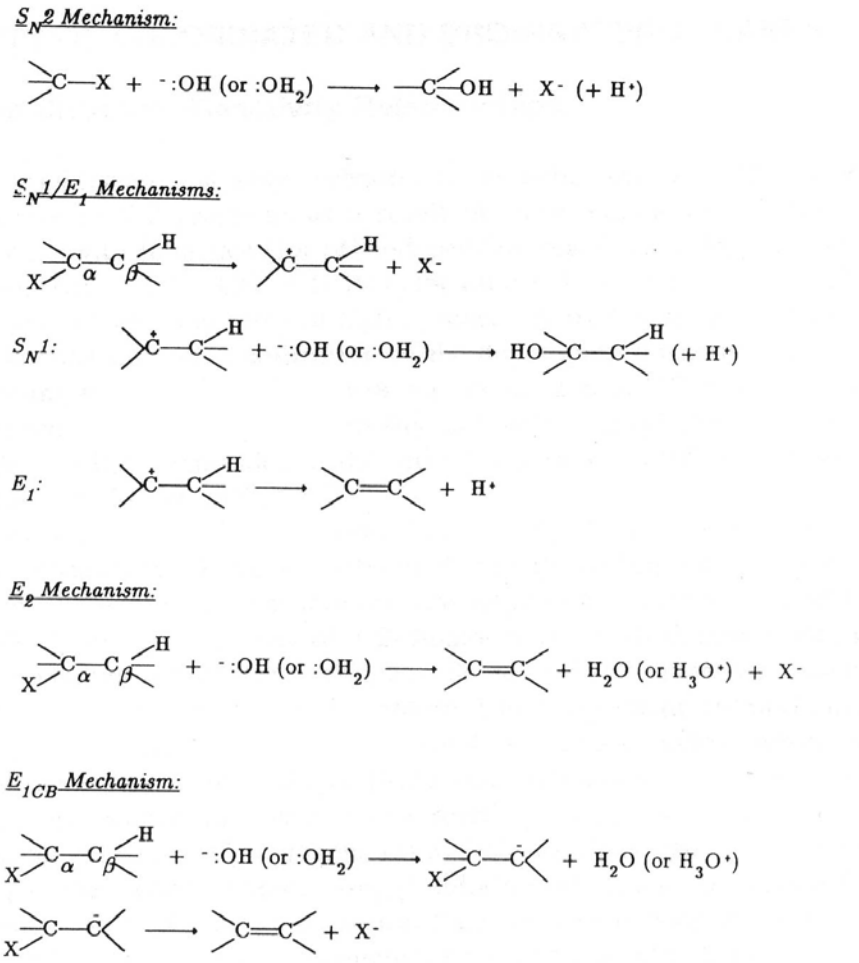

Figure 2.4 Principle mechanisms for polyhalogenated alkanes in aqueous solution (*80*).

2.3.2 Transformation by Electron Transfer

Reductive dechlorination is the transformation of chlorinated hydrocarbons that involves electron transfer and it is the major degradation process in reducing environments. The reported pathways of reductive dechlorination include hydrogenolysis, α-elimination, β-elimination, hydrogenation, and coupling. (*9,18,22,23,81-86*). Hydrogenolysis is a reduction process that breaks carbon-chlorine bonds and replaces chlorine with hydrogen. Elimination reactions remove two chlorine atoms that are bound to the same carbon atom (α-elimination) or that are bound on two adjacent carbon atoms (β-elimination) and the products contain multiple carbon bonds, e.g. a dichloro-ethane would be converted to ethene. Hydrogenation is a reaction that results in the addition of hydrogen (H_2) to compounds. Examples include converting acetylene to ethene.

Beside of all reductive dechlorination pathways, chlorinated ethanes (e.g. 1,1,1-TCA) have been reported to follow a coupling reaction, which is a process that connects two alkyl groups together.

2.3.2.1 Reductive Dechlorination of Chlorinated Ethenes

Reductive dechlorination of chlorinated ethenes such as PCE and TCE has been reported to follow the pathways shown in Figure 2.5, which are initiated by either hydrogenolysis or β-elimination reactions. The transformation products of reductive dechlorination of chlorinated ethenes vary according to the reductant being tested (*18,22,23,32,81-83*).

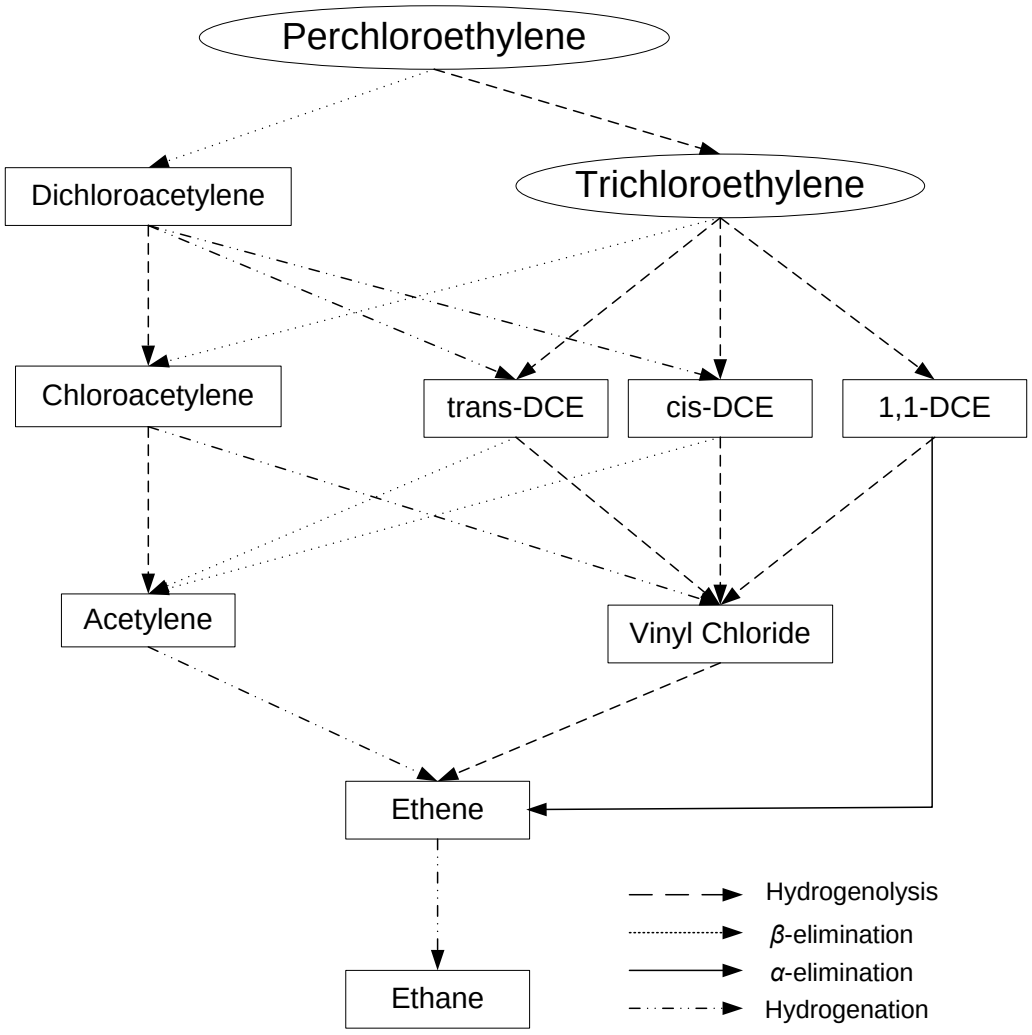

Figure 2.5 Reduction pathways for PCE and TCE (*82*).

Ethene and ethane have been reported to be the primary transformation products of chlorinated ethenes being reduced by Fe(0). Small amounts of chlorinated intermediates, such as TCE and DCEs, as well as longer-chain coupling products are also found (*82*). Dechlorination of chlorinated ethenes on Fe(0) followed mainly the *β*-elimination pathway. The production of dichloroacetylene was formed by *β*-elimination of PCE, and the production of chloroacetylene and acetylene was occurred via both *β*-elimination and hydrogenolysis (*82*). Several possible pathways for PCE and TCE degradation were suggested, including PCE → dichloroacetylene → chloroacetylene → acetylene → ethene → ethane and TCE → chloroacetylene → acetylene → ethene → ethane (*82*). Figure 2.6 shows the hypothesized reaction mechanism for PCE reduction by Fe(0). Reaction steps 3a) and 4a) in Figure 2.6 represent *β*-elimination that produces dichloroacetylene. Steps 3b) and 4b) show hydrogenolysis that produces TCE (*82*).

Acetylene has been reported as the primary transformation product of PCE and TCE degradation by several reductants that contain Fe(II), including pyrite, magnetite, green rust and Fe(II) in mixtures of Portland cement. Accumulation of acetylene without accumulation of DCEs or VC indicates that degradation followed the *β*-elimination pathway (*18,22,23*).

On the other hand, TCE has been reported as the primary product of PCE reduction by Zn(0) with lesser amounts of both *trans*-DCE and acetylene being found along with trace amounts of ethene and *cis*-DCE. This supports a pathway for PCE degradation by Zn(0) that begins with hydrogenolysis followed by *β*-elimination, i.e. PCE → TCE → *trans*-DCE → acetylene (*81*).

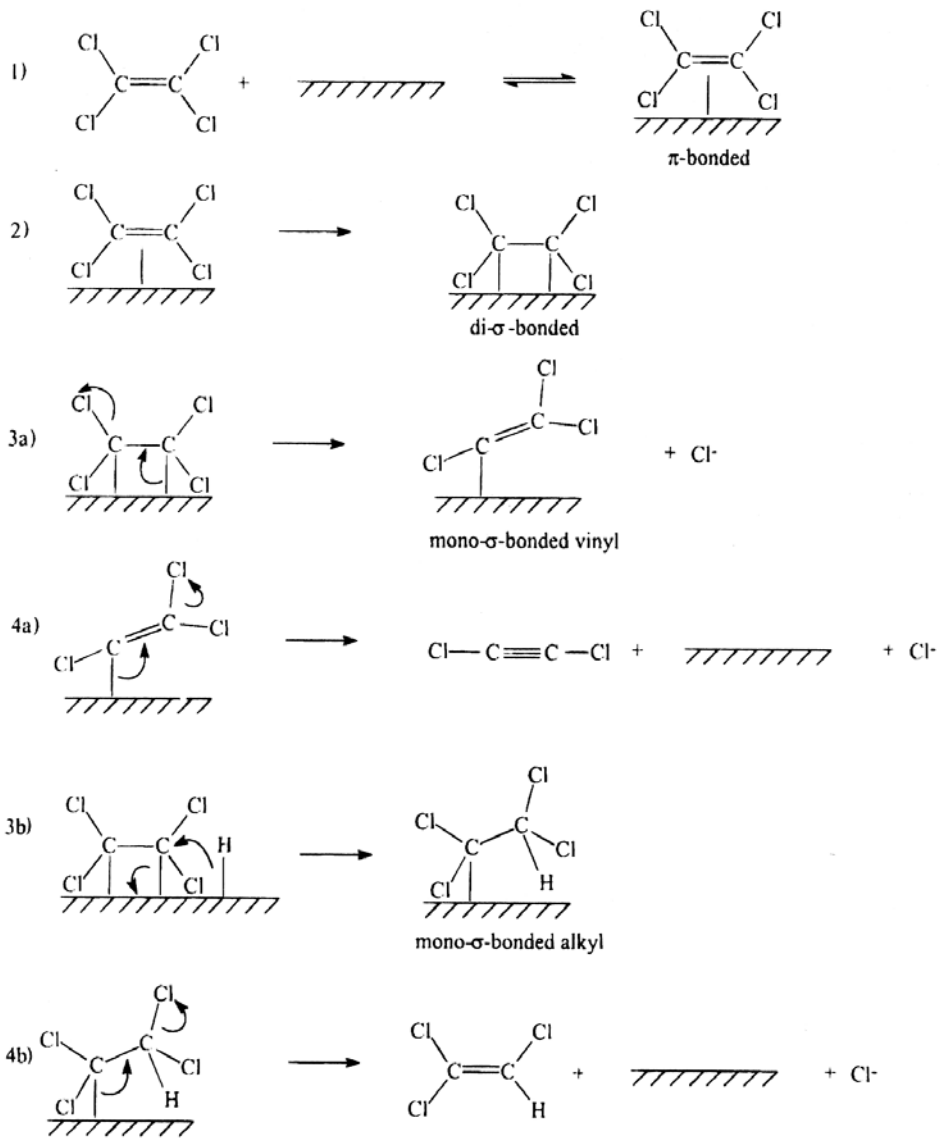

Figure 2.6 Hypothesized mechanism of PCE reduction on Fe(0) (*82*).

2.3.2.2 Reductive Dechlorination of Chlorinated Ethanes

Reductive dechlorination of chlorinated ethanes, such as 1,1,1-TCA, is complicated because of the existence of radicals and α-chloroorganometallic compounds (e.g. $H_3C-\ddot{C}-Cl$ and $H_3C-\ddot{C}-H$ carbenoid) (*9,86*). Figure 2.7 shows the hypothesized pathway for degradation of 1,1,1-TCA dechlorination on Fe(0).

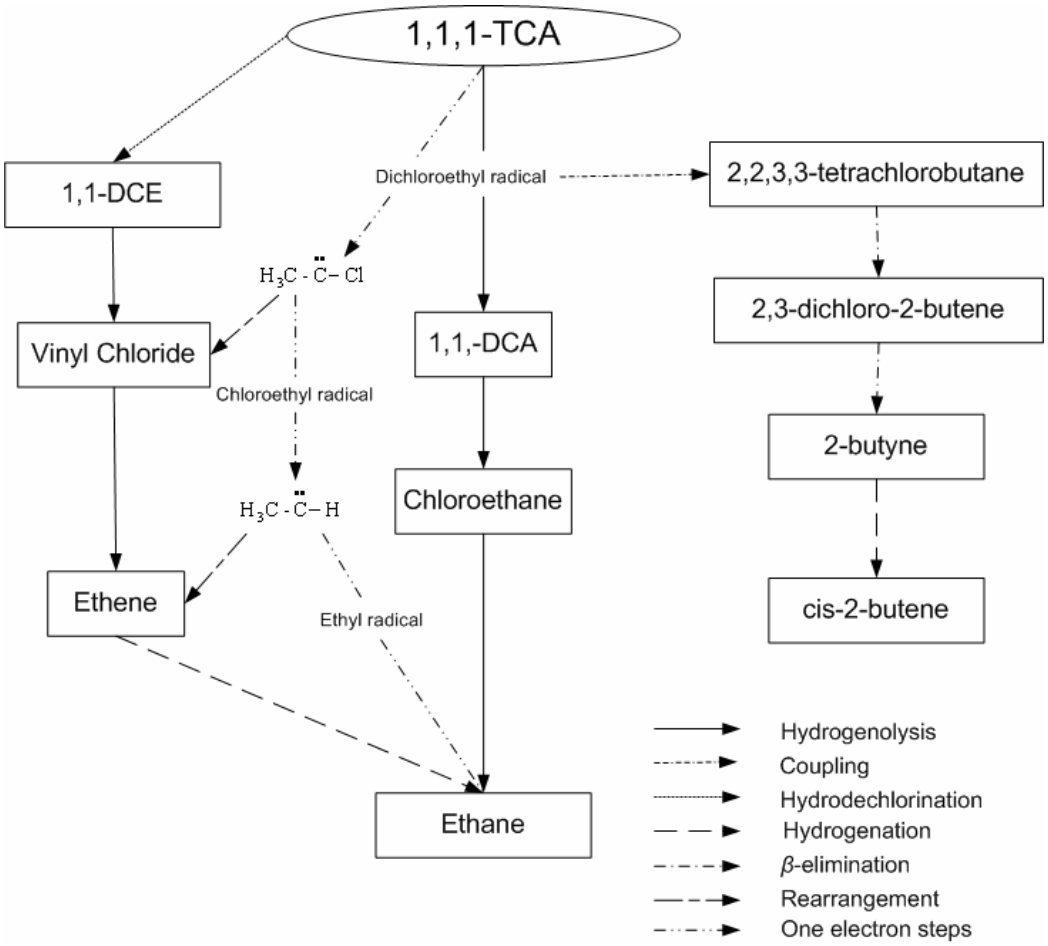

Figure 2.7 Hypothesized reduction pathways of 1,1,1-TCA (*9,86*).

The product distribution of 1,1,1-TCA differed both quantitatively and qualitatively depending on the type of reductant. Reductants that have been evaluated include Fe(0), other zero-valent metals, bimetallic materials (e.g. nickel-plated iron and copper-plated iron), green rust, and Fe(II) with Portland cement (*9,21,32,85,86*).

The main product of 1,1,1-TCA reaction with Fe(0) at pH 7.5 was 1,1-DCA along with some ethane, cis-2,3-dichloro-2-butene, ethene, and a trace of 2-butyne. The reduction of 1,1,1-TCA on copper-plated iron showed a different product distribution that included 1,1-DCA, ethane, ethene, cis-2,3-dichloro-2-butene, 2-butyne, and 1,1-DCE. Because chloroethane was not detected, it was suggested that $H_3C\text{-}\ddot{C}-Cl$ and $H_3C\text{-}\ddot{C}-H$ existed as carbine-metal complexes, rather than as free radicals (*9*). Moreover, the detection of 1,1-DCE implied that the hydrodechlorination pathway was active.

On the other hand, the reduction of 1,1,1-TCA on Fe(II) with Portland cement showed that nearly all of it was transformed to 1,1-DCA. However, under some conditions trace amounts of ethane were found (*21*).

The product distribution for degradation of 1,1,1-TCA by green rust with the addition of Ag (AgGR) included chloroethane (CA) as the main product and ethane, *n*-butane, 1,1-DCA, and ethene as minor products (*86*). Because CA was not reduced by AgGR, it was suggested that the pathway from CA to ethane was not active (*86*).

CHAPTER III

MATERIALS AND METHODS

3.1 Experimental Plan

Two experimental objectives were developed to demonstrate the ability of a modified Fe(II)-DS/S process to remove three representative chlorinated hydrocarbons (PCE, TCE, and 1,1,1-TCA) present as DNAPLs. First, experimental and analytical procedures were developed. This included an extraction procedure for DNAPLs and synthesis procedures for several iron-based reductants. One contained ferrous iron and Portland cement and was identified as "Fe(II)+C". The other contained ferrous iron, ferric iron and lime and was called an iron-solid mixture (ISM). The ISM was used by itself and with Portland cement. A gas-chromatographic analysis procedure was modified to detect target compounds and their probable chlorinated and non-chlorinated products. A batch slurry reactor generally was used for kinetic studies. To achieve the second objective, kinetic experiments were conducted to characterize the ability of ISM by itself and in combinations with Portland cement to dechlorinate PCE, TCE, and 1,1,1-TCA DNAPLs.

3.2 Materials

Organic chemicals used were: perchloroethylene (PCE, 99.9+%, HPLC grade, Aldrich), trichloroethylene (TCE, 99.5+%, Fisher Scientific), 1,1,1-trichloroethane

(1,1,1-TCA, 99.5+%, anhydrous, Aldrich), 1,1-dichloroethene (1,1-DCE, 97%, Aldrich), *cis*-dichloroethene (*cis*-DCE, 97%, Aldrich), *trans*-dichloroethene (*tans*-DCE, 98%, Aldrich), and 1,1-dichloroethane (1,1-DCA, 99.5%, Chem Service). Methanol (99.8%, HPLC grade, EM) was used as an extractant and as a solvent to prepare stock solutions of target compounds when necessary. Hexane (99.9%, HPLC grade, EM) was used as extractant and it was spiked with 1,2-dibromopropane (1,2-DBP, 97%, Aldrich) as an internal standard.

Standard curves for non-chlorinated products were prepared using a mixture of nitrogen gas with 1 % carbon monoxide, carbon dioxide, methane, ethylene, ethane, and acetylene (Micro MAT 14, Alltech Associates, Inc.)

Iron solid mixtures (ISMs) were synthesized by combining ferrous chloride (99+%, tetrahydrate, Sigma), ferric chloride (98+%, hexahydrate, Sigma), and calcium hydroxide (Fisher Scientific). Fe(II)+C mixtures were prepared by combining ferrous chloride with Portland cement (type 1, Capitol Cement), for which the chemical composition is shown in Table 3.1. Each chemical was dissolved into de-aerated deionized water, which purified by the Barnstead Nanopure system and purged with gas consisting of 95% nitrogen and 5% hydrogen for at least 24 hours in an anaerobic chamber. Sodium hydroxide (97+%, ACS grade, EM) was used to adjust pH.

Table 3.1 Chemical composition of Portland cement (*71*)

CaO	SiO_2	Al_2O_3	Fe_2O_3	MgO	SO_3	Loss on ignition	Insoluble Residue	Total (wt %)
64.85	20.26	5.46	2.52	1.26	3.20	1.65	0.1	99.3

3.3 Experimental Procedures

3.3.1 Synthesis of Iron-Based Reductants with and without Portland Cement

Various concentrations (i.e. 225, 424, 660, 789 mM) of ferrous chloride were mixed with a constant concentration (100 mM) of ferric chloride for the experiment using ISM to dechlorinate PCE DNAPL. For the experiments evaluating different types of reductants, the ISM was prepared with 225 mM ferrous chloride and 100 mM ferric chloride. Because 1,1,1-TCA was more easily degraded than chlorinated ethenes, lower concentrations of ferrous chloride (20, 80 mM) and ferric chloride (10 mM) were used to make the ISMs.

Calcium hydroxide was added at doses estimated to achieve pH 12 and 5 N sodium hydroxide was used if necessary to achieve the desired pH. This ISM suspension was allowed to react for 2 hours with vigorous mixing in an anaerobic chamber. ISM was identified by its concentration of ferrous iron, for example a mixture identified as "225 mM ISM ($[Fe(II)]_{ISM}$ = 225 mM)" would contain 225 mM ferrous iron.

The mass ratio of Portland cement to water was set to values of 0.05 and 0.1 for conventional mixtures of Fe(II)+C. Portland cement was stored at least 2 days in an anaerobic chamber in order to eliminate oxygen. Ferrous chloride was used as a source of ferrous iron and it was vigorously mixed with Portland cement for 2 hours in an anaerobic chamber. The final pH of 12 was maintained using 5 N sodium hydroxide. Each mixture was identified in terms of its ferrous iron concentration and its cement concentration. For example, "225 mM Fe(II)+5%C ($[Fe(II)]_{Fe(II)+5\%C}$ = 225 mM)" indicated a mixture containing 225 mM ferrous iron with 5% Portland cement.

The third reductant was a mixture of ISM and Portland cement (ISM+C). It was synthesized by first preparing ISM, adjusting the pH to 12 with 5 N sodium hydroxide, and then mixing it with Portland cement. After ISM was mixed with Portland cement, the adjustment to achieve pH 12 was repeated. These mixtures were identified in the same manner as the other reductants. "225 mM ISM +5%C ($[Fe(II)]_{ISM+5\%C}$ = 225 mM)" meant that the concentration of ferrous iron was 225 mM and the concentration of Portland cement was 5%.

These three types of reductants were introduced into the batch slurry reactors as a suspension. The reproducibility of transferring this suspension was determined by measuring the total iron concentration in solutions after transfer using the Ferrozine method. The average relative errors for analysis of ferrous and total iron were 0.01 and the average percent recoveries from seven samples of ferrous and total iron were 97.5 % and 98 %, respectively.

3.3.2 Preliminary Experiments

A 24-mL glass vial with triple-layer closures (rubber septa, lead foil, and Teflon film) was used as batch slurry reactors. The appropriateness of this reactor system has been demonstrated by other researchers (*18,22,25*). All samples were prepared in triplicate and controls were prepared in duplicate. Every experiment was conducted with freshly prepared suspensions of reductants and all glass vials stayed in an anaerobic chamber for at least 24 hours before use as reactors.

The effect of pH on reaction kinetics is usually important and often complicated. The optimum pH was reported as pH 12 for dechlorination of 0.24 mM PCE by Fe(II)+C

(*18*) and as pH 12.5 for dechlorination of 0.245 mM 1,1,1-TCA by Fe(II)+C (*21*). An optimum pH was not observed for degradation of 0.25 mM TCE by Fe(II)+C, but increasing pH over the range from 10 to 13.5 slightly increased rate constants (*20*). A preliminary kinetic test for degradation of 3.08 mM PCE by ISM showed that the rate constant at pH 12 (7.12E-2 day^{-1}) was greater than that at pH 10 (2.57E-2 day^{-1}). Based on literature reviews and preliminary tests, it was decided to conduct all experiments at pH 12.

Before each kinetic experiment was conducted, a preliminary three-point test was carefully planed and conducted. The preliminary test was planned using data collected from the literature for degradation constants obtained at lower concentrations of chlorinated hydrocarbons (0.245 mM). These rate constants were called reference constants ($k_{rc\_Fe(II)}$) and are shown in Table 3.2. Data were obtained for experiments conducted with low chlorinated hydrocarbon concentrations (0.245 mM) and with two types of reductants. One was a mixture of ferrous iron and Portland cement and the other was a mixture of ferrous iron, ferric iron, NaOH and chloride (Fe(II)-Fe(III)-Cl).

These data were used to estimate rate constants expected in preliminary kinetic tests at high concentration of targets. First, the average value of the rate constant over different ferrous iron concentrations was calculated using data collected at the low concentration of target organic. This value was multiplied by the ratio of the target concentrations used to obtain the data and the target concentration to be used in the preliminary experiment in order to obtain an estimate of the rate constant (estimated $k_{rc\_Fe(II)}$), which were shown in the last row of Table 3.2.

Table 3.2 Reference ferrous normalized rate constants at pH 12 (*21,25,71*)

		Fe(II)+10 % C			Fe(II)-Fe(III)-Cl [e]
		PCE	TCE	1,1,1-TCA	PCE
		$k_{rc\_Fe(II)}$ (d^{-1} mM^{-1})	$k_{rc\_Fe(II)}$ (d^{-1} mM^{-1})	$k_{rc\_Fe(II)}$ (hr^{-1} mM^{-1})	$k_{rc\_Fe(II)}$ (d^{-1} mM^{-1})
Fe(II) (mM)	4.9	-	-	3.14E-2	-
	9.8	2.86E-3	-	4.23E-2	4.84E-3
	19.6	4.03E-3	-	4.41E-2	2.91E-3
	39.2	2.55E-3	1.79E-4	4.92E-2	2.09E-3
	98	1.63E-3	4.69E-4	-	8.49E-3
	196	6.63E-4	4.49E-4	-	6.60E-4
Average.		2.35E-3	3.66E-4	4.18E-2	2.27E-3
Low/High Conc.		≈0.10	≈0.02	≈0.02	≈0.10
Estimated $k_{rc\_Fe(II)}$		2.35E-4[a]	7.31E-6[b]	8.35E-4[c]	2.27E-4[d]

[a] and [d] : high $[PCE]^{o}_{total}$ = 3.08 mM, low [PCE] = 0.245 mM.

[b] : high $[TCE]^{o}_{total}$ = 12.0 mM, low [TCE] = 0.245.

[c] : high $[1,1,1\text{-TCA}]^{o}_{total}$ = 11.7 mM; low [1,1,1-TCA]= 0.245 mM.

[e] : [Fe(III)] = 0.4 mM, simple mixing was used for solid synthesis, results from unpublished previous research.

The half-life for the target compound expected in the preliminary kinetic experiment was estimated with the assumptions that the degradation reaction would follow second-order kinetics and that the concentration of the target compound in the aqueous phase would be constant at its solubility. The values for the solubilities of PCE, TCE, and 1,1,1-TCA were assumed to be 0.9, 10.4, and 11.2 mM respectively. These values were obtained from toxicological profiles published by ATSDR (Agency for Toxic Substances & Disease Registry). The half-life can be calculated as one-half of the

initial total concentration divided by the rate of removal expected at initial concentrations of ferrous iron and target concentration in solution (solubility).

$$t_{1/2} = \frac{0.5 \times [\mathrm{CH}]^{o}_{total}}{k_{est\_rc\_Fe(II)} \times [\mathrm{Fe(II)}]_{solid} \times [\mathrm{CH}]_{sol}} \qquad (3.1)$$

where $t_{1/2}$ is the half-life, $k_{est\_rc\_Fe(II)}$ is the estimated reference rate constant for conditions of high concentration of target (last row in Table 3.2), $[\mathrm{Fe(II)}]_{solid}$ is concentration of ferrous iron as solid reductant, $[\mathrm{CH}]^{o}_{total}$ is the total concentration of chlorinated hydrocarbons in aqueous and non-aqueous phase, and $[\mathrm{CH}]_{sol}$ is solubility of chlorinated hydrocarbons. The value of 0.5 means that 50% of the initial amount of target compound in all phases would be degraded at $t_{1/2}$.. The time frame of preliminary tests was roughly limited to 30 days, so if a half-life was estimated to be larger than 15 days, the sampling times were fixed at 4 hours, 15 days, and 30 days. If a half-life was estimated to be smaller than 15 days, the sampling times were 4 hours, half-life, and the time of 90 % removal of chlorinated hydrocarbons.

Table 3.2 shows that there were no data for degradation of TCE and 1,1,1-TCA by Fe(II)-F(III)-Cl. Therefore, the rate constants estimated for degradation of TCE and 1,1,1-TCA by Fe(II)+C were applied to design experiments using Fe(II)-F(III)-Cl.

After conducting a three-point preliminary test, the data were analyzed by non-linear, least squares regression using EXCEL SOLVER to calculate apparent first-order rate constants. The sampling times for ten-point kinetic experiments were calculated using rate constants from the three-point preliminary tests to be equally spaced over a time period that would correspond to 0% to 90% degradation of the target compound.

3.3.3 Kinetic Experiments for Chlorinated Ethenes/Ethanes

Kinetic experiments on PCE degradation by ISM were conducted at various initial PCE concentrations (3.08, 6.16, 8.62, 12.3 mM) and at various initial ferrous iron concentrations (225, 424, 660, 789 mM).

Kinetic experiments for the effects of reactant types were conducted with three target compounds at three initial concentrations (PCE, 3.08 mM; TCE, 12.0 mM; 1,1,1-TCA, 11.7 mM) using three reductants (ISM, ISM+C, Fe+C). A reductant concentration of 225 mM of ferrous iron was used for experiments with chlorinated ethylenes (PCE and TCE). Concentrations of 20 and 80 mM ferrous iron with 10 mM ferric iron were used for the experiments with a 1,1,1-TCA. The lower concentrations of iron were used, because reference rate constants and a preliminary test showed that 1,1,1-TCA was degraded more rapidly. The effect of cement mass (5% and 10%) in Fe(II)+C system on degradation of PCE, TCE, and 1,1,1-TCA was examined. A mixture of PCE, TCE, and 1,1,1-TCA, each at a concentration of about 12 mM, was examined using 225 mM ISM and 225 mM Fe+C as reductants.

Batch kinetic experiments were started by filling a 24-mL glass vial with the suspension of reductants in a way to minimize headspace and then spiking it with the chlorinated hydrocarbon. The vial was closed rapidly using a triple-layer closure, and mixed on a vortex mixer to maintain a homogeneous suspension. All reactors were mounted on a 360-degree tumbler that was rotated at 7 rpm. When it was time to take a sample, the extraction procedure was applied and the extractant analyzed by gas-chromatography with electron capture detector (GC-ECD).

3.3.4 Experiments for Production of Non-Chlorinated Products

Triplicate three-point experiments were conducted to measure formation of non-chlorinated products resulting from degradation of PCE, TCE, and 1,1,1-TCA by ISM and Fe+C. The sampling times were calculated from the results of previous kinetic experiments. The first sample was taken at 4 hours and the second sample was taken at the estimated half-life. The time for the last sample was chosen in the same way as was done for the last sample in experiments used to characterize degradation kinetics. For example, if the ferrous normalized rate constant for 3.08 mM PCE dechlorination by 225 mM ISM was 4.44E-4 d^{-1} mM^{-1} and the solubility of PCE was 0.9 mM, then the half-life would be 17 days. This would result in sampling times of 4 hours, 17 days, and the time for the last sample in experiments used to characterize degradation kinetics. Table 3.3 shows the concentrations of reactants used in the experiments to measure products of degradation of PCE, TCE, and 1,1,1-TCA.

Table 3.3 The conditions for non-chlorinated products experiments at pH 12

Target chlorinated organics	Conc. (mM)	$[Fe(II)]_{ISM}$ (mM)	$[Fe(II)]_{Fe(II)+C}$ (mM)
PCE	3.08	789	225 [a]
TCE	12.0	225 and 789	80 [b] and 225 [a]
1,1,1-TCA	11.7	80	80 [b]

[a] : $[Fe(II)]_{Fe(II)+5\%C}$, [b] : $[Fe(II)]_{Fe(II)+10\%C}$

3.4 Analytical Procedures

3.4.1 Extraction for DNAPLs

An extraction procedure was developed for measuring total concentration of chlorinated hydrocarbons that were present in two phases (DNAPL and aqueous). The procedure was capable of achieving high extraction efficiency and was based on separate analyses of the aqueous and non-aqueous phases as is described in Figure 3.1.

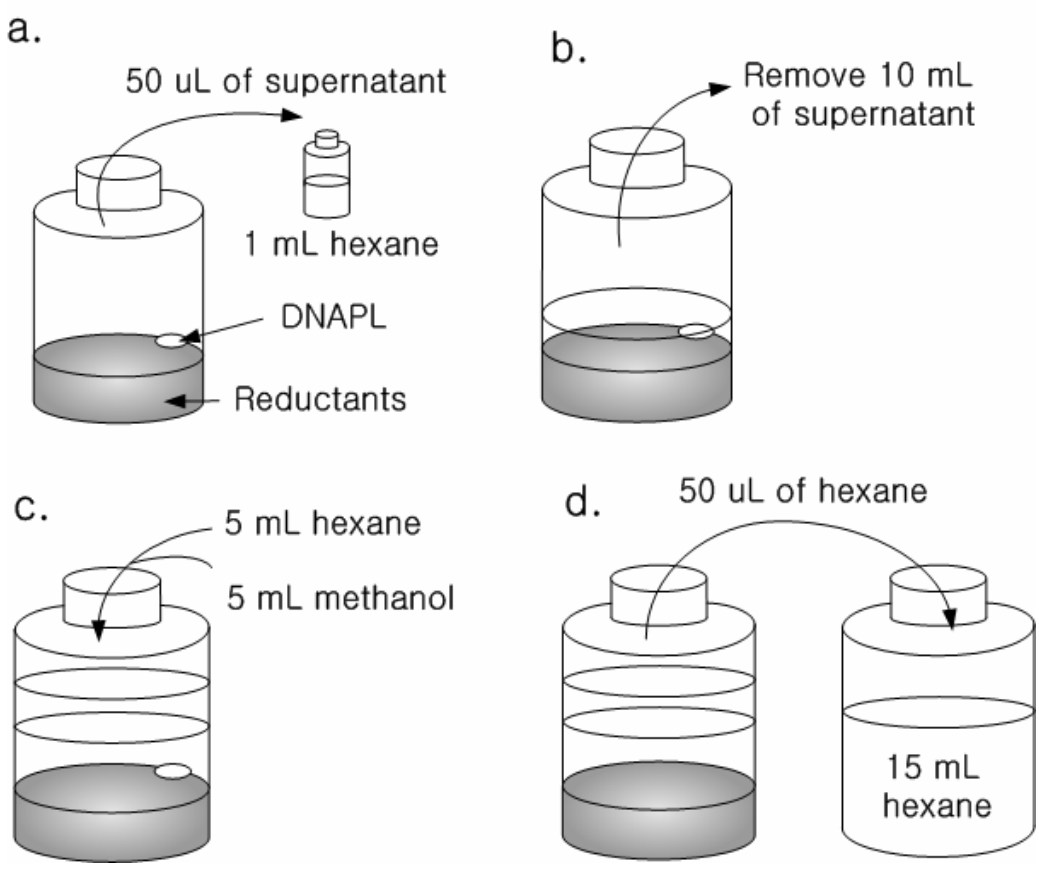

Figure 3.1 An example scheme of extraction procedure.

A sample was centrifuged at 250 rpm for 10 min and the triple-layer closure was carefully opened. An aqueous sample was taken and transferred into a 2-mL micro-vial filled with 1 mL of extractant, which was hexane that contained 1,2-DBP as internal standard. This hexane (a. in Figure 3.1) was used to determine the concentration in the aqueous phase. Then more water was removed to allow room to add a 50:50 methanol**:**hexane extractant for analysis of the amount of target in both the aqueous and the non-aqueous phases (c. in Figure 3.1). The vial containing the two phases and the extractant were mounted on an orbital shaker and shaken at 250 rpm for 1 hour, which was shown to be sufficient time for extraction of the target chlorinated hydrocarbons from both phases. After extraction, the 2-mL micro-vial containing the extract of the aqueous phase was directly mounted on the auto-sampler for GC analysis. At the same time, the extract of both phases was diluted with hexane to adjust its concentration to a range that would be more suitable for analysis (d. in Figure 3.1) and was transferred into a 2-mL micro-vial for GC analysis.

3.4.2 GC Analysis for Chlorinated Ethenes/Ethanes

Gas chromatography with electron capture detection (GC-ECD) was used for analysis of target organics and their chlorinated degradation products in hexane extracts that contained 1,2-dibromopropane (1,2-DBP) as an internal standard. A DB-VRX column (60 m x 0.25 mm) was used with a temperature profile (35 °C for 8 min, ramped to 170 °C at 10 °C/min, 170 °C for 1 min). Ultra-high purity nitrogen was used as carrier gas. These GC-ECD conditions were used to analyze perchloroethylene (PCE), trichloroethylene (TCE), 1,1,1-trichloroethane (1,1,1-TCA), 1,1-dichloroethene (1,1-

DCE), cis-1,2-dichloroethene (cis-DCE), trans-1,2-dichloroethene (trans-DCE), and 1,1-dichloroethane (1,1-DCA). Standard curves for each compound were prepared for quantification. Method detection limits (MDL) measured for these chlorinated compounds are given in Table 3.4.

Table 3.4 Method detection limits (MDL) and retention time (RT) of chlorinated hydrocarbons on GC-ECD

	PCE	TCE	1,1,1-TCA	1,1-DCE	cis-DCE	trans-DCE
MDL (mM)	1.06E-5	1.97E-5	3.45E-4	1.09E-3	3.09E-3	4.68E-2
RT (min)	16.8	13.3	11.3	5.52	9.51	7.32

The MDLs in Table 3.4 show that the analytical procedure could measure concentrations of chlorinated target compounds and their expected degradation products at low enough concentrations to accurately determine degradation kinetics. One exception is 1,1-DCA, so this method was not used for its analysis. It is believed that a trace amount of 1,1-DCA was detected during degradation of 1,1,1-TCA, but it was not possible to quantify its concentration with the procedure that was used.

3.4.3 Preparation of Headspace Analysis

Headspace analysis was used to measure concentrations of non-chlorinated products (acetylene, ethylene, and ethane). The reactor was opened and a 10-mL aqueous sample was rapidly transferred into a 24-mL glass vial with triple-layer closure.

The vial was shaken for 15 min on orbital shaker and then put in a safe place for 1 hour to allow equilibrium to be reached between the aqueous and the gas phases. This procedure was shown to recover over 90% of non-chlorinated products. A 100-µL sample of gas from the headspace was manually injected into a GC-FID using a gas-tight syringe.

3.4.4 GC Analysis for Non-Chlorinated Products

Headspace samples were analyzed by gas chromatography with a GS-Alumina Column (30 m x 0.53 mm) and a frame ionization detector (FID). The temperature of injector was 150 °C and the temperature of the detector was 200 °C. The oven temperature was held at 80 °C for 20 minutes. The split ratio was 7:1 and flow rate of ultra high purity nitrogen as a carrier gas was 5.1 ml/min. The ignition gases were hydrogen and zero air. Before each analysis, the column was cleaned by operating it at 100 °C for 1 min before cooling it to the operating temperature.

Quantification was conducted using a standard gas mixture containing acetylene, ethylene, ethane, and methane. Table 3.5 shows MDL, retention time, and Henry's Law constant for the non-chlorinated products detected by GC-FID. The dimensionless Henry's Law coefficients were calculated for 25 ºC using published regression equations (National Institute Standards and Technology, NIST). Methane is included in Table 3.5 because it was in the calibration standard, even though it is not considered a possible degradation product. The sequence of retention times in Table 3.5 agrees with information provided by the manufacturer of the GS-Alumina column (*87*).

Moreover, additional headspace samples were also analyzed by GC-MS (Agilent 6890N with mass selective detector) in order to quantify trace intermediates or products. Capillary column (HP-5MS) was used and the oven temperature was held at 80 °C for 6 minutes. The temperature of injector was 150 °C and the volume of injected sample was 20 μL. The split ratio was 7:1 and flow rate of ultra high purified helium (UHP He) as carrier gas was 8.1 ml/min.

Table 3.5 Maximum detection limits (MDL) and retention time (RT) of non-chlorinated products on GC-FID

	Methane	Ethane	Ethylene	Acetylene
Dimensionless H	-	16.0	7.9	0.93
MDL (mM)	2.79E-2	2.58E-2	2.11E-2	2.15E-2
RT (min)	1.8	1.9	2.2	4.6

3.4.5 Iron Analysis

Iron was measured in the dissolved phase, in the solid phases, and in all phases. The amount of iron in the solid phase that was present in forms such as magnetite would not be measured by this procedure, because it is not soluble in acid. However, the amount of iron in such solids was calculated as the difference in the total amount of iron added and the amount measured in all phases.

The Ferrozine method was used for iron analysis (*88*). A sample for analysis of ferrous iron was diluted as needed and introduced into 1 mL of acid quenching solution

(0.7M HNO_3). If analysis of both ferrous and ferric iron was desired, the diluted sample was added to 1 mL of reductant solution (10% hydroxylamine; $NH_2OH{\cdot}HCl$). The acid quenching solution prevents oxidation of ferrous iron and the reductant solution reduces ferric iron to ferrous iron. For both analyses, 1 mL of colorimetric solution (1 : 4 = Ferrozine (3-(2-pyridyl)-5,6-bis (4-phensylsulfonic acid)-1,2,4-triazine, monosodium salt) : 10% ammonium acetate; $NH_4C_2H_3O_2$) was added, mixed well, and allowed to react for 2 to 5 min for complete color development. Absorbance of these solutions was measured at 562 nm using a UV-VIS spectrophotometer (G1103A, Hewlett Packard) and it was used to calculate iron concentrations using a standard curve.

To separate iron between dissolved and solid phases, suspensions containing iron were filtered with 0.45-μm membrane filters. Analysis of iron in the dissolved phase typically showed levels less than 2 ppm total iron. Therefore, it was assumed that iron was exclusively in the solid phase. Moreover, the results of total iron analysis showed that all of the iron in the solid phase was dissolved by a solution of 10% hydroxylamine.

3.5 Kinetic Modeling

An appropriate model was adopted to describe results in each kinetic study. Such models included first-order, Langmuir-Hinshelwood, and competitive adsorption models. Kinetic data was analyzed to determine values of rate constants using the "nlinfit" function in MATLAB to conduct non-linear regressions. Values for the initial concentration and assumed coefficients were inputted manually and model predictions required by the non-linear regression routine were provided by numerically solving the

batch material balance equation using the MATLAB function “ode45”. The code for the MATLAB programs needed to conduct these regressions is shown in Appendix A.

CHAPTER IV

RESULTS AND DISCUSSION

4.1 Reductive Dechlorination of PCE DNAPL by ISM

Experiments were conducted for the purposes of 1) understanding and designing experimental procedures for DNAPL conditions and 2) evaluating iron solid mixtures (ISMs) as reductants to degrade chlorinated hydrocarbons that are present as DNAPL.

4.1.1 Effectiveness of Reactor System Containing DNAPL

4.1.1.1 Effects of Extractant with Methanol

An extraction procedure was designed and its extraction efficiency was evaluated. The octanol-water partition coefficients of target organics were used as estimates of the hexane-water partition coefficients in order to estimate extraction efficiency during the design of the procedure. The value of octanol-water partition coefficient for PCE that was used was 300. Moreover, the use of methanol in combination with hexane was evaluated as a method of increasing extraction efficiency. It has been reported that combining a polar solvent with a non-polar extractant enhances the rate of desorption of sorbed compounds, especially in systems that contain solid phases (*89*).

Extraction and dilution procedures were evaluated that were appropriate to concentrations of contaminants above their solubility. First, the volume ratio of extractant (hexane and methanol) to water that would achieve 99% extraction efficiency

was calculated assuming equilibrium. This calculation showed that a volume ratio of 0.33 would achieve 99 % extraction efficiency. Therefore, 99 % extraction efficiency could be expected with the use of 5 mL of both hexane and methanol as long as the volume of water was kept below 30 mL.

Experiments showed that methanol did not affect the efficiency of extracting PCE DNAPL, if solids were not present. Recoveries of PCE DNAPL at concentrations between 3 mM to 60 mM ranged from 92 % to 99 %.

However, extraction of PCE DNAPL in the presence of an iron-based solid mixture showed that applying methanol was critical to achieving better extraction efficiency. The average recovery of PCE DNAPL in the presence of solids using only hexane was 68 %, with a standard deviation of 13% (n=4), while an average extraction efficiency of 97 % was achieved with a standard deviation of 2% (n=4) by using methanol with hexane. These results confirmed that adding methanol increased recovery of PCE DNAPL in existence of solids and that adequate extraction efficiencies could be obtained. This documents the appropriateness of these extraction and dilution procedures.

4.1.1.2 Chlorinated Hydrocarbons in Aqueous and Non-Aqueous Phases

Chlorinated hydrocarbons as DNAPLs can be partitioned among the aqueous, gaseous, sorbed, and non-aqueous phases in an experimental system. However, the system used in these experiments was a batch slurry reactor without headspace, so no gaseous phase was present. The sampling and extraction procedures were designed to extract the target organic compound in two steps. The first step extracted the targets

from the aqueous phase and the second extracted them from all phases (aqueous, non-aqueous liquid, and sorbed).

Figure 4.1 shows the concentrations of PCE in the aqueous and non-aqueous phases (liquid and sorbed) during an experiment to evaluate the ability of ISM to dechlorinate PCE when present at concentrations above its solubility.

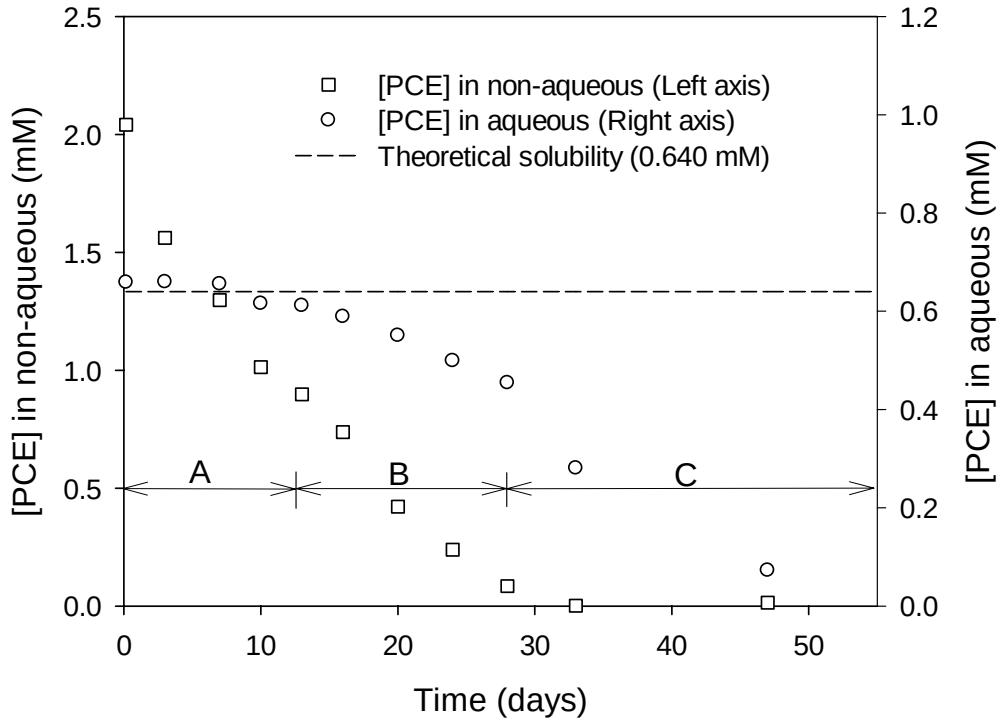

Figure 4.1 PCE DNAPL reduction in aqueous and non-aqueous phases. Symbols are average values of measured PCE concentrations. Dashed line represents theoretical solubility (0.640 mM). Experimental conditions were: $[PCE]^{o}_{total}$ = 3.08 mM and $[Fe(II)]_{ISM}$ = 789 mM at pH 12.

PCE in the non-aqueous phase was reduced by a zero-order rate, as indicated by the linear plot of concentration as a function of time. The concentration of PCE in the aqueous phase remained constant at the beginning of the experiment, even though total PCE was being degraded (A in Figure 4.1). This was due to continuous dissolution of PCE from the DNAPL into aqueous phase. However, midway through the experiment (B in Figure 4.1), the concentration of PCE in the aqueous phase began to be reduced, even though PCE DNAPL still existed in system. After 30 days of reaction time when the NAPL had completely dissolved, reduction of PCE in aqueous phase appeared to follow a first-order rate (C in Figure 4.1).

A hypothesis is presented to explain the experimental observations of zeroth-order reduction of PCE while maintaining a nearly constant concentration. The hypothesis is based on the assumption that PCE dechlorination occurs only in the aqueous phase, so that PCE must be transported from the DNAPL to the solution before being degraded. A constant aqueous concentration of PCE would occur when the net rates of removal by chemical reduction and of formation by dissolution of DNAPL are equal. However, midway through the experiment (B in Figure 4.1), the concentration of PCE in aqueous phase began to decline, which indicates that the rate of removal was higher than the rate of dissolution. The dissolution rate is affected by two factors that could cause the reduction. One is the surface area of DNAPL droplets and the other is the concentration gradient between the surface of the DNAPL and the solution. Because of the DNAPL droplet volume would decrease with time, the surface area would decrease, which would tend to lower the transfer rate and cause a decreased

concentration. The decrease in concentration in solution would tend to mitigate the effect of lower interfacial area of DNAPL, because it would increase the concentration gradient between DNAPL surface and solution. Although the concentration in solution could be constant at any value, the observed concentration is very close to the solubility, which supports the observation that mass transfer from DNAPL droplets is rapid. After all of the DNAPL disappeared, PCE was removed from solution with first-order behavior, because the concentration would decrease as PCE was dechlorinated. Although TCE accumulated in these experiments, it was assumed that TCE did not change the characteristics of the system in a way that would affect any of the reaction rates. These hypotheses were used to develop a kinetic model to interpret the removal of chlorinated compounds present as DNAPL and the model considered the rate of removal from aqueous solution as the rate-limiting step.

4.1.1.3 Effect of $[Fe(II)]_{ISM}$ on Solubility of PCE DNAPL

The solubility of chlorinated hydrocarbons has been generally defined as the concentration in the aqueous phase that exists in equilibrium with the pure NAPL. However, this equilibrium concentration was found to vary with the concentration of ISM as shown in Figure 4.2.

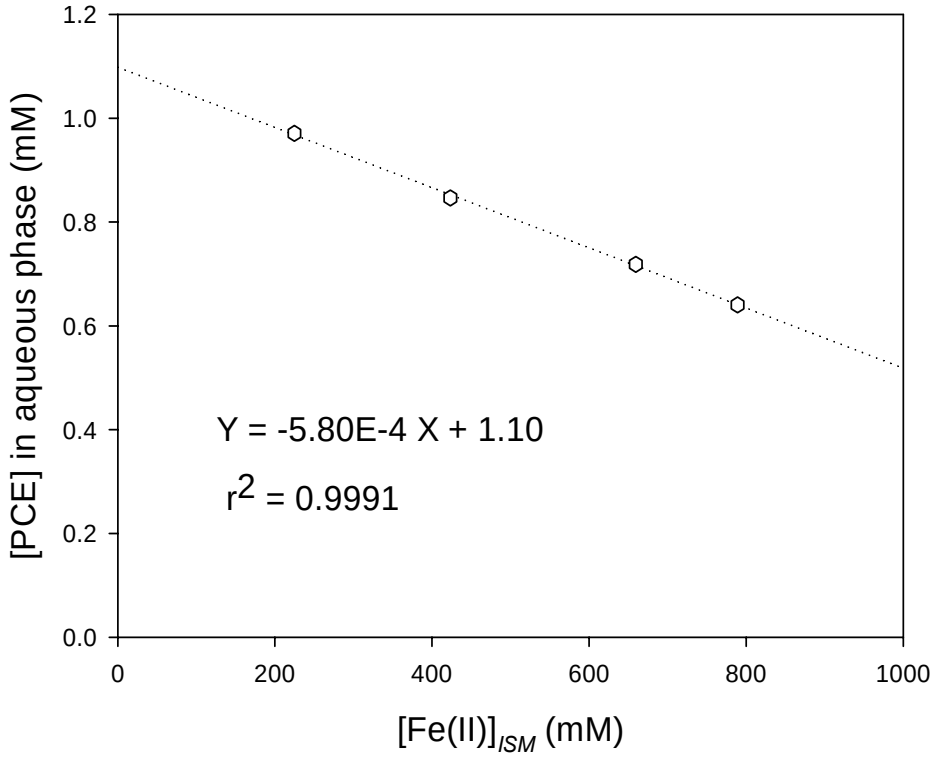

Figure 4.2 A relationship between the solubility of PCE and the concentration of ferrous iron in ISM ($[Fe(II)]_{ISM}$ = 225, 424, 660, and 789 mM). $[PCE]^{o}_{total}$ = 3.08 mM at pH 12.

The results shown in Figure 4.2 mean that the activity of PCE in the aqueous phase at equilibrium decreased with increasing $[Fe(II)]_{ISM}$ in the system. The factors most commonly reported to affect solubility of organic compounds in water were temperature and chemical composition of the solution (*69*). In the present study, increasing $[Fe(II)]_{ISM}$ could increase concentrations of ions such as Ca^{2+} and Cl^{-} in solution, and this might cause decreasing solubility, which is commonly referred to as "salting out."

4.1.2 Evaluation of Kinetic Data

A kinetic model was developed to describe degradation in a batch system that contains contaminants both in the aqueous phase and in the non-aqueous phase. This model is shown in Equations 4.1 to 4.3.

$$\frac{d[\mathrm{CH}]_{total}}{dt} = -k_{app} \times [\mathrm{CH}]_{sol} \qquad \text{if } [\mathrm{CH}]_{total} > [\mathrm{CH}]_{sol} \qquad (4.1)$$

$$\frac{d[\mathrm{CH}]_{total}}{dt} = -k_{app} \times [\mathrm{CH}]_{total} \qquad \text{if } [\mathrm{CH}]_{total} < [\mathrm{CH}]_{sol} \qquad (4.2)$$

$$k_{app} = k_{Fe(II)} \text{ x } [\mathrm{Fe(II)}]_{solid} \qquad (4.3)$$

, where k_{app} is the apparent first-order rate constant, $k_{Fe(II)}$ is the ferrous-iron-normalized rate constant or second-order rate constant, $[\mathrm{CH}]_{total}$ is the total concentration of chlorinated hydrocarbons in both aqueous and non-aqueous phases, $[\mathrm{CH}]_{sol}$ is solubility of chlorinated hydrocarbons, and $[\mathrm{Fe(II)}]_{solid}$ is the concentration of ferrous iron in the solid reductants.

The model was based on the assumption that the mass transfer between the non-aqueous phase and aqueous phase is fast enough to maintain the concentration in the aqueous phase approximately equal to its equilibrium value. The experimental results showed that aqueous concentration was constant at the very beginning of reaction and it began to decrease midway through experiment, while DNAPL was still present. This decrease can be explained by the decrease in surface area of the DNAPL that results in lower dissolution rates. Although the aqueous-phase concentration did not remain

totally constant while DNAPL was present, its value did not change greatly, so it will be assumed constant in the kinetic model for simplicity.

The model also assumes that there is no direct reaction between the contaminant in the non-aqueous phase and the solid-phase reductants, so all degradation occurs in the solution. The rate of degradation was assumed to follow a rate model that is first order in the concentration of chlorinated hydrocarbons in the aqueous phase. The concentration of chlorinated hydrocarbon in the aqueous phase was assumed to be equal to the solubility as long as its total concentration (aqueous + non-aqueous) was greater than the solubility. The solubility was assumed to be affected by the concentration of solids present.

4.1.3 Experimental Results

4.1.3.1 Reductive Dechlorination of PCE DNAPL by Fe(II) in ISM

Batch kinetic experiments were conducted to evaluate the effects of target concentrations and reductant doses on dechlorination of PCE DNAPL at pH 12. Previously, it was reported that pH 12 was approximately the optimum for PCE reduction in Fe(II)-based DS/S (*18*). The controls were prepared to introduce only chlorinated hydrocarbons without ISM into the de-aerated deionized water, which had been purged with gas consisting of 95% nitrogen and 5% hydrogen for at least 24 hours in an anaerobic chamber. The pH of the de-aerated deionized water was 5.1 in the anaerobic chamber. The symbols and error bars in figures represent the average value and standard deviation of triplicates, respectively. The lines are non-linear predictions of the kinetic model, which used values of solubility of PCE that were obtained from phase

equilibrium experiments and values of kinetic coefficients that were obtained by non-linear regression using the nlinfit function in MATLAB.

Results of kinetic experiments on degradation of 3.08 mM PCE DNAPL by different doses of $[Fe(II)]_{ISM}$ (i.e. 225, 424, 660, and 789 mM) at pH 12 is shown in Figure 4.3. The data (n = 78) from controls of all experiments taken at the same reaction time were averaged and shown as a single symbol. The first-order rate constant was determined to be 4.40E-3 (± 1.40E-3) day^{-1}. The good fits of predicted lines demonstrated the soundness of the kinetic model, which was based on the assumption that the rate was first-order in aqueous phase concentration. The data showed a removal rate that tended to be constant at high total concentrations when the DNAPL was present and tended to decrease with concentration at lower concentrations after the DNAPL had dissolved. A constant rate of removal is predicted by the model that assumes the rate is proportion to the solution concentration, because the solution concentration is constant at a value near the solubility. Increasing degradation rates were observed with increasing $[Fe(II)]_{ISM}$.

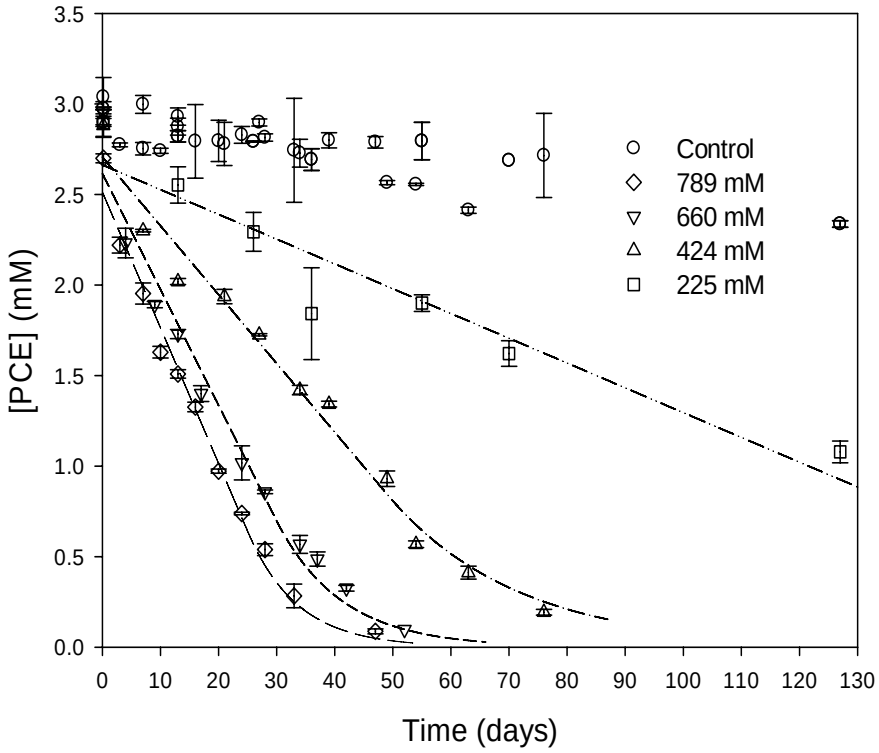

Figure 4.3 Effect of dose of $[Fe(II)]_{ISM}$ on reductive dechlorination of PCE. $[PCE]^{o}_{total}$ = 3.08 mM and $[Fe(II)]_{ISM}$ = 225 to 789 mM.

Figure 4.4 shows results from experiments investigating the effect of various concentrations of PCE DNAPL (i.g. 3.08, 6.16, 8.62 and 12.3 mM) on its degradation with $[Fe(II)]_{ISM}$ = 789 mM. The lines are predictions of the kinetic model and their constant slopes show that the concentration of DNAPL did not affect degradation rates of PCE. This is expected, because the concentration of PCE in the aqueous phase, which controls the rate, remained nearly constant at the solubility. The average first-order rate constant for various PCE DNAPL concentrations was 0.120 (day^{-1}) with a standard

deviation of 2.65E-3. This relative constancy of the rate constants with various initial PCE DNAPL concentrations supports the validity of the kinetic model.

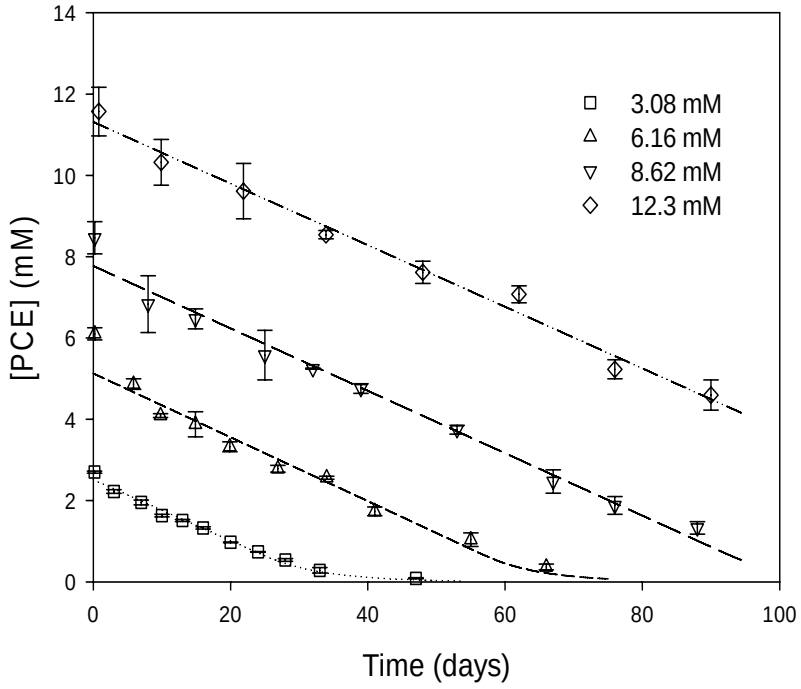

Figure 4.4 Dechlorination of various concentrations of PCE DNAPL by $[Fe(II)]_{ISM}$ = 789 mM at pH 12. $[PCE]^{o}_{total}$ = 3.08 to 12.3 mM.

Table 4.1 shows the degradation rate constants that were obtained from the experiments for the effects of PCE DNAPL concentration and $[Fe(II)]_{ISM}$. It includes the value of the solubility of PCE DNAPL that was assumed valid for each experimental condition and the half-lives of degradation.

Table 4.1 First-order rate constants for PCE DNAPL reduction by ISM

exp[a]	$[Fe(II)]_{ISM}$ (mM)	$[PCE]_{sol}$ [b] (mM)	$[PCE]^{o}_{total}$ [c] (mM)	k_{app} [c] (day^{-1})	$t_{1/2}$ [d] (day)	n[e]
1	225	0.971	2.66 (±0.302)	1.41E-2 (± 5.20E-3)	97.1	21
2	424	0.847	2.71 (±0.164)	4.47E-2 (±5.90E-3)	35.8	30
3	660	0.719	2.62 (±0.212)	8.91E-2 (±1.51E-2)	20.4	30
4	789	0.640	2.52 (±0.127)	0.117 (±1.27E-2)	16.8	31
5	789	0.640	5.13 (±0.317)	0.123 (±1.68E-2)	32.6	30
6	789	0.640	7.77 (±0.411)	0.120 (±1.30E-2)	50.6	30
7	789	0.640	11.3 (±0.452)	0.118 (±1.36E-2)	74.8	24

[a] : All conditions are contained [Fe(III)]=100 mM at pH=12, which are mainly achieved by $Ca(OH)_2$ and finally adjusted by NaOH.

[b] : Solubilities of PCE were obtained from phase equilibrium experiments in which equilibrium concentrations of PCE in the aqueous phase were measured in presence of DNAPL.

[c] : Values in parenthesis represented 95% confidence intervals from using nlparci function in Matlab.

[d] : Half-lives from the equation of $t_{1/2} = \frac{0.5 \times [\text{PCE}]^{o}_{total}}{k_{app} \times [\text{PCE}]_{sol}}$, where $[PCE]^{o}_{total}$ = initial total PCE DNAPL concentration (mM), $[PCE]_{sol}$ = solubility of PCE DNAPL, and k_{app} = first-order rate constant.

[e] : Number of data points.

4.1.3.2 Dechlorination Products of PCE DNAPL

The chlorinated and non-chlorinated products of degradation of 3.08 mM PCE DNAPL by 789 mM ISM ($[Fe(II)]_{ISM}$ = 789 mM) are shown in Figure 4.5. This figure shows total concentrations of PCE, TCE, acetylene, ethene and ethane as functions of reaction time. The average recovery of controls was 90 % with standard deviation of 1.6 %. Experimental data showed that some error bars were smaller than the symbols.

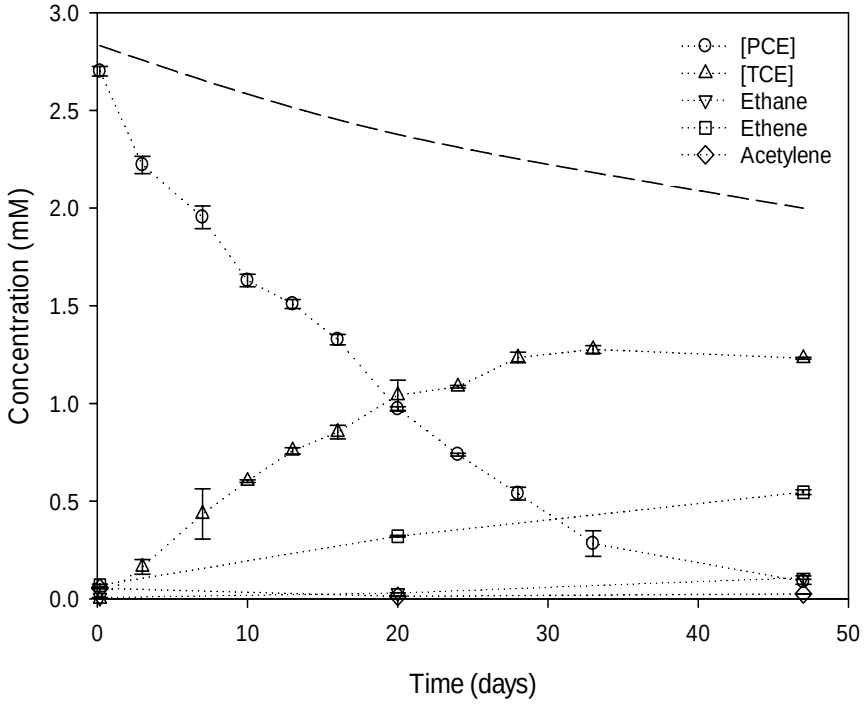

Figure 4.5 Dechlorination products of PCE DNAPL by ISM at pH 12. $[PCE]^{o}_{total}$ = 3.08 mM and $[Fe(II)]_{ISM}$ = 789 mM. Dashed line is the measured total carbon balance.

The total concentration of PCE declined at a constant rate when DNAPL existed, and it slowed when DNAPL disappeared. The major chlorinated product was TCE,

which accumulated during PCE degradation. The ratio of TCE production to PCE DNAPL removal reached a maximum of 48.3 % at 33 days and dropped to 40.1 % at the end of the experiment where only 3 % of initial PCE remained. DCEs (i.e. 1,1-DCE or trans/cis-DCE) were identified on GC-MS, but these compounds could not be quantified because of small peaks.

The non-chlorinated products that were detected were ethane, ethene, and acetylene. Ethene was the major non-chlorinated product, and the maximum ratio of ethene production to PCE DNAPL removal was 18.3 % at 47 days. The amount of acetylene present was higher at the beginning of the experiment and the amount of ethane present increased during the experiment. The carbon balance was 91 % at the beginning, and 64.5 % at 47 days. This could be caused by production of unidentified compounds or by errors in experimental procedures.

Accumulation of TCE might be explained by 1) the existence of non-active sites on the reductant that could bond with TCE; 2) lower reactivity of TCE on ISM than observed for PCE; or 3) the amount of reductants added was not enough to degrade all chlorinated compounds to non-chlorinated compounds.

4.1.4 Discussion

4.1.4.1 Reaction Kinetics

The observed rate constants for degradation of PCE DNAPL are shown in Figure 4.6 as functions of the concentration of Fe(II). The symbols show average values of triplicates, and the error bars show 95% confidence intervals. The lines represent power law equations fitted to the rate constants for PCE DNAPL dechlorination.

The behavior of the apparent first-order rate constants implies that k_{app} at low Fe(II) doses of ISM increases more slowly with an increase in the dose than at high doses. This behavior is different than that reported for conventional Fe(II)-DS/S, which showed a saturation relationship between reductant reactivity and dose of Fe(II) (*18,20*). This might imply that the type of reductant synthesized during the present research and/or its physical properties (i.e. particle size, structure of reductant, etc.) were different from the reductant generated in conventional Fe(II)-DS/S. Moreover, this might show that it is possible to synthesize different types of reductants when chemical composition is varied (i.e. when higher concentrations of Fe(II) are used). For example, at lower Fe(II) doses, a less reactive reductant might be synthesized than at higher Fe(II) doses. The possibility of forming different types of iron-based reductants is supported by the observation that the color of solids produced differed at different Fe(II) doses. Suspensions prepared with lower Fe(II) doses were almost a dark gray and suspensions prepared with higher Fe(II) doses were greenish.

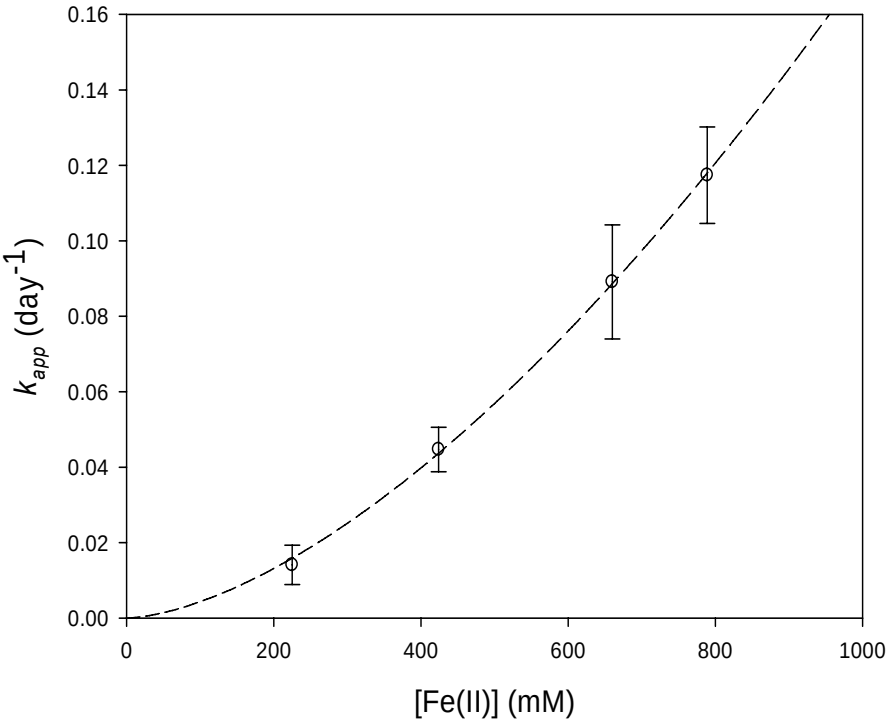

Figure 4.6 PCE DNAPL removal rate constants using various concentration of Fe(II) in ISM. The equation of line is $y = a * x^{b}$, where a = 2.75E-6 (± 8.54E-7), b = 1.60 (± 4.73E-2), and $r^2 = 0.9996$. The number in parenthesis was calculated by standard error.

Generally, the rate constant and half-life ($t_{1/2}$) are independent of the initial concentration when first-order kinetics is observed. However, the half-life for removal of DNAPL in these experiments depended on the initial DNAPL concentration. Moreover, the half-lives were almost proportional to the initial DNAPL concentration. This behavior can be demonstrated by applying the relationship for calculating the half-life to two systems with different total concentrations, identified by the subscripts 1 and 2.

$$\frac{t_{1/2,1}}{t_{1/2,2}} = \frac{\dfrac{0.5 \times [\text{PCE}]^{o}_{total,1}}{k_{app,1} \times [\text{PCE}]_{sol,1}}}{\dfrac{0.5 \times [\text{PCE}]^{o}_{total,2}}{k_{app,2} \times [\text{PCE}]_{sol,2}}} \approx \frac{[\text{PCE}]^{o}_{total,1}}{[\text{PCE}]^{o}_{total,2}} \qquad (4.4)$$

, where $t_{1/2}$ is the half-life, k_{app} is the first-order rate constant, $[\text{PCE}]^{o}_{total}$ is the initial total concentration of PCE in all phases, and $[\text{PCE}]_{sol}$ is aqueous equilibrium concentration of PCE (solubility). Equation 4.4 shows that the half-life would be nearly proportional to the total PCE concentration, because the rate constants should be the same and the solubilities should not be greatly different. Moreover, Equation 4.5 may be used when $[\text{PCE}]^{o}_{total}$ is the same, but solubilities are different.

$$\frac{t_{1/2,1}}{t_{1/2,2}} = \frac{k_{app,2} \times [\text{PCE}]_{sol,2}}{k_{app,1} \times [\text{PCE}]_{sol,1}} \qquad (4.5)$$

If PCE exists with other compounds as a DNAPL mixture, then the solubility of PCE depends on its mole fraction in the DNAPL mixture. Equation 4.5 would apply to this situation, because there are different solubilities with the same total concentration. Even though Equation 4.5 will not be used for any further discussions, it indicates that

the solubility can be important in evaluating kinetics of removal when DNAPL are present.

A variety of different types of reductants were used to generate data shown in Figure 4.7. This figure includes results from experiments that used a low initial concentration of PCE (0.242 mM) and various reductants produced in the presence and absence of Portland cement. The ferrous-iron-normalized rate constants ($k_{Fe(II)}$) were compared for each type of reductant. The reductants include: soluble components of acid-extracted Portland cement (PCX) combined with Fe(II) (Fe(II)-PCX); a solution prepared to simulate the composition of acid-extracted cement extract but without addition of Ca, Al, and Mg combined with Fe(II) (MSCXFe); green rust prepared by coprecipitation (Fe(II)Fe(III)Cl-GR); a mixture of $FeCl_2$, $FeCl_3$, and NaCl (Fe(II)Fe(III)Cl); and Friedel's salts (*25,42,90*). All suspensions were adjusted to pH 12 except Fe(II)-PCX, which was at pH 11.8 (*25*). In most experiments, no chlorinated products were measured. However, TCE was produced when MSCXFe was used as reductant (*25*). This might suggest that Al or Mg has a role in determining the pathways of reductive dechlorination of PCE.

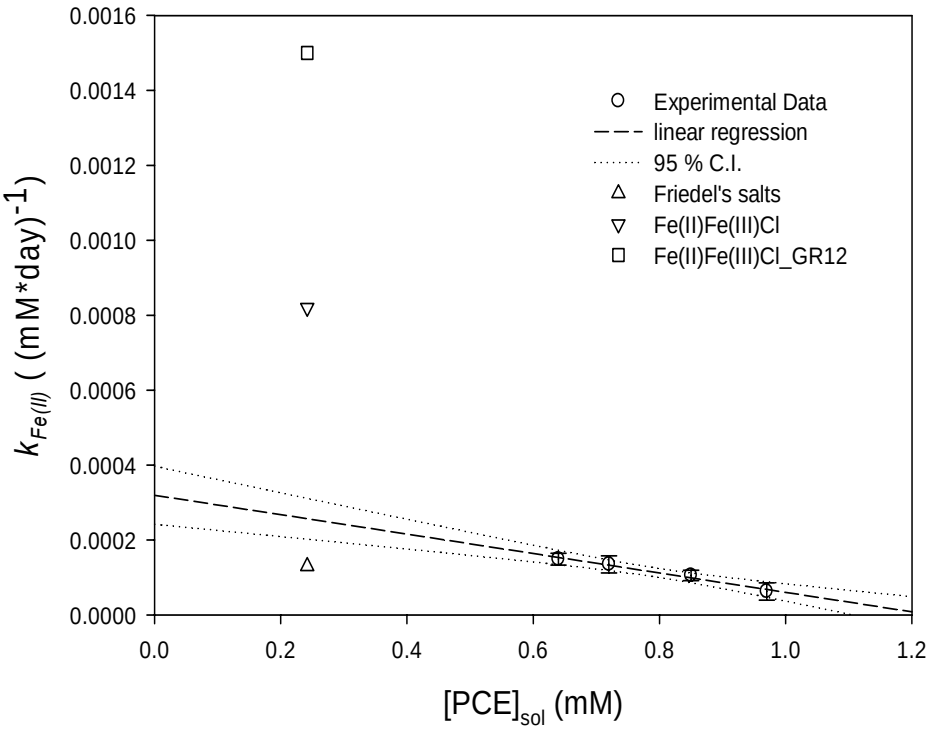

Figure 4.7 Effects of types of various reductants and the relationship of aqueous equilibrium concentration versus the ferrous-iron-normalized rate constants. The linear equation of line is y = -2.59E-4 * x + 3.19E-4 with $r^2 = 0.978$. Rate constants for Fe(II)-PCX ($k_{Fe(II)}$ = 1.10E-2 (mM*day)$^{-1}$) and MSCXFe ($k_{Fe(II)}$ = 3.80E-3 (mM*day)$^{-1}$) were considered in the analysis, but were not depicted in this figure due to their relatively large values.

There have been many efforts to identify the active agent in the Fe(II)-DS/S system, and it was reported that Fe(II), Fe(III), and Cl might be the most essential elements for producing the active agent (*25*). It was suggested that the solid reductants formed from acid-extracted soluble components of Portland cement were more reactive than the solids formed by hydration of cement (*25*). Unlike surface-bound Fe(II) in iron oxides, the mixing times (2 hours to 20 hours) used to synthesize the solids from cement extracts did not affect the reactivities of the solids (*25,91*). It was reported that Portlandite and Friedel's salts were the major solids products identified in suspensions produced by combining an extract of 10 % Portland cement with Fe(II) and that the addition of Fe(II) caused a reduction of particle size (*25*). The reduction of particle size would increase the reduction rates because of larger surface areas. Moreover, it was concluded that Portlandite combined with Fe(II) was not an active reducing agent (*25*).

On the other hand, Friedel's salts were not detected when cement was absent. Portlandite and GR_Cl were reported as solids that were detected by XRD in non-cement systems (*25*). However, detection of GR_Cl was not certain, because the high intensity of peaks from Portlandite hindered identification of the third-most intense peak of GR_Cl. Moreover, it was reported that the formation of ferrous hydroxide solid was observed when $FeCl_2$, $FeCl_3$, and NaCl (Fe(II)Fe(III)Cl) were combined with a solution that contained a number of minor elements present in cement extracts (*25*). This research identified the potentially active agents in cement systems primarily to be LDHs, such as Friedel's salts, calcium aluminum hydrate, and green rust chloride. Moreover, these

LDHs showed smaller solid particle size at pH 12 than at neutral pH, which was suggested as a responsible reason for the higher reactivity at higher pH (*25*).

A reductant was synthesized during the present research using a mixture of $FeCl_2$, $FeCl_3$, and $Ca(OH)_2$ at high concentrations. This could have synthesized an active reductant that was an LDH such as a substituted form of Friedel's salt ($Ca_2(Al,Fe)(OH)_6(Cl,OH)\cdot 2H_2O$) in which Al is substituted by Fe(III). Other possible LDHs include chloride and hydroxide green rust (GR_Cl and GR_OH)). Possible active reductants that are not LDHs include ferrous hydroxide, Portlandite, and β-$Fe_2(OH)_3Cl$ (*25,50,57,60*). In addition to these solid phases that incorporate Fe(II) into their structure, surface-bound Fe(II) could also play a role in dechlorination. The identities of the reductants formed in this research are not clear, but the present results show that they could degrade PCE DNAPL and that increased rates of dechlorination occur when increased amounts of Fe(II) are added. Moreover, if a combination of LDHs can be produced by Fe(II) and cement, the combination might show higher rates of dechlorination than a single LDH.

Comparisons of rate constants obtained with different types of reductants was made to determine if it is reasonable to assume that they contain the same kinds of compounds that are responsible for dechlorination. Unfortunately, it is beyond the scope of this research to analyze solids to determine their chemical forms. It has been reported that the separation and identification of these types of reductants is difficult, especially in slurry systems (*25*). Moreover, it seemed that it would be difficult for XRD analysis to distinguish solids in such systems, because of similar structure, overlapping peaks, and

the presence of amorphous solids. Because of this difficulty, there was no attempt to identify the chemical form of the iron complexes synthesized in this research.

4.1.4.2 Reduction Pathways

It has been reported that trace amounts of TCE were detected when a low concentration of PCE (0.24 mM) was degraded by a mixture of ferrous iron and cement. Because only small amounts of TCE were found, it was suggested that β-elimination was the major reductive dechlorination pathway. However, when PCE present as DNAPL was degraded by ISM, it seemed to follow a combination of the hydrogenolysis and β-elimination pathways.

PCE present as DNAPL could possibly be degraded by the hydrogenolysis, β-elimination, α-elimination or hydrogenation pathways as shown in Figure 2.5. The identification of products of PCE degradation could demonstrate which of these pathways is active during reaction with ISM. The hydrogenolysis pathway of PCE degradation leads to the sequential formation of TCE, DCEs (dichloroethenes), VC (vinyl chloride) and ethene. The β-elimination pathway leads from PCE to dichloroacetylene, chloroacetylene, and acetylene. When TCE is degraded through the β-elimination pathway it first produces chloroacetylene which is converted to acetylene. When DCEs are degraded by β-elimination the first product is acetylene.

Accumulation of TCE (Figure 4.5) shows that the hydrogenolysis pathway is important. However, because TCE accumulated to only half the initial concentration of PCE (Figure 4.5) it may not be the only pathway. The major non-chlorinated product was ethene, which could be formed by hydrogenolysis or by β-elimination. There was no

direct evidence of accumulation of VC, which indicates that the ethene was probably formed by *β*-elimination. The accumulation of acetylene also indicates that *β*-elimination was active. Although peaks associated with DCE were found during GC-MS, the analysis procedure was not able to identify the peaks as 1,1-DCE, trans-DCE or cis-DCE.

It was reported that dechlorination of PCE and TCE on Fe(II)-DS/S system produced mostly acetylene (about 80 % of PCE and TCE) (*20*). It was reported that dichloroacetylene and chloroacetylene reacted very rapidly with zero-valent iron (*82*). If this were applicable to ISM, some possible pathways to produce acetylene by *β*-elimination or combinations of hydrogenolysis and *β*-elimination are: 1) PCE → dichloroacetylene → chloroacetylene → acetylene, 2) PCE → TCE → chloroacetylene → acetylene, and 3) PCE → TCE → trans/cis-DCE → acetylene. The second pathway is the most likely pathway to produce acetylene because of relatively high reactivity of chloroacetylene.

Moreover, the fact that relatively larger amounts of acetylene accumulated at the initial sampling time (4 hours) might mean that *β*-elimination of trans/cis-DCE or chloroacetylene to produce acetylene dominates at the beginning of PCE dechlorination. The major final product, ethene, could be accumulated through 1) trans/cis-DCE → acetylene → ethene or 2) DCEs (trans/cis-DCE or 1,1-DCE) → VC → ethene. However, it was reported the very slow rate constant of VC dechlorination (*20*), and present analysis did not detected VC. This might imply that ethene could be produced via trans/cis-DCE → acetylene → ethene.

Therefore, the main pathway for degradation of PCE DNAPL by ISM appears to be through combined pathways that include both hydrogenolysis and β-elimination. Such pathways would be: 1) PCE→ TCE → trans/cis-DCE → acetylene → ethene, and 2) PCE→ TCE → chloroacetylene → acetylene → ethene. Ethene can also be converted to ethane.

4.2 DNAPL Reductive Dechlorination by ISM and Fe(II)+C

Previously, PCE DNAPL reduction by ISM showed that it is possible to synthesize reductants for chlorinated organics without using Portland cement. To extend this work, the effects of the type of reductant and type of target chlorinated hydrocarbon were evaluated. Target chlorinated hydrocarbons were PCE, TCE, and 1,1,1-TCA and they were present as DNAPLs. The types of reductants were ISM, ISM with Portland cement (ISM+C), and ferrous iron with Portland cement (Fe(II)+C). The latter reductant is produced by conventional Fe(II)-DS/S technology. It was used for comparison with other reductants to evaluate their relative abilities to degrade chlorinated hydrocarbons as DNAPLs.

4.2.1 Effectiveness of Experimental Systems Containing DNAPLs

The appropriateness of the experimental system was demonstrated by experiments showing the effectiveness of the extraction procedure and by a phase equilibrium experiment. The extraction procedure was verified previously for application to PCE DNAPL, but was evaluated for other effectiveness with other target compounds. This procedure separately extracts, the aqueous phase by addition of

hexane and both phases by adding a mixture of methanol and hexane. This procedure was applied to extraction of TCE and 1,1,1-TCA DNAPL in the same way that it was applied to PCE DNAPL.

The extraction efficiency for TCE and 1,1,1-TCA with and without solids showed that the extraction procedure could be used for those target organics. The recovery of TCE present initially at 12.0 mM was 97 % with solids present and 98 % without solids being present. The recovery of 1,1,1-TCA initially present at 11.7 mM was 91 % with solids present and 95 % without solids being present. This shows that the extraction procedure could be used generally for analysis of these target compounds present as DNAPL.

Phase equilibrium experiments for TCE and 1,1,1-TCA were also conducted. The solubility of TCE was measured as 7.45 mM in the presence of ISM with $[Fe(II)]_{ISM}$ = 225 mM. The solubility of 1,1,1-TCA in the presence of ISM with $[Fe(II)]_{ISM}$ = 80 mM was measured as 7.57 mM. The value of 0.971 mM for PCE solubility in the presence of ISM with $[Fe(II)]_{ISM}$ = 225 mM was measured previously. Each experiment system with various reductants showed small differences in solubility of chlorinated hydrocarbons, but the values for solubility presented in this paragraph were used to simplify comparisons of reactivity of different reductants.

4.2.2 Evaluation of Kinetic Data

Generally, a first-order rate model was applied to interpret kinetics of degradation of chlorinated hydrocarbons, but other models such as the Langmuir-Hinshelwood model (L-H model) were used in some cases, depending on the

experimental data. It was reported that TCE reduction by soil minerals followed a modified Langmuir-Hinshelwood model (ML-H model). This model used the concept of the reductive capacity, which was the total concentration of chlorinated compound that could be reduced by a specific concentration of reductant (*22*).

The Langmuir-Hinshelwood model was further modified by assuming that the aqueous concentration of a chlorinated hydrocarbon would be equal to its solubility whenever the compound existed as DNAPL. The rate equation for the modified Langmuir-Hinshelwood model (ML-H model) combined with the material balance equation for a batch reactor is shown below.

$$\frac{d[\mathrm{CH}]_{total}}{dt} = -\frac{k_{LH} \times [\mathrm{RC}] \times [\mathrm{CH}]_{sol}}{1/K + [\mathrm{CH}]_{sol}} \qquad \text{if } [\mathrm{CH}]_{total} \geq [\mathrm{CH}]_{sol} \qquad (4.6)$$

$$\frac{d[\mathrm{CH}]_{total}}{dt} = -\frac{k_{LH} \times [\mathrm{RC}] \times [\mathrm{CH}]_{total}}{1/K + [\mathrm{CH}]_{total}} \qquad \text{if } [\mathrm{CH}]_{total} < [\mathrm{CH}]_{sol} \qquad (4.7)$$

$$[\mathrm{RC}] = [\mathrm{RC}]^{o} - ([\mathrm{CH}]^{o}_{total} - [\mathrm{CH}]_{total}) \qquad (4.8)$$

, where k_{LH} is modified Langmuir-Hinshelwood (ML-H model) rate constant, K is the sorption coefficient, $[\mathrm{RC}]^{o}$ is initial concentration of reductive capacity that is represented as the total amount of chlorinated hydrocarbons that could be reduced by the reductant per unit volume of water, [RC] is the reductive capacity at any time, $[\mathrm{CH}]_{total}$ and $[\mathrm{CH}]^{o}_{total}$ are the total concentration of target compound present in both aqueous and non-aqueous phases at time t and at time zero, $[\mathrm{CH}]_{sol}$ is solubility of chlorinated hydrocarbons.

If the value of K is small ($K <<< 1$) so that $1/K$ is much larger than $[\mathrm{CH}]_{sol}$, then the rate equation (Equation 4.6) becomes second-order (Equation 4.9). If K is large

enough ($K >>> 1$) so that $1/K$ is much less than $[CH]_{sol}$, then the denominator of the ML-H rate equation would be equal to $[CH]_{sol}$. Therefore, the kinetics of such a system could be expressed with a rate equation that is first order in concentration of reductive capacity. The first-order rate constant would equal to the product of the ML-H rate constant (k_{LH}) and sorption constant (K). Therefore, if K is large, the dechlorination rate is affected by both reductant capacity and target concentration. Equation 4.9 and 4.10 present a second-order rate model with k_2 as the second-order rate constant.

$$\frac{d[CH]_{total}}{dt} = -k_2[RC][CH]_{sol} \qquad \text{if } [CH]_{total} \geq [CH]_{sol} \qquad (4.9)$$

$$\frac{d[CH]_{total}}{dt} = -k_2[RC][CH]_{total} \qquad \text{if } [CH]_{total} < [CH]_{sol} \qquad (4.10)$$

4.2.3 Experimental Results

All experiments were conducted under anaerobic conditions at pH 12. Triplicate samples and duplicate controls were prepared for all kinetic experiments. The input concentrations of chlorinated hydrocarbons were 3.08 mM PCE, 12.0 mM TCE, and 11.7 mM 1,1,1-TCA. PCE and TCE were present as DNAPLs, but 1,1,1-TCA was totally soluble. These three chlorinated hydrocarbons were tested with three types of reductants, which were ISM, ISM+C, Fe(II)+C. The effect of Portland cement doses of 5 % and 10 % was tested.

4.2.3.1 The Effects of Reductant Types on PCE DNAPL Dechlorination

Three types of reductants containing 225 mM ferrous chloride were tested for their abilities to dechlorinate 3.08 mM PCE present in both the aqueous phase and as a

DNAPL. The types of reductants used were ISM, ISM+C, and Fe(II)+C at two Portland cement doses (5 % and 10 %). The solubility of PCE DNAPL was assumed to be 0.971 mM.

Figure 4.8 shows the results of these experiments and they indicate that reductants that contained cement (ISM+C, Fe(II)+C) showed the fastest dechlorination rates for PCE DNAPL. Dechlorination of PCE DNAPL by Fe(II)+C and ISM+5%C was completed within 60 days, while ISM was able to degrade only about 39 % of initial PCE within the same reaction time. The lines in Figure 4.8 are predictions made by the modified first-order model using values of coefficients determined by non-linear regression. Figure 4.8 shows that the model predictions approach zero-order behavior as expected when DNAPL was present. The last few data points are lower than the predictions of the model for Fe(II)+C. This could be caused by having fewer experimental data points in the region of first-order behavior than in the region of zero-order behavior, or it could be due to the inability of the kinetic models to describe PCE DNAPL dechlorination by Fe(II)+C over the entire range of conditions. Moreover, the dose of cement did not seem to have much of an effect on kinetics of PCE DNAPL dechlorination under these conditions.

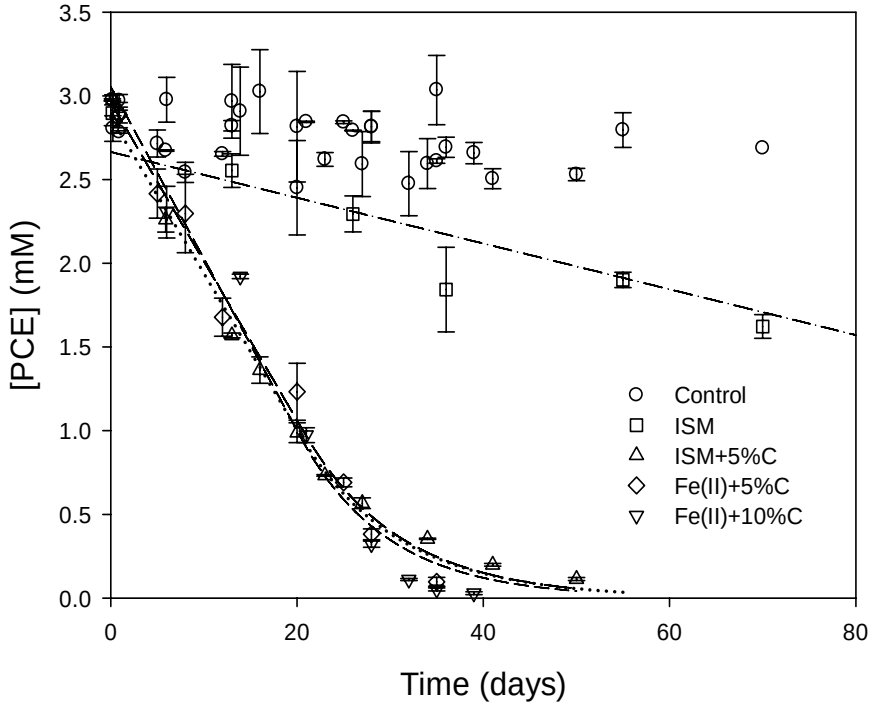

Figure 4.8 PCE DNAPL dechlorination ($[PCE]^{o}_{total}$ = 3.08 mM) by different types of reductants. [Fe(II)] = 225 mM at pH 12.

The rate coefficients for various kinetic models (zero, modified first-order, and ML-H model) were calculated and evaluated to better understand the reaction kinetics. Data from experiments with ISM and ISM+5%C were not used in this analysis, because they were well-fitted by the modified first-order model. The modified first-order rate constants for ISM and ISM+5%C were 1.41E-2 (± 5.20E-3) day^{-1} and 9.62E-2 (± 8.70E-3) day^{-1}, respectively. The average relative absolute errors of prediction lines for ISM and ISM+5%C were 6.30E-2 and 5.57E-2, respectively.

Table 4.2 shows coefficients for the zero-order, the modified first-order, the modified second-order and the ML-H (modified Langmuir-Hinshelwood) models for PCE DNAPL dechlorination by Fe(II)+C. The non-linear regression routine used to calculate kinetic coefficients required initial guesses for the coefficients and it was found that the final values depended to some extent on the initial guesses. Five sets of initial guesses for rate coefficients (k_0, k_1, and k_2) were used that were separated by a factor of 10 and ranged from 10^{-3} to 10. All three coefficients had the same initial value. Twenty-five sets of initial guesses for rate coefficients of the ML-H model (k_{LH} and K) were used that varied by a factor of 10 and ranged from 10^{-3} to 10. All combinations of the five values were used to give twenty-five sets of initial guesses. The initial guesses for PCE and reductive capacity ($[RC]^o$) were fixed at 3.08 mM and 28.1 mM, respectively. The initial guess for reductive capacity was calculated as the stoichiometric amount of PCE that could be reduced to ethene by reaction with 225 mM of Fe(II). Values of rate coefficients shown in Table 4.2 are those that provided the minimum relative average absolute error.

Table 4.2 Rate coefficients of various models

exp	Reductant	Zero-order		Modified first-order		ML-H model				n
		k_0 (mM/day)	r.a.e.[a]	k_1 (day^{-1})	r.a.e.[a]	k_{LH} (day^{-1})	K (mM^{-1})	$[RC]^o$ (mM)	r.a.e.[a]	
9	Fe(II)+5%C	8.40E-2	7.13E-2	9.78E-2 (±1.59E-2)	6.69E-2	5.0E-3	5.73	22.5	4.87E-2	23
10	Fe(II)+10%C	8.06E-2	1.53E-1	0.106 (±2.43E-2)	1.31E-1	3.18E-4	11.5	320	6.59E-2	24

[a] : Relative average absolute errors (r.a.e. = average of absolute errors / average of the data), where the absolute errors are the absolute value of (data – model)

The zero-order model showed slightly higher relative average absolute errors (r.a.e.) than the other models. Because of its simplicity and reasonable ability to fit the experimental data, the modified first-order model was accepted as the primary kinetic explanation for removal of PCE DNAPL by Fe(II)+C. The ML-H model showed lower relative average absolute error, but used a greater number of coefficients than the modified first-order model. Interestingly, the reductive capacity with Fe(II)+5%C was 22.5 mM, which is close to its theoretical value (28.1 mM) for complete conversation of PCE to ethene by 225 mM Fe(II). The rate coefficients for the ML-H model with Fe(II)+10%C cannot be accepted because of an unreasonably high reductive capacity (320 mM), which is greater than the theoretical value (28.1 mM). Moreover, the modified second-order model also had a reductive capacity that was much higher than the theoretical maximum value (28.1 mM) with both Fe(II)+5%C and Fe(II)+10%C. Therefore, these values were not accepted. Comparison of the rate constants in Table 4.2 shows that the effect of cement on the rate of PCE dechlorination was negligible.

The yield of TCE produced by reduction of PCE DNAPL by various types of reductants is shown in Figure 4.9. The yields were calculated as the TCE concentration at a certain time divided by the concentration of PCE removed at that time. The value for the initial PCE DNAPL concentration used in these calculations (2.91 mM) was calculated as the average initial PCE concentration measured in 4 sets of triplicate samples (n=12).

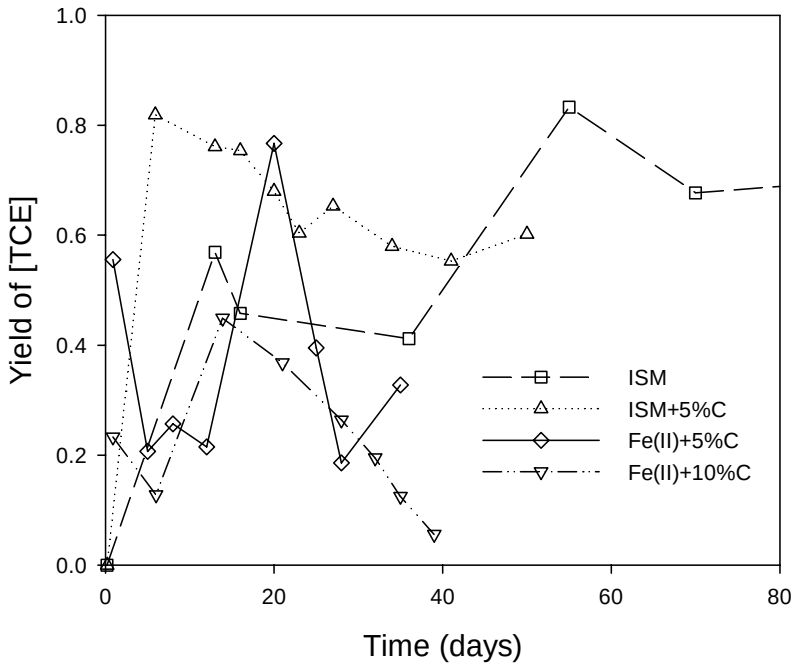

Figure 4.9 Yields of TCE from PCE DNAPL dechlorination ($[PCE]^{o}_{total}$ = 3.08 mM). [Fe(II)] = 225 mM and pH 12.

The behavior of TCE was different depending on whether ISM or Fe(II)+C were used. In systems with ISM, the yield of TCE reached 55% early in the experiment and continuously increased until 127 days. In the system with ISM+5%C, it reached 81 % at

the very beginning of PCE reduction, and slowly decreased to about 60% when PCE was almost completely reduced. On the other hand, the amounts of TCE produced with Fe(II)+C were smaller. Increasing the amount of Portland cement appeared to accelerate the reduction of TCE. For the system with Fe(II)+5%C, the TCE yield was 40 % early in the experiment, reached a maximum of 76 %, and decreased to 33 % at 40 days. The TCE yield by Fe(II)+10%C was 18 % early in the experiment, reached a maximum of 44 %, and decreased to 6 % at the end of PCE DNAPL dechlorination.

The observations on TCE yields suggest that Portland cement with ferrous iron (Fe(II)+C) was able to more efficiently degrade both the target (PCE) and its reaction intermediate (TCE). Lower levels of accumulation of TCE might occur if PCE were being reduced by β-elimination, which would not produce TCE, or if TCE were being reduced effectively by β-elimination with Fe(II)+C, which would usually accumulate no chlorinated compounds. It was reported that when lower concentrations of PCE were dechlorinated using Fe(II)+C, only transitory, trace amounts of TCE were detected and acetylene was the dominant product. This implies that the pathway for PCE dechlorination on Fe(II)+C was primarily via β-elimination (*18*). Moreover, the observation that dichloroacetylene is rapidly dechlorinated would explain why dichloroacetylene was not detected as an intermediate.

On the other hand, TCE accumulation with ISM could indicate that ISM was not as reactive as Fe(II)+C for TCE dechlorination. Moreover, TCE accumulated during relatively fast degradation of PCE with ISM+5%C. Accumulation of TCE with ISM and ISM+5%C could mean that the reductants formed by reaction of Fe(II) with cement

(Fe(II)+C) are more reactive than those formed by ISM even when cement is present. The ability of ISM to reduce PCE more rapidly and to avoid accumulation of TCE might be improved by introducing elements that are contained in cement. It has been reported that an acid-extract of cement that did not contain its major constituents (Ca, Al, and Mg) accumulated TCE to levels as high as 10 % of the initial PCE concentration (0.245 mM), while no TCE was accumulated with major constituents (*25*). This suggests that these major constituents might improve the rates of TCE removal. Calcium was present at high levels during formation of ISM, so potential improvement would be limited to addition of Al or Mg.

In addition to TCE, trace amounts of DCEs were detected by GC-MS. 1,1-DCE and/or trans/cis-DCE were detected in experiments with ISM, and trans/cis-DCE was detected in experiments with Fe(II)+C. Because only trace amounts of DCEs were detected, it could not be considered to be an important measurement. In addition, the analysis of non-chlorinated products showed that there was no significant qualitative difference in the non-chlorinated products found in experiments with different types of reductants. Non-chlorinated products of dechlorination of PCE DNAPL by both Fe(II)+C and ISM were acetylene, ethene, and ethane. Ethene was the major non-chlorinated product and more acetylene was detected at the beginning of each experiment. Moreover, production of acetylene was 2.50E-2 mM at 47 days with 789 mM of Fe(II) in ISM, while it was 3.26E-2 mM at 35 days with 225 mM Fe(II)+5%C. This might indicate that PCE was reduced with Fe(II)+C more favorably via *β*-

elimination, while the reductive pathway for PCE with ISM was a combination of hydrogenolysis and β-elimination.

4.2.3.2 The Effect of Reductant Types on TCE DNAPL Dechlorination

TCE DANPL was dechlorinated by three types of reductants (ISM, ISM+C, and Fe(II)+C). Figure 4.10 shows that TCE DNAPL was reduced effectively by Fe(II)+C, but it was not completely removed and the rate of removal appeared to be approaching zero at the end of the experiment. In addition, Portland cement doses did not affect the kinetics of dechlorination of TCE DNAPL in the same way it did for kinetics of dechlorination of PCE DNAPL. Unlike the rate of PCE DNAPL dechlorination, the rate of TCE DNAPL dechlorination was similar with ISM and ISM+C. The observation of less reactivity with ISM and ISM+C might imply that ISM could have the ability to bind TCE on non-reactive solid surfaces or could have fewer reactive sites for TCE compared to Fe(II)+C.

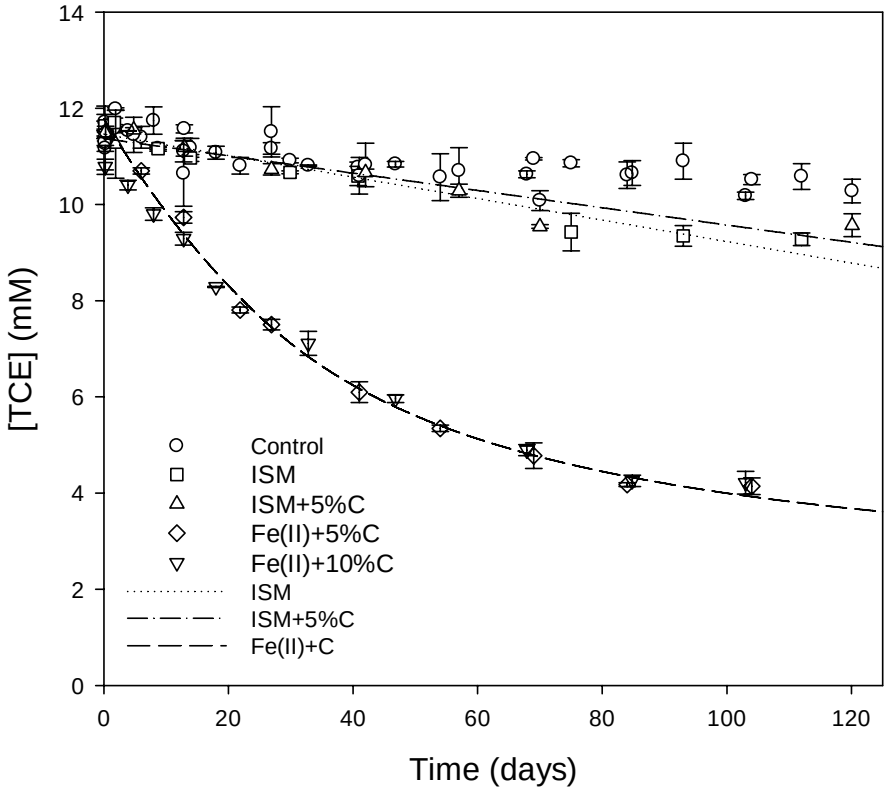

Figure 4.10 Dechlorination of TCE DNAPL ($[TCE]^{o}_{total}$ = 12.0 mM) by various types of reductants. [Fe(II)] = 225 mM, and pH 12.

The behavior of being removed fast initially and then dramatically more slowly suggests the necessity of using kinetic models like second-order or Langmuir-Hinshelwood model (L-H model) to describe kinetics of TCE removal, because they describe the effect of reductive capacity which can decrease to levels that reduce rates of dechlorination. The reductive capacity has been used to describe kinetics of reduction by natural minerals in which the target compound first adsorbs on the surface of the mineral. A modified Langmuir-Hinshelwood model has been used to describe kinetics in

such systems. The relationship between sorption coefficient (K) and aqueous target concentration in ML-H model is important to understand the kinetics of system. If K is extremely small (K <<< 1), then the rate equation for reduction becomes second-order. If K is extremely large (K >>> 1), the rate equation for reduction becomes first-order in the concentration of reductive capacity (k_{app} * [RC]). The concentration of reductive capacity changes with time, because it is being consumed by the reaction. Moreover, reductive capacity also can be used in the second-order model. The theoretical reductive capacity of 225 mM of Fe(II) would be 37.5 mM if TCE were reduced completely to ethene.

The kinetic models (zero, modified first-order, modified second-order, and modified L-H model) were tested for their ability to describe kinetics of TCE dechlorination on ISM and Fe(II)+C. To determine coefficients, non-linear regressions were conducted with the nlinfit function in MATLAB, which minimizes the sum of squares by adjusting coefficient with the Marquardt-Levenberg algorithm. Initial values for the initial concentrations of TCE DNAPL and the reductive capacity were chosen to be 12.0 mM and 37.5 mM, respectively. Initial values of rate coefficients (k_0, k_1, k_2, k_{LH}, and K) were chosen to range from 10^{-3} to 10 with each value differing by one order of magnitude. The values of coefficients calculated by nlinfit were affected by the initial values chosen, so the values of the coefficients were chosen to be those with positive values and with the minimum relative average absolute errors. Rate coefficients for TCE on ISM and ISM+C are shown in Table 4.3.

Table 4.3 The kinetic coefficients for TCE DNAPL dechlorination with ISM

		Zero-order		Modified first-order		Modified second-order				
exp	Reductants	k_0 (mM/day)	r.a.e.[a]	k_1 (day^{-1})	r.a.e.[a]	k_2 ($day^{-1}mM^{-1}$)	$[RC]^{o}$[a] (mM)	r.a.e.[a]	$\frac{[RC]^{o}}{[Fe(II)]}$	n
11	ISM	2.23E-2 (±4.80E-5)	1.72E-2	3.0E-3 (±6.0E-4)	1.72E-2	1.70E-3 (±1.70E-3)	3.27	1.17E-2	1.45E-2	27
12	ISM+5%C	1.80E-2 (±6.0E-3)	1.79E-2	2.40E-3 (±8.0E-4)	1.79E-2	1.70E-3 (±2.40E-3)	2.68	1.46E-2	1.19E-2	25

[a] : Relative average absolute errors (r.a.e. = average of absolute errors/average of the data),

The comparison of kinetic models showed that the modified second-order model was better able to describe kinetics of removal with ISM and ISM+5%C, as indicated by it having the smallest relative average absolute errors. However, the wide range of the 95 % confidence interval for the second-order rate constant indicates that the value has a large degree of uncertainty, which makes it less attractive as a representative value. The zero-order and modified first-order models showed the same relative average absolute errors. Previous research showed that a first-order rate model was appropriate for describing removal of low concentrations of TCE with Fe(II)+C [20]. Therefore, the modified first-order model had the dual advantages of being able to describe zeroth-order kinetics observed with constant aqueous concentration in the presence of DNAPL and first-order kinetics with variable dissolved concentrations in the absence of DNAPL. The rate coefficients (k_{LH} and K) in the ML-H model for TCE on ISM and ISM+C were

not tabulated because of a wide distribution of values that were calculated by the regression.

Rate coefficients for degradation of TCE with Fe(II)+C and other reductants are shown in Table 4.4. Values for the ML-H sorption coefficient (*K*) for dechlorination of TCE have been reported for some minerals (pyrite, magnetite, and green rust) and they range from 0.345 to 0.76 mM^{-1} (*22,23*). Moreover, a value for *K* of 0.003 mM^{-1} was calculated when a low concentration of TCE (0.25 mM) was degraded by mixtures of Portland cement and Fe(II) (10 to 400 mM) (*20*). These values serve as guides in choosing values of parameters to accept in the present research.

The second-order and ML-H models was described the experimental data for TCE dechlorination with Fe(II)+5%C. Moreover, because of a small value for *K* in the ML-H model, this model became equivalent to the second-order model and the product of the ML-H coefficients (k_{LH} x *K*) was equivalent to the second-order rate constant. In the calculation of the ML-H model for Fe(II)+5%C, the average value for product (k_{LH} x *K*) was 3.0E-3 (±1.18E-4) ($day^{-1}mM^{-1}$), and reductive capacity was 9.21 – 9.28 mM. Although the average absolute errors were the same for both models, the second-order model was chosen because the coefficients (k_{LH} and *K*) of ML-H were dependent upon each other.

Table 4.4 The kinetic coefficients for TCE DNAPL dechlorination

exp	Reductants	Modified second-order		Modified L-H					
		k_2 ($day^{-1}mM^{-1}$)	r.a.e.[a]	k_{LH} (day^{-1})	K (mM^{-1})	r.a.e.[a]	$[RC]^o$ (mM)	$\frac{[RC]^o}{[Fe(II)]}$	n
13	Fe(II)+5%C	3.10E-3 (±1.0E-3)	2.13E-2	0.402-46.2	6.81E-5 - 0.008	2.13E-2	9.28[b] (±1.11)	4.12E-2 (±4.93E-3)	29
14	Fe(II)+10%C	2.50E-3 (±8.0E-4)	1.53E-2	2.30E-2	1.46E+6 - 9.54E+7	1.37E-2	9.01[b] (±1.21)	4.0E-2 (±5.38E-3)	29
	pyrite[c]	N.A.	N.A.	1.59	0.345	-	0.124	8.69E-4	-
	Magnetite[d]	N.A.	N.A.	0.254	0.503	-	0.023	4.34E-4	-
	GR_SO_4[e]	N.A.	N.A.	0.9	0.76	-	0.101	2.77E-4	-
	Polished Fe[of]	N.A.	N.A.	2.03E-4	63.9	3.47E-2	5.55E+2	2.37E-2	-
	Fe(II)+10%C[g]	0.186	5.71E-2	N.A.	N.A.	N.A.	1.58[b]	3.95E-2	-

[a] : Relative average absolute errors (r.a.e. = average of absolute errors/average of the data), in which the errors represent the absolute value of (data – model)

[b] : Initial reductive capacity was calculated from the modified second-order model.

[c] : From (*22*), [TCE] = 0.25 mM and [Fe(II)] = 142.7 mM (94.8 mg Fe(II)/g pyrite * 0.084 g pyrite/g water * 1 g/mL water * 24 mL volume * 0.747 mM/mg) at pH 8

[d] : From (*22*), [TCE] = 0.25 mM and [Fe(II)] = 232.5 mM (205.9 mg Fe(II)/g pyrite * 0.063 g pyrite/g water * 1 g/mL water * 24 mL volume * 0.747 mM/mg)at pH 7

[e] : From (*23*), [TCE] = 0.25 mM and [Fe(II)] = 83.2 mM (464 mg Fe(II)/g pyrite * 0.01 g pyrite/g water * 1 g/mL water * 24 mL volume * 0.747 mM/mg)at pH 7

[f] : From (*92*), [TCE] ≈ 210 μM degraded by polished zero-valent iron at neutral pH in one of two different mixed-batch system (I). The values were calculated from regenerated data by using the ML-H model. $[RC]^o/[Fe(II)]$ was defined as the ratio of reductive capacity of zvi and the concentration of zvi used (i.e. 2.34E+7 μM when 30g of pure zvi was introduced 23 mL deionized water). Initial value for $[RC]^o$ = 7.8E+6 μM by Fe(0) reduced to Fe(II).

[g] : From (*20*), [TCE] = 0.25, [Fe(II)] = 40 mM, and the cement from different sources at pH 12.8. The values were calculated from regenerated data by using the ML-H model. Initial value for $[RC]^o$ = 6.67 mM by Fe(II) reduced to Fe(III)

TCE dechlorination on Fe(II)+10%C showed constant values of rate constant (k_{LH}) and initial reductive capacity ($[RC]^o$). Because of the large sorption coefficients (K) on Fe(II)+10%C, the dechlorination rate could be expressed by the product of k_{LH} and [RC]. It would not be possible to calculate a zero-order rate constant for Fe(II)+10%C unless the reductive capacity was unchanged. Reductive capacity was defined by the ability of reductant to remove targets, and it should change during a redox reaction that consumes the reductant. Therefore, the zeroth-order rate model was not evaluated, but the second-order model was evaluated and it was able to explain the experimental data well.

The comparison of the kinetic models showed that the modified first-order model was generally better in describing removal of TCE with ISM and the modified second-order model was better in describing removal of TCE with Fe(II)+C. The prediction line in Figure 4.10 was made by the second-order model with coefficients calculated for the experiment with Fe(II)+5%C. The good fit to the data shows that the second-order model is an appropriate model for dechlorination of TCE DNAPL by Fe(II)+C.

Moreover, Table 4.3 and Table 4.4 show the ratio of the reductive capacity to the concentration of ferrous iron ($[RC]^o$/[Fe(II)]). This dimensionless ratio was used to measure the ability of ferrous iron in a reductant to dechlorinate TCE. Values of this ratio for reductants studied in this research are two orders of magnitude higher than those for solid minerals (pyrite, magnetite, and green rust) and 1.7 factors higher than polished ZVI. The effect of cement dose (i.e. 5 % and 10 %) could be neglected. Despite the different initial concentrations of TCE (i.e. 0.25 mM and 12.0 mM), it was observed

that the ratio of reductant capacity and ferrous iron had similar values in the Fe(II)-DS/S system. Moreover, the theoretical stoichiometry shows that one mole of TCE degraded to ethene needs six moles of ferrous iron to be reduced to ferric iron. This makes a theoretical stoichiometric ratio of 0.167, which means that 10 mM of ferrous iron can remove 1.67 mM of TCE. The observed ratio in the Fe(II)-DS/S system means that 100 mM ferrous iron could remove 3.95 to 4.12 mM of TCE, whether it exists as DNAPL or not. The lower ratios observed for Fe(II)-based iron compounds (1.45E-2) indicates that they are less reactive with TCE than mixtures of Portland cement and Fe(II).

No intermediates were detected by GC-ECD in experiments with ISM and Fe+C, but DCEs (i.e. 1,1-DCE and/or 1,2-DCE) were detected by GC-MS. The aqueous sample that was extracted for analysis by GC-ECD was diluted because of the high concentrations of the target compound. This would make it more difficult to detect low concentrations of products. Headspace analysis with GC-MS was used to analyze non-chlorinated products. Ethene was the major non-chlorinated products of TCE DNAPL dechlorination detected by GC-FID, but ethane and acetylene were also detected. It has been reported that acetylene was a major product of dechlorination of lower concentrations of PCE and TCE, and that ethene was the major product of 1,1-DCE dechlorination by Fe(II)-DS/S [20]. The maximum production of acetylene with Fe(II)+5%C was 4.21E-2 mM at 104 days using an Fe(II) dose of 225 mM, and it was 3.42E-2 mM at 112 days with ISM at an Fe(II) dose of 789 mM. This might indicate that TCE degraded with Fe(II)+C followed the β-elimination pathway like PCE. Moreover, acetylene was found at a concentration of 1.53E-2 mM after 104 days of degradation by

Fe(II)+5%C with an Fe(II) dose of 80 mM. This might imply that TCE was affected by the Fe(II) doses when degraded by Fe(II)+5%C but not by cement doses, because similar rate constants were observed for cement doses of both 5 % and 10 % .

4.2.3.3 The Effect of Reductant Types on 1,1,1-TCA DNAPL Dechlorination

Experiments were conducted with an initial concentration of 1,1,1-TCA DNAPL of 11.7 mM and an initial ferrous iron concentration of 80 mM, except for one experiments to evaluate the effect of a different initial Fe(II) concentration of 20 mM. The effect of cement dose was also tested. Kinetic models were evaluated by graphical and statistical analysis of experimental data. The modified first-order model was better for ISM systems (ISM and ISM+5%C) and the modified second-order model was generally better for Fe(II)+C systems (Fe(II)+5%C and Fe(II)+10%C). Data from experiments with 1,1,1-TCA was more complicated and showed different behavior than that from experiments with chlorinated ethenes (i.e. PCE and TCE). Data from experiments with ISM are shown in Figure 4.11 (a) and they agree well with the modified first-order model. 1,1,1-TCA showed better reactivity with ISM than with ISM+5%C. Degradation of 1,1,1-TCA DNAPL by ISM was completed within a week and it was predicted that degradation of 1,1,1-TCA DNAPL by ISM+5%C would be completed within about 17 days. However, dechlorination of 1,1,1-TCA DNAPL by Fe(II)+C showed more complex behavior than that with ISM and made it more difficult to determine kinetic coefficients. Figure 4.11 (b) shows how the modified second-order model was able to describe experimental data of 1,1,1-TCA DNAPL dechlorination by

Fe(II)+C. The rate coefficients of the kinetic models were determined and the prediction line agreed well with the experimental data for Fe(II)+5%C.

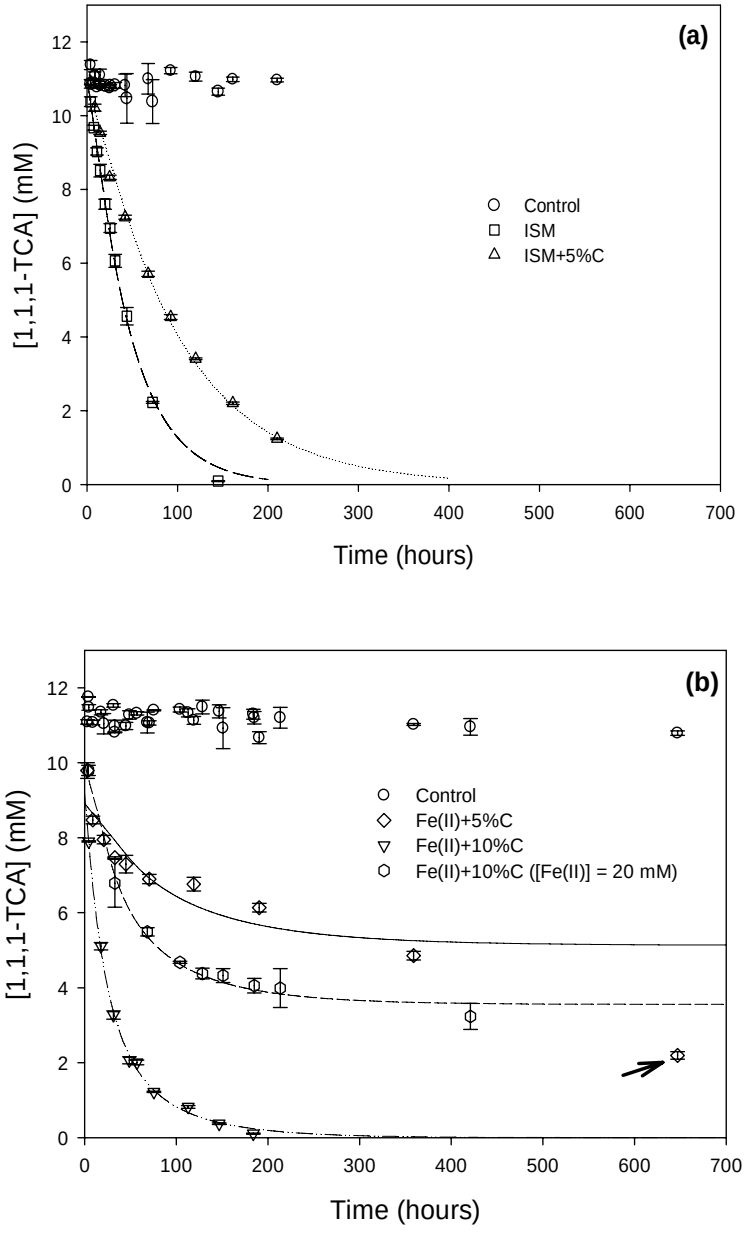

Figure 4.11 1,1,1-TCA DNAPL dechlorination by various types of reductants; a) ISM and b) Fe(II)+C with two cement doses (5%, 10%) at a Fe(II) dose of 80 mM and one cement dose (10%) at a Fe(II) dose of 20 mM.

Table 4.5 summarizes values of rate coefficients for degradation of 1,1,1-TCA. The modified first-order model was not able to accurately describe experimental data for Fe(II)+10%C, which showed rapidly decreasing concentrations at the beginning of the experiment that dramatically slowed when the concentration of 1,1,1-TCA went below 1 mM. Moreover, the modified first-order model predicted lower initial concentrations than other models. The low levels of removal at the end of the experiment indicates that there was not a sufficient amount of active reductant to degrade all of the 1,1,1-TCA.

Table 4.5 The modified first-order rate constant for 1,1,1-TCA

exp	Reductants	k_1 (hour^{-1})	$[1,1,1\text{-TCA}]^{o}_{total}$ (mM)	r.a.e.	n
15	ISM	2.24E-2 (± 1.60E-3)	11.0 (± 0.261)	1.89E-2	30
16	ISM+5%C	1.05E-2 (± 9.0E-4)	10.8 (± 0.330)	2.74E-2	29
18	Fe(II)+10%C	2.81E-2 (± 4.10E-3)	8.63 (± 0.691)	8.96E-2	29

The rate constant for 1,1,1-TCA with ISM was twice that with ISM+5%C. This might mean that cement adversely affected 1,1,1-TCA dechlorination. The lower reactivity with ISM+C might be caused by some component of cement, such as silica, (SiO_2). It has been reported that a dissolved silica concentration of 0.17 mM decreased the reactivity of granular iron for 1,1,1-TCA by 30% (*78*). It has been reported that less than 10 μg/g of dissolved silica was detected in porewater of hydrated cement at pH in the range 12 - 13 (*93*). Therefore, it is not likely that reactivity would be affected by

silica. However, ISM might react with cement hydration products in a way that changed its reactivity.

Table 4.6 shows that rate constants for 1,1,1-TCA degradation with Fe(II)+C. Various kinetic models (zero, modified first-order, modified second-order, and ML-H) were used to evaluate experiment data. A modified first-order model was chosen as provided the best fit for 1,1,1-TCA with ISM, but rate coefficients for the ML-H model were tabulated for comparisons. Generally, the modified second-order and ML-H model showed the best fits to data for degradation of 1,1,1-TCA with Fe(II)+C.

Table 4.6 Rate coefficients for degradation of 1,1,1-TCA DNAPL with Fe(II)+C

		Modified second-order			Modified L-H					
exp	Reductants	k_2 ($hour^{-1}mM^{-1}$)	$[RC]^o$ (mM)	r.a.e.	k_{LH} ($hour^{-1}$)	K (mM^{-1})	$[RC]^o$ (mM)	r.a.e.	$\frac{[RC]^o}{[Fe(II)]}$	n
17	Fe(II)+5%C	1.70E-3 (±1.70E-3)	3.96 (±1.44)	5.09E-2	4.32 - 103	1.64E-5 - 5.34E-4	3.96	5.09E-2	4.95E-2 [a] (±1.80E-2)	27 [b]
18	Fe(II)+10%C	3.20E-3 (±1.60E-3)	14.1 (±3.80)	3.97E-2	6.57E-2	0.113	10.9	3.78E-2	0.136 [c]	27
19	Fe(II)+10%C [d]	2.60E-3 (±2.0E-4)	6.82 (±0.48)	2.17E-2	6.16	4.27E-4	6.79	2.16E-2	0.341 [a] (±2.40E-2)	23
15	ISM [e]	N.A.	N.A.	N.A.	1.48E-2	1.15	14.9	5.45E-3	0.186 [c]	30

[a] : Initial reductive capacity from the modified second-order model was used.
[b] : Total number of data points was 30, but coefficients were calculated using only 27 points. The last data points were excluded.
[c] : Initial reductive capacity from the modified L-H model was used.
[d] : [Fe(II)] = 20 mM.
[e] : Coefficients were from the experiment for 11.7 mM of 1,1,1-TCA reduced by 80 mM of Fe(II) in ISM.

Rate coefficients of the modified second-order and ML-H models for 1,1,1-TCA DNAPL degradation on Fe(II)+5%C were determined. Initial values for k_2, k_{LH}, and K were chosen to range from 10^{-3} to 10 and to differ by a factor of 10. Initial values for the coefficients of the ML-H model (k_{LH} and K) were chosen to range from 10^{-3} to 10 and to differ by a factor of 10. Each value of one coefficient was paired with all of the values of the other coefficient to give 25 sets of initial values. Initial values for 1,1,1-TCA concentration and reductive capacity were 11.7 mM and 13.3 mM, respectively for 80 mM of Fe(II) doses. In addition, initial value of reductive capacity for 20 mM of Fe(II) doses was 3.33 mM. The values of the coefficients in the model were determined as those values calculated by the regression routine that had the lowest relative average absolute errors. If the lowest relative average absolute errors were similar, then the model with fewer variables was chosen. At the same time, experimental data were screened to exclude errors.

The last data point (identified by the arrow in Figure 4.11 (b)) was excluded from the regressions, because when it was included, large values for the sorption coefficient (K) (49.5 to 9.1E+7 mM^{-1}) were calculated and the model did not do well in predicting the data obtained at the beginning of the experiment. A large value of the sorption coefficient can make the denominator of the rate equation in the ML-H model (Equation 4.6) equal the solubility ($[CH]_{sol}$), which cancels the solubility in the numerator, resulting in the rate being proportional to the concentration of reductive capacity. Therefore, the observed kinetics would be first-order with respect to reductive capacity, which changes as the target compound is reduced. A second-order model was evaluated,

but it did not fit the experiment data well when all data points were used in the calibration. Therefore, the last point was excluded, because none of kinetic models (modified first, modified second, and ML-H) interpreted experiment data properly when it was included.

The products of the ML-H rate coefficients (k_{LH} and K) for Fe(II)+5%C in Table 4.6 were exactly the same as the values of the second-order rate constant (k_2). Moreover, the initial reductive capacities and relative average absolute errors were also the same in both models. The predictions of both models fit well with the experiment data. The second-order model was chosen to describe removal of 1,1,1-TCA on Fe(II)+5%C, as was done for TCE on Fe(II)+5%C. Lower relative average absolute errors were calculated when the ML-H model was used to describe data for experiments with Fe(II)+10%C using 80 mM Fe(II) than when the modified second-order model was used. Therefore, rate coefficients of the ML-H model were used for further calculations, such as calculating the ratio of $[RC]^o/[Fe(II)]$. The ML-H model had the lower relative average absolute errors with data for the experiment for 1,1,1-TCA reduced by 20 mM of Fe(II) in Fe(II)+10%C. However, the sorption coefficient of the ML-H model was relatively small, so 1/K was larger than the aqueous concentration. Therefore, the ML-H model becomes equivalent to the second-order model. The product of k_{LH} and K was 2.63E-3 ($hr^{-1}mM^{-1}$), which is close to the value of the second-order rate constant (2.60 E-3 $hr^{-1}mM^{-1}$).

Increasing doses of cement and Fe(II) tend to change the preferred kinetic model from the modified second-order model to the ML-H model. This might mean that

increasing cement and Fe(II) doses affected the surface properties of the reductant, which affected the value of the sorption coefficient in the ML-H model.

The experimental results and the kinetic analysis show that kinetics of dechlorination of 1,1,1-TCA by ISM and Fe(II)+C were complicated. Removal with ISM was best described by the modified first-order model. With Fe(II)+C, both cement and Fe(II) doses affected not only dechlorination rates, but also the best kinetic model. However, the addition of cement to ISM slowed dechlorination rates for 1,1,1-TCA DNAPL. The rate with ISM was faster than with Fe(II)+5%C and similar to rates with Fe(II)+10%C, when the same dose of Fe(II) (80 mM) was used.

Table 4.6 shows that the reductive capacity of Fe(II)+C increased by a factor of 2.8, when the cement doses increased by a factor of 2.0 (5 % to 10 %) and the same dose of ferrous iron (80 mM) was used. When the ferrous iron concentration was increased by a factor of 4.0 (20 mM to 80 mM) with the same cement dose (10 %), the reductive capacity increased by a factor of 1.6. This suggests that the dosage of cement affects the ability to produce effective reductants for 1,1,1-TCA DNAPL in the Fe(II)+C system more than the dosage of Fe(II). However, unlike chlorinated ethenes, reactivity of ISM for dechlorination of 1,1,1-TCA DNAPL was higher without cement. The rate with ISM was twice that with ISM+C (Table 4.5).

The analysis of non-chlorinated products showed that for both ISM and Fe(II)+C, ethane was the major product and ethene was a secondary product. Moreover, analysis by GC-MS detected 1,1-DCA (1,1-dichloroethane) and some of coupling products (e.g. 2-butyne) as reaction intermediates.

The effects of both ferrous iron and cement doses on dechlorination of 1,1,1-TCA DNAPL indicate that there are differences in the characteristics of ISM and Fe(II)+C or that a chlorinated ethane (i.e. 1,1,1-TCA) has a different reactivity on Fe(II)-based reductants than do chlorinated ethenes. Dechlorination of chlorinated ethenes with ISM was not as fast as with Fe(II)+C, when the same Fe(II) doses were used. Moreover, kinetics with Fe(II)+C generally were interpreted best by the second-order or the ML-H model, while kinetics with ISM were generally interpreted best by the modified first-order model.

4.2.3.4 Comparisons of Rate Coefficients for DNAPL Dechlorination

To compare rates constants among the Fe(II)+C systems in which different kinetic models were used to describe results, a corrected first-order initial rate constant (k_{app}) was calculated using rate coefficients of either the modified L-H model (equation 4.11) or the modified second-order model (equation 4.12). Moreover, these corrected first-order initial rate constants were compared with rate constants of the first-order model, which was used to describe results with ISM.

$$k_{app} \cong \frac{k_{LH} \times ([\mathrm{RC}]^{o} - ([\mathrm{CH}]^{o}_{total} - [\mathrm{CH}]_{sol}))}{1/K + [\mathrm{CH}]_{sol}} \qquad (4.11)$$

$$k_{app} \cong k_{2} \times ([\mathrm{RC}]^{o} - ([\mathrm{CH}]^{o}_{total} - [\mathrm{CH}]_{sol})) \qquad (4.12)$$

The rate coefficients for degradation of PCE, TCE and 1,1,1-DCA DNAPLs are shown in Table 4.7 for comparison. Fe(II)+5%C had higher dechlorination rate constants (k_{app}) for degradation of PCE DNAPL and TCE DNAPL than did ISM by factors of

about 7.0 and 5.0, respectively. The small effect of Portland cement dose (5 % and 10 %) on k_{app} for degradation of chlorinated ethenes by Fe(II)+C can be ignored. However, the effect of both cement and Fe(II) doses on the dechlorination rates of the chlorinated ethane (1,1,1-TCA DNAPL) was significant. Rates were observed to increase by a factor of about 8.0 when cement dose increased from 5 to 10 % and the same dose of Fe(II) (80 mM) was used. Moreover, the effect of Fe(II) dose on degradation of 1,1,1-TCA was significant with the rate increasing by a factor of about 3.0 when [Fe(II)] was increased from 20 to 80 mM in Fe(II)+10%C. The lower reactivity of TCE and 1,1,1-TCA on ISM+5%C compared to ISM shows some adverse effects of adding cement, which may be due to silica (SiO_2). Some papers have reported that dissolved silica can decrease the reactivity of granular iron for reducing chlorinated hydrocarbons (TCE and 1,1,1-TCA) (*78,94*). Because the concentration of dissolved silica in the presence of hydrated cement is low, it might not affect dechlorination rates, so no adverse effects of silica were assumed to occur.

Table 4.7 Rate coefficients of various types of targets and reductants

exp	Targets	Reductants	k_1 [a] (day^{-1})	k_{app} (day^{-1})	$[CH]^o_{total}$ (mM)	$[RC]^o$ (mM)	$\frac{[RC]^o}{[Fe(II)]}$	$t_{1/2}$ [b] (day)	n
1	[PCE] (3.08 mM)	ISM	1.41E-2 (±5.20E-3)	N.A.	2.66	2.19 [c]	9.73E-3	97.2	21
8		ISM+5%C	9.62E-2 (±8.70E-3)	N.A.	2.87	N.A.	N.A.	15.4	30
9		Fe(II)+5%C	9.78E-2 (±1.59E-2)	N.A.	2.96	22.5 [c]	0.100	15.6	23
10		Fe(II)+10%C	0.106 (±2.43E-2)	N.A.	3.05	N.A.	N.A.	14.8	24
11	[TCE] (12.0 mM)	ISM	3.0E-3 (±6.0E-4)	N.A.	11.5	3.27 [d]	1.45E-2	257	27
12		ISM+5%C	2.40E-3 (±8.0E-4)	N.A.	11.4	2.68 [d]	1.19E-2	319	25
13		Fe(II)+5%C [e]	N.A.	1.59E-2	11.6	9.28 (±1.11)	4.12E-2 (±4.93E-3)	49.0	29
14		Fe(II)+10%C [e]	N.A.	1.34E-2	11.1	9.01 (±1.21)	4.0E-2 (±5.38E-3)	55.6	29
15	[1,1,1-TCA] (11.7 mM)	ISM	0.538 (±3.84E-2)	N.A.	11.0	14.9 [c]	0.186	1.35	30
16		ISM+5%C	0.252 (±2.16E-2)	N.A.	10.8	N.A.	N.A.	2.83	29
17		Fe(II)+5%C [e]	N.A.	9.47E-2	9.21	3.96 (±1.44)	4.95E-2 (±1.80E-2)	6.43	27
18		Fe(II)+10%C [f]	N.A.	0.880	9.31	10.9	0.136	6.99E-2	27
19		Fe(II)+10%C [g]	N.A.	0.255	10.3	6.82 (±0.48)	0.340 (±2.40E-2)	2.67	23

[a] : Values in parenthesis represent 95% confidence intervals from using nlparci function in Matlab.

[b] : Half-lives calculated from $t_{1/2}$ = 0.5 x $[CH]^o_{total}$ / (k_{app} x $[CH]_{sol}$), where $[CH]^o_{total}$ is initial concentration of DNAPLs, $[CH]_{sol}$ is solubility ($[PCE]_{sol}$ = 0.97, $[TCE]_{sol}$ = 7.45, and $[1,1,1\text{-}TCA]_{sol}$ = 7.57 mM).

[c] : Reductive capacity from the ML-H model was used.

[d] : Reductive capacity from the modified second-order model was used.

[e] : The corrected first-order initial rate constants (k_{app}) and reductive capacity from the modified second-order model were used.

[f] : The corrected first-order initial rate constants and reductive capacity from the ML-H model were used.

[g] : [Fe(II)] = 20 mM. The corrected first-order initial rate constants (k_{app}), and reductive capacity from the modified second-order model were used.

The order of dechlorination rate constants (reactivity), half-life, and the ratio of the initial concentrations of reductive capacity to ferrous iron ($[RC]^o/[Fe(II)]$) were compared. ISM reduced target compounds with the order of reactivity being 1,1,1-TCA > PCE > TCE as indicated by values of k_{app}. Based on the corrected first-order initial rate constants, the order of reactivity with Fe(II)+C was 1,1,1-TCA > PCE > TCE. The order of reactivity with Fe(II)-DS/S has been reported as TCE > 1,1-DCE > PCE > VC when lower concentrations of target compounds were used (*20*). This difference between PCE and TCE in the order of reactivity might be caused by higher initial concentrations ($[PCE]^o_{total}$ = 3.08 mM and $[TCE]^o_{total}$ = 12.0 mM) used in this research. Initial degradation rates of TCE have been reported to increase linearly with increasing initial TCE concentration (below 0.5 mM) and surface saturation behavior has been found at high concentration of TCE (above 1.0 mM) (*20*). Data from the current research shows that when the ratios $[RC]^o/[Fe(II)]$ were similar, rate constants for degradation of PCE were the same in the presence and absence of DNAPL. Therefore, dechlorination rates for PCE increased linearly with the dissolved PCE concentration when PCE was reduced with Fe(II)+C at high initial concentrations. Since rates of TCE removal tend to reach a maximum at low concentrations, but rates of PCE removal continue to increase with higher initial concentrations, it is reasonable to observe a change in relative reactivity of PCE and TCE at higher initial concentrations used in this research.

The order of half-lives on ISM and Fe(II)+C were the same (TCE > PCE > 1,1,1-TCA). However, if PCE concentration were same as other the other target compounds (approximately 12.0 mM) and rate constants for PCE were constant with the same Fe(II)

doses in reductants, then the order of half-lives would change to PCE > TCE > 1,1,1-TCA. The order of $[RC]^o/[Fe(II)]$ was 1,1,1-TCA > TCE > PCE on ISM and PCE > 1,1,1-TCA > TCE on Fe(II)+5%C. If the same Fe(II) doses were used with both reductants, the order of $[RC]^o/[Fe(II)]$ might be more similar.

The ratio of initial concentrations of reductive capacity and ferrous iron ($[RC]^o/[Fe(II)]^0$) showed a somewhat different tendency for change than that of the rate constants. The theoretical reductive capacity for PCE and TCE were 28.1 mM and 37.5 mM respectively, when 225 mM of Fe(II) was used. The theoretical reductive capacities for 1,1,1-TCA were 13.3 mM and 3.33 mM, respectively, when 80 and 20 mM of Fe(II) were used.

The theoretical stoichiometry for degradation of PCE to ethene is 0.125 mole PCE/mole Fe(II) compared to the measured values of $[RC]^o/[Fe(II)]^0$ of 9.73E-3 (ISM) and 0.100 (Fe+5%C). The low values of $[RC]^o/[Fe(II)]$ for PCE DNAPL dechlorination by ISM means that most of the Fe(II) was not involved in reacting with PCE, while high values of $[RC]^o/[Fe(II)]$ on Fe(II)+5%C indicates that most of Fe(II) was reacted with PCE. The method used to form ISM in which dissolved irons were precipitated at high pH, might have converted substantial amounts of iron into compounds that were structural backbones and not able to react. This would mean that Fe(II) was more structurally incorporated into ISM than adsorbed onto its surface, because adsorbed Fe(II) is probably more reactive. It was pointed out that mechanism of reaction by sorbed Fe(II) could not be excluded because various solids existed in cement hydration (*18*). Moreover, it was reported that surface-bound Fe(II) might be the most important

factor in reductive transformations in the subsurface (*95*). The theoretical stoichiometric ratios for conversion of PCE to TCE and acetylene on 225 mM of Fe(II) were 0.5 and 0.167 mole PCE/mole Fe(II) respectively.

The theoretical stoichiometric ratio for degradation of TCE to ethene is 0.167 mole TCE/mole Fe(II). This can be compared to the measured values of $[RC]^o/[Fe(II)]^0$ of 1.45E-2 (ISM), 1.19E-2 (ISM+5%C), 4.12E-2 (Fe(II)+5%C), and 4.0E-2 (Fe+10%C). The lower values of $[RC]^o/[Fe(II)]$ were observed for TCE DNAPL on ISM, and this indicates again that Fe(II)+C reduced target compounds more effectively than ISM. The ability of the modified second-order kinetic models to describe observed results with Fe(II)+C could mean that TCE limited by surface-mediated reaction. Other possible explanations are that 1) species of ferrous iron other than sorbed or structurally incorporated might have a role in reducing TCE, or 2) other elements, possibly Al or Mg, in cement might be imbedded in solid phases and play a role as catalysts.

The theoretical stoichiometric ratio for degradation of 1,1,1-TCA to ethane is 0.167 mole PCE/mole Fe(II). The measured values of $[RC]^o/[Fe(II)]$ were 0.186 (ISM), 4.95E-2 (Fe(II)+5%C), and 0.136 (Fe(II)+10%C). Moreover, a high value of $[RC]^o/[Fe(II)]$ (0.340) was observed for degradation of 1,1,1-TCA by Fe+10%C with 20 mM Fe(II). The theoretical stoichiometric ratios for conversation of 1,1,1-TCA to 1,1-DCA and ethene are 0.5 and 0.25, respectively. Therefore, it could high value observed for $[RC]^o/[Fe(II)]$ could be due to incomplete dechlorination of 1,1,1-TCA.

4.2.3.5 Reduction Mechanisms for DNAPL Dechlorination

The experimental results showed that chlorinated ethenes (PCE DNAPL and TCE DNAPL) were transformed via a combination of the *β*-elimination and hydrogenolysis pathways using either ISM or Fe(II)+C. In particular, the accumulation of TCE from degradation of PCE DNAPL and the lower reactivity for TCE DNAPL by ISM could imply that ISM tended to reduce PCE both to dichloroacetylene (via *β*-elimination) and to TCE (via hydrogenolysis), but that it was less effective in reducing TCE. The lower effectiveness might be due to the fact that TCE was so strongly adsorbed on iron oxides that it delayed further dechlorination (*82,96*).

On the other hand, the higher reactivity for TCE DNAPL by Fe(II)+C compared to ISM could imply that Fe(II)+C reduced chlorinated ethenes (PCE and TCE) more favorably via *β*-elimination. Analysis of non-chlorinated products showed that both PCE DNAPL and TCE DNAPL produced ethene as a major product with ethane and acetylene as minor products and DCEs only in trace amounts. The lack of detection of other intermediates (i.e. VC and chloroacetylene) from degradation of TCE DNAPL on Fe(II)+C might mean that TCE DNAPL was transformed via *β*-elimination with little hydrogenolysis. The product of TCE degradation via *β*-elimination would be chloroacetylene, which would not accumulate because it is rapidly converted to acetylene. In contrast, the major products of TCE degradation via hydrogenolysis would be DCEs and VC, which would accumulate because they are degraded relatively slowly (*18,20,82*). Moreover, it was reported that TCE dechlorination by elemental iron mainly followed the *β*-elimination pathway and dechlorination of chlorinated ethenes (PCE and

TCE) in Fe(II)-DS/S system followed the β-elimination pathway because of high recovery of acetylene (about 80 %) as a major product (*6,20*). In both ISM and Fe(II)+C, the initial production of acetylene followed by production of ethene might show that hydrogenation of acetylene was occurring. Similarly, the ethane that was detected might have been formed by hydrogenation of ethene.

It might be also possible that ISM converted PCE no farther than to TCE, because it lost its reactivity, because of low ratio of $[RC]^o/[Fe(II)]$. Column tests of TCE reduction by granular iron have shown that the iron surface was observed to be deactivated as the columns aged (*94*). The slow reduction of TCE with ISM could support this possibility. Moreover, degradation of both PCE DNAPL and TCE DNAPL produced acetylene. This indicates that ISM could follow the same reductive pathways as Fe(II)+C.

A chlorinated ethane (1,1,1-TCA DNAPL) was transformed via hydrogenolysis to 1,1-DCA and ethane as a major products with both ISM and Fe(II)+C. No 1,1-DCE was detected by any GC analysis indicating that hydrodechlorination was not important. Moreover, ethene was detected and could have formed via one electron transfer with rearrangement. Unidentified coupling products were detected and could have formed via coupling followed by β-elimination.

These results imply that the initial stage of transformation of chlorinated ethenes was more likely via both β-elimination and hydrogenolysis, while it was via hydrogenolysis for the chlorinated ethane. Several authors have reported mechanisms of transformation of chlorinated hydrocarbons and they have been correlated by linear free

energy relationship (LFER) and experiment data analysis. One study examined the electrochemical reduction of chlorinated ethenes (PCE, TCE, and DCE isomers (trans-DCE, cis-DCE, and 1,1-DCE)) and ethanes (pentachloroethane (PCA), tetrachloroethane isomers (1,1,1,2-TeCA and 1,1,2,2-TeCA), 1,1,1-TCA and 1,1,2-TCA) using a porous nickel cathode. This study showed that the predictions of kinetics of dechlorination of chlorinated ethenes based on bond enthalpy calculations based on ethane were not accurate. Therefore, it was suggested that the transformation mechanisms for chlorinated ethenes and ethanes were different. It concluded that the predominant reaction pathways for both chlorinated ethenes and chlorinated ethanes (e.g. 1,1,1-TCA) were sequential hydrogenolysis, while polychlorinated ethanes (e.g. PCA and TeCAs) were mainly transformed via elimination (*74*). On the other hand in Fe(II)-DS/S, it was reported that low concentrations of chlorinated ethenes (i.e. PCE and TCE) were transformed through β-elimination and that chlorinated ethanes, especially 1,1,1-TCA, were transformed predominantly through hydrogenolysis (*18,20,21*).

Dechlorination rates of PCE and TCE with ISM were slower than with Fe(II)+C. 1,1,1-TCA showed similar reactivity with ISM and with Fe(II)+10%C. The ratios of $[RC]^o/[Fe(II)]$ observed with ISM and with Fe(II)+C support the higher reactivity for PCE and TCE observed with Fe(II)+C. Moreover, the ratio of $[RC]^o/[Fe(II)]$ with ISM also showed that there are similar amounts of active Fe(II) for reaction with 1,1,1-TCA in solids of Fe(II)+10%C. Analysis of non-chlorinated products indicated that chlorinated ethenes (PCE and TCE) are mainly degraded with Fe(II)+C via *β*-elimination, because there was less accumulation of TCE and more production of

acetylene. Lower production of DCEs also supports this pathway for them. The reductive pathway for degradation of PCE and TCE with ISM was a combination of hydrogenolysis and β-elimination. Dechlorination of 1,1,1-TCA with both ISM and Fe(II)+C appears to be via hydrogenolysis.

4.2.4 Discussion

Experimental results show that the reductant synthesized with ferrous iron as a major element could reduce chlorinated hydrocarbons (PCE, TCE, and 1,1,1-TCA) existing as DNAPLs. Mainly two types of reductants (ISM and Fe(II)+C) were tested to determine their ability to dechlorinate DNAPLs. The chemical form of the active reductant in each system has not been clearly identified. With this difficulty of identification, experiments on dechlorination of low concentrations of PCE (0.24 mM) suggest that: 1) the major elements that increased reactivity were Fe(II), Fe(III), Cl, and Ca in the Fe(II)+C system; 2) the iron complexes synthesized without cement were difficult to identify by XRD due to their amorphous state, (previously, the synthesis of iron compounds without cement produced solids that were identified as ferrous hydroxides by XRD analysis); and, 3) the formation procedure for solid reductants can be an important factor in determining their characteristics as active reducing agents (*25*). However, the experimental results from this research showed that chlorinated ethenes (i.e. PCE and TCE DNAPL) were dechlorinated effectively by Fe(II)+C. and that a chlorinated ethane (i.e. 1,1,1-TCA DNAPL) was dechlorinated as well by ISM as by Fe(II)+C when the same dose of Fe(II) was used.

Previously, results with ISM were presented that increasing the concentration of ferrous iron leads to increased rates of dechlorination of 3.08 mM PCE DNAPL. The kinetics was well explained by a first-order model, which was a mathematical interpretation of the reaction conditions with and without a NAPL phase. Despite the reactivity of ISM for PCE DNAPL dechlorination, the addition of cement was observed to increase rates of dechlorination. Unlike dechlorination of PCE DNAPL, dechlorination of TCE DNAPL showed that modified second-order model with reductive capacity interpreted the experimental data more precisely. This was observed more clearly when TCE DNAPL was dechlorinated by Fe(II)+C.

A small increase in reactivities for PCE and its product (TCE) were observed when cement dose was changed from 5 % to 10 % with Fe(II)+C. This might imply that trace elements in cement could have a role in forming active reductants that contain Fe(II). However, adding cement to ISM did not facilitate dechlorination of TCE DNAPL, while it did improve reactivity toward PCE DNAPL. This reduced effect of cement addition in ISM is consistent with the observation of increased yield of TCE (i.e. intermediate) from PCE DNAPL dechlorination with both ISM and ISM+5%C. Moreover, the increased reactivity for PCE resulting from the addition of cement to ISM could indicate the inability of PCE to sorb on non-reactive sites.

On the other hand, 1,1,1-TCA DNAPL dechlorination behaved differently. With the same dose of Fe(II) (80 mM), ISM reduced 1,1,1-TCA DNAPL as completely as did Fe(II)+10%C. However, kinetics of removal by ISM were interpreted by the first-order mechanism and those of Fe(II)+C were complicated, which generally interpreted with

the modified second-order, but 80 mM of Fe(II) in Fe(II)+10%C interpreted well with the ML-H model. In experiments with Fe(II)+C, 1,1,1-TCA DNAPL was dechlorinated rapidly at first and then more slowly and finally seemed to reach equilibrium. Both cement and Fe(II) doses accelerated 1,1,1-TCA DNAPL dechlorination in the Fe(II)+C system, but the existence of cement in the ISM system reduced the dechlorination rates compared to ISM itself.

Because of the heterogeneity of the cement itself and of its hydration products, the assumption that there are several different active reducing agents is reasonable. In addition to that, ISM might need other elements, such as Al or Mg to dechlorinate intermediates/products effectively. The incorporation of other elements, such as Al or Mg, into solids formed in ISM could increase its reactivity to that of Fe(II)+C. It has been suggested that the active reducing agents in Fe(II)-DS/S are forms of LDH. Other elements, such as Al or Mg, might rearrange the structure of LDHs to change the width of interlayer or to enlarge or breaks the structure of the LDHs resulting in formation of more surfaces that can support reactions. Similarly, the reduction of structural Fe in Fe-rich smectites electronically disordered the crystal structure and, as a result, shifted electron density distribution of sorbed chlorinated hydrocarbons in a way that promoted their reaction via radical pathways (*97*). If this were to happen in a low crystallinity or amorphous structure, it could increase the reactivity of ISM for chlorinated hydrocarbons. Another possible explanation is the core/shell model of catalyst involvement. This model describes a system where the core is Fe^0 and the shell is an iron oxide with an embedded catalyst (Ni or Pd). In this system, the Fe^0 core donates

electrons, which travel through the iron oxide/catalyst shell to reduce adsorbed TCE (*96,98*). Unfortunately, the present experiment data cannot be used to verify this model.

These results raised again questions about whether: 1) the reductant synthesized from each system had similar reactivity; and, 2) the reduction of chlorinated ethenes (i.e. PCE and TCE) had different reductive transformation mechanisms than the chlorinated ethane (i.e. 1,1,1-TCA). The experimental data, including intermediate/product analysis, suggest that chlorinated ethenes are transformed via both β-elimination and hydrogenolysis pathways and that the chlorinated ethane is likely transformed via hydrogenolysis by the Fe(II)-based reductants studied in this research. Moreover, rate constants and the ratio of $[RC]^o/[Fe(II)]$ could indicate that the reductant synthesized from each system (i.e. ISM and Fe(II)+C) had different reactivity. Fe(II)+C shows better reactivity for chlorinated ethenes (PCE and TCE) than ISM and they show similar rates for 1,1,1-TCA, when the same concentration of Fe(II) are used.

4.3 DNAPL Mixture Dechlorination by ISM and Fe(II)+C

Dechlorination of a DNAPL mixture by ISM and Fe(II)+C was investigated. The DNAPL mixture contained PCE (12.2 mM), TCE (12.0 mM), and 1,1,1-TCA (11.7 mM), and was adjusted to pH 12. Experimental and analytical procedures were the same as described previously, except for the extraction procedure. A kinetic model was developed to interpret interactions between DNAPLs.

4.3.1 Adjustment of Experimental Systems Containing DNAPL Mixture

The extraction procedure was modified in order to obtain good extraction efficiency. The concentrations in the aqueous phase were determined by introducing 20 μL of aqueous sample into 1 mL of hexane. This volume ratio was chosen in order to achieve better extraction efficiency for all of three targets. After removing an appropriate volume of water to make space in the reaction vials for the extractant, 5 mL of hexane and 5 mL of methanol were added to extract target compounds from the aqueous and non-aqueous phases. After extraction, 25 μL of extractant was diluted with 10 mL of hexane before analysis to reduce the concentrations to levels that are easier to analyze. Standard curves for the target compounds (PCE, TCE, and 1,1,1-TCA) were prepared and they showed a high degree of linearity ($r^2 > 0.998$).

The effective solubility of a compound in a non-aqueous mixture is expressed as its water solubility multiplied by its mole fraction in the non-aqueous phase (Raoult's Law). Although the relative concentrations of target compounds in the DNAPL mixture might change over time, the mole fractions of each target compound were calculated using initial concentrations. Therefore, the theoretical effective solubility of PCE, TCE,

and 1,1,1-TCA in the DNAPL mixtures were calculated as 0.330 mM (0.971 x 0.340), 2.49 mM (7.45 x 0.334), and 2.47 mM (7.57 x 0.326), respectively.

4.3.2 Modification of Competitive Adsorption Model for DNAPL Mixture

Previously, various kinetic models (zero-order, first-order, second-order, and ML-H model) were used to explain removal of individual target compounds present as DNAPL. However, a competitive adsorption model is needed to describe the possibility of competition of different target compounds for the same active sites. The competitive model is derived with following assumptions: 1) chlorinated hydrocarbons (A, B, and C) are adsorbed on available surface sites ([≡S]); and 2) the adsorption reactions are at equilibrium. This analysis uses the concept of the total surface site concentration, which is defined as the concentration of surface sites that are bound with chlorinated hydrocarbons plus those that are not bound. Equation 4.13 through 4.15 describes the sorption and desorption reactions that are assumed at equilibrium, and Equation 4.16 through 4.18 results from equating the forward and reverse rates of the reactions.

$$[\equiv S] + [A] \underset{k_{r,a}}{\overset{k_{f,a}}{\leftrightarrow}} [\equiv S - A] \tag{4.13}$$

$$[\equiv S] + [B] \underset{k_{r,b}}{\overset{k_{f,b}}{\leftrightarrow}} [\equiv S - B] \tag{4.14}$$

$$[\equiv S] + [C] \underset{k_{r,c}}{\overset{k_{f,c}}{\leftrightarrow}} [\equiv S - C] \tag{4.15}$$

where, [A], [B], and [C] are concentrations in solution of a chlorinated hydrocarbon, [≡S] is the concentration of available surface sites, [≡S-A], [≡S-B], and [≡S-C] are the concentration of each compound adsorbed onto the surface, $k_{f,a}$, $k_{f,b}$, and

$k_{f,c}$ are rate constants for the adsorption reactions of compounds, and $k_{r,a}$, $k_{r,a}$, and $k_{r,a}$ are rate constants for the desorption reaction of compounds.

Equations 4.16 through 4.18 result from assuming equilibrium and equating the forward and reverse rates of the reactions.

$$[\equiv \mathrm{S} - \mathrm{A}] = \frac{k_{f,a}}{k_{r,a}}[\equiv \mathrm{S}][\mathrm{A}] \qquad (4.16)$$

$$[\equiv \mathrm{S} - \mathrm{B}] = \frac{k_{f,b}}{k_{r,b}}[\equiv \mathrm{S}][\mathrm{B}] \qquad (4.17)$$

$$[\equiv \mathrm{S} - \mathrm{C}] = \frac{k_{f,c}}{k_{r,c}}[\equiv \mathrm{S}][\mathrm{C}] \qquad (4.18)$$

Equation 4.19 is a balance on concentrations of surface sites, where $[\equiv S]_T$ is the total concentration of surface sites.

$$[\equiv S] = [\equiv S]_T - [\equiv S - A] - [\equiv S - B] - [\equiv S - C] \qquad (4.19)$$

Algebraic manipulation of Equation 4.16 and substitution into equations 4.17 and 4.18 results in equation 4.20 and 4.21.

$$[\equiv \mathrm{S} - \mathrm{B}] = \frac{\frac{k_{f,b}}{k_{r,b}}[\mathrm{B}]}{\frac{k_{f,a}}{k_{r,a}}[\mathrm{A}]}[\equiv \mathrm{S} - \mathrm{A}] \qquad (4.20)$$

$$[\equiv \mathrm{S} - \mathrm{C}] = \frac{\frac{k_{f,c}}{k_{r,c}}[\mathrm{C}]}{\frac{k_{f,a}}{k_{r,a}}[\mathrm{A}]}[\equiv \mathrm{S} - \mathrm{A}] \qquad (4.21)$$

[≡S-B] in equation 4.20 and [≡S-C] in equation 4.21 can be substituted into equation 4.19, and the result can be used to substitute for [≡S] in equation 4.16. Then, equation 4.16 becomes equation 4.22.

$$[\equiv \mathrm{S}-\mathrm{A}] = \frac{k_{f,a}}{k_{r,a}}[\mathrm{A}]([\equiv \mathrm{S}]_T - [\equiv \mathrm{S}-\mathrm{A}] - \frac{\frac{k_{f,b}}{k_{r,b}}[\mathrm{B}]}{\frac{k_{f,a}}{k_{r,a}}[\mathrm{A}]}[\equiv \mathrm{S}-\mathrm{A}] - \frac{\frac{k_{f,c}}{k_{r,c}}[\mathrm{C}]}{\frac{k_{f,a}}{k_{r,a}}[\mathrm{A}]}[\equiv \mathrm{S}-\mathrm{A}]) \tag{4.22}$$

This can be used to develop a simple relationship for surface site concentrations as functions of concentrations.

$$[\equiv \mathrm{S}-\mathrm{A}] = \frac{[\equiv \mathrm{S}]_T K_a[\mathrm{A}]}{1 + K_a[\mathrm{A}] + K_b[\mathrm{B}] + K_c[\mathrm{C}]} \tag{4.23}$$

$$K_a = \frac{k_{f,a}}{k_{r,a}}, K_b = \frac{k_{f,b}}{k_{r,b}}, K_c = \frac{k_{f,c}}{k_{r,c}}$$

Equation 4.23 can be rearranged and generalized to give equation of 4.24.

$$q_i = \frac{Q_{o,i} K_i [\mathrm{CH}_i]}{1 + \sum_{j=1}^{n} K_j [\mathrm{CH}_j]} \tag{4.24}$$

where, q_i is the concentration of the i^{th} compound adsorbed on the surface, $Q_{o,i}$ is maximum adsorption capacity of the i^{th} compound, K is sorption coefficient for the i^{th} compound, n is number of chlorinated hydrocarbons, and subscripts i and j represent different types of chlorinated hydrocarbons.

Equation of 4.24 can be used to describe rates of degradation that are assumed to be first-order in the surface concentration. Then, the overall rate equation is,

$$\gamma_i = -k_i q_i = -\frac{k_i Q_{oi} K_i [\mathrm{CH}_i]}{1 + \sum_{j=1}^{n} K_j [\mathrm{CH}_j]} = -\frac{k_{max,i} K_i [\mathrm{CH}_i]}{1 + \sum_{j=1}^{n} K_j [\mathrm{CH}_j]} \qquad (4.25)$$

where, k_i is pseudo-first-order rate constant for the reduction of a chlorinated hydrocarbon, and k_{max} is product of the rate constant (k_i) and the maximum adsorption capacity ($Q_{o,i}$).

Finally, this rate equation can be modified by the assumption that the concentrations in solution are constant and equal to the solubility whenever the DNAPL is present.

$$\gamma_i = \frac{d[\mathrm{CH}_i]_{total}}{dt} = -\frac{k_{max,i}[\mathrm{CH}_i]_{eff.sol}}{1/K_i + \sum_{j=1}^{n} \frac{K_j}{K_i} [\mathrm{CH}_j]_{eff.sol}} \qquad \text{if } [\mathrm{CH}_i]_{total} \geq [\mathrm{CH}_i]_{eff.sol} \qquad (4.26)$$

$$\gamma_i = \frac{d[\mathrm{CH}_i]_{total}}{dt} = -\frac{k_{max,i}[\mathrm{CH}_i]_{total}}{1/K_i + \sum_{j=1}^{n} \frac{K_j}{K_i} [\mathrm{CH}_j]_{total}} \qquad \text{if } [\mathrm{CH}_i]_{total} < [\mathrm{CH}_i]_{eff.sol} \qquad (4.27)$$

$[\mathrm{CH}_i]_{total}$ is total concentration of i^{th} compounds in aqueous and non-aqueous phase, and $[\mathrm{CH}_i]_{eff.sol}$ is the effective solubility of i^{th} compounds. If the sum of product of adsorption constants (K) and concentration are very small ($\sum K \cdot [\mathrm{CH}_i] <<< 1$), then the model equations (4.26 and 4.27) could be converted to the first-order model. [82].

Moreover, this Langmuir-Hinshelwood model can be adapted to a system in which the solid phase acts as a reactant, not as a catalyst. This can be done by assuming that when a reaction occurs at a site, it is no longer able to react. Therefore, the number of sites that are initially present and available for adsorption would become the number of sites that can react with the target compound and reduce it. With this assumption, the

maximum adsorption capacity can be replaced with the reductive capacity. The reductive capacity is defined as a maximum concentration of target compound that could be reduced by the reductant surface.

$$k_{max,i} = k_i[\mathrm{RC}_i] \tag{4.28}$$

where, k_i is pseudo-first-order rate constant for the reduction of the i^{th} compound, and $[\mathrm{RC}_i]$ is concentration of available reductive capacity for the i^{th} compound. Then, concentration of available reductive capacity at any time can be calculated from the definition of reductive capacity.

$$[\mathrm{RC}_i] = [\mathrm{RC}_i]^o - ([\mathrm{CH}_i]^o_{total} - [\mathrm{CH}_i]_{total}) \tag{4.29}$$

where, $[\mathrm{RC}_i]^o$ is initial reductive capacity for the i^{th} compound, $[\mathrm{CH}_i]_{total}$ and $[\mathrm{CH}_i]^o_{total}$ are total concentrations of the i^{th} compound in both the aqueous and non-aqueous phases at any time and at time equal to zero, respectively.

If it is assumed that the reaction occurs at same sites, then the total initial reductive capacity ($[\mathrm{RC}]^o_{sum}$) is the sum of each initial reductive capacity.

$$[\mathrm{RC}]^o_{sum} = \sum_{i=1}^{n} [\mathrm{RC}_i]^o \tag{4.30}$$

4.3.3 Experimental Results

Dechlorination of target compounds (PCE, TCE, and 1,1,1-TCA) present as a DNAPL mixture were tested using two types of reductants (ISM and Fe(II)+C) that contained 225 mM of Fe(II). All appropriate models (zero, modified first-order, modified second, or ML-H model) were evaluated for their ability to describe removal of each target compound and then the competitive adsorption model was evaluated if necessary.

The solubility in DNAPL mixture was determined. At the beginning of reaction with DNAPL mixture, the solubilities for three targets could be the calculated effective solubility (0.330 mM for PCE, 2.49 mM for TCE, and 2.47 mM for 1,1,1-TCA). Therefore, using calculated solubility for 1,1,1-TCA was accepted. However, because 1,1,1-TCA was dechlorinated rapidly, the equilibrium concentration of PCE and TCE could not be equaled to those calculated solubilities. The measured average chlorinated hydrocarbon concentrations in aqueous phase with both reductants were 0.474 (± 0.281) mM for PCE (n=57) and 2.60 (± 0.467) mM for TCE (n=60). The higher measured aqueous concentrations for both PCE and TCE (0.474 mM for PCE, 2.60 mM for TCE) than the calculated solubilities (0.330 mM for PCE, 2.46 mM for TCE) imply that mole fractions change in system due to fast disappearance of 1,1,1-TCA. The calculated solubilities for binary DNAPL system are 0.489 (0.971 x 0.504) mM for PCE and 3.70 (7.45 x 0.496) mM, respectively. The lower measured aqueous concentrations than the calculated solubilities for binary DNAPL system (0.489 mM for PCE, 3.70 mM for

TCE) might indicate that there were reaction intermediates in system, and they reduced activities of targets in solution.

Therefore, the measured average aqueous concentrations of the target compounds in the aqueous phase were used as the effective solubility for PCE and TCE (0.474 mM and 2.60 mM, respectively). The calculated solubility (2.47 mM) was used for 1,1,1-TCA.

4.3.3.1 The Effects of Reductant Types on Dechlorination of DNAPL Mixture

Figure 4.12 shows that the DNAPL mixture was dechlorinated by both ISM and Fe(II)+5%C. The average recovery of controls were 91.4 +/- 3.3 % for PCE (n=20), 93.4 +/- 2.8 % for TCE (n=20), and 93.3 +/- 2.9 % for 1,1,1-TCA (n=20). The range is given as a relative standard deviation. Data for controls are not shown in Figure 4.12 because of they overlapped with sample data. Filled symbols in Figure 4.12 represent data from the experiment conducted with ISM and empty symbols represent data from the experiment conducted with Fe(II)+C. Circles represent PCE; triangles represent TCE; and squares represent 1,1,1-TCA. The lines are predictions made by the modified first-order kinetic model.

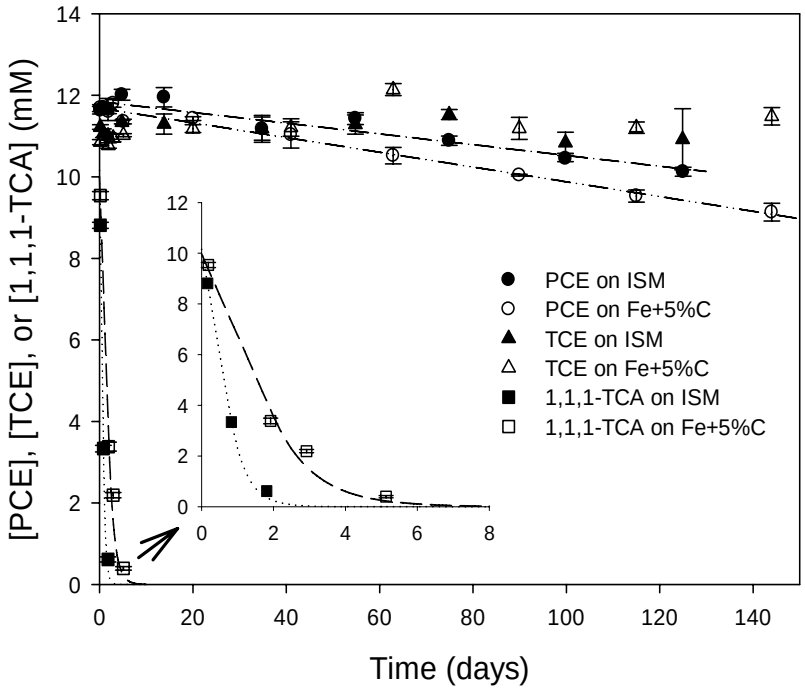

Figure 4.12 The dechlorination of DNAPL mixture by ISM and Fe(II)+5%C.

Figure 4.12 shows that 1,1,1-TCA DNAPL was removed relatively very rapidly with both ISM and Fe(II)+5%C compared to removal of chlorinated ethenes (PCE and TCE). Moreover, the dechlorination rate of 1,1,1-TCA on ISM was faster than with Fe(II)+5%C. PCE was reduced more rapidly using Fe(II)+5%C than with ISM. These observations agree with previous experiments conducted with the individual target compounds. Because TCE was reduced relatively well by Fe(II)+5%C compared to ISM in experiments where it was the only target compound, it was expected that TCE would be reduced by Fe(II)+5%C in the DNAPL mixture. However, the TCE in DNAPL mixtures was maintained at its initial concentration in both ISM and Fe(II)+5%C with

slightly up and down from the steadiness. This resistance of TCE to degradation might be explained by either the exhaustion of reductant ability or by balance between the rates of production and removal of TCE. It could be possible that TCE was reduced on reductant at the same rate that it was produced from PCE dechlorination.

PCE reduction to ethene requires 8 moles of Fe(II) per mole of PCE. Reduction of TCE to ethene requires 6 mole of Fe(II) per mole of TCE. and reduction of 1,1,1-TCA to ethane requires 6 mole of Fe(II) per mole of 1,1,1-TCA. Therefore, 240 mM of Fe(II) would be enough to stoichiometrically reduce all of the target compounds. However, a dose of 225 mM of [Fe(II)] was used in these experiments in order to be comparable with previous experiments.

The order of reactivity on ISM was observed to be 1,1,1-TCA > PCE > TCE in experiments with individual target compounds. This order was the same whether reactivity was measured by half-life or $[RC]^o/[Fe(II)]$. The modified first-order model usually did well in correlating experimental data obtained with ISM.

On the other hand, the order of reactivity measured by half-life with Fe(II)+5%C was 1,1,1-TCA > PCE > TCE, while the order of reactivity measured by $[RC]^o/[Fe(II)]$ was PCE > 1,1,1-TCA > TCE. The kinetics of dechlorination was more complicated on Fe(II)+5%C. The modified second-order model best described removal of 1,1,1-TCA and TCE and the modified first-order model best described removal of PCE. Even though the best kinetic model was chosen based on its ability to best predict observed data, coefficients of the ML-H model were calculated for previous results when

necessary. Rate coefficients for each target compound in the DNAPL mixture were calculated for both ISM and Fe(II)+5%C.

4.3.3.2 Interpretation of Rate Coefficients for Targets in DNAPL Mixture

First, the rate constants and the average relative errors for dechlorination 1,1,1-TCA DNAPL in the DNAPL mixture were calculated for ISM (n=9) and Fe(II)+5%C (n=12). The concentration of Fe(II) was 80 mM for experiments with 1,1,1-TCA by itself and was 225 mM for experiments with the DNAPL mixture. Solubility was 7.57 mM for both individual and 2.47 mM for DNAPL mixture. Rate coefficients for 1,1,1-TCA in both individual and DNAPL mixture are shown in Table 4.8. Because the modified first-order model was described experimental data for 1,1,1-TCA with ISM, the modified first-order model was applied to targets in DNAPL mixture, and as the same manner, the modified second-order model was used for Fe(II)+5%C. Moreover, the corrected first-order initial rate constants are also tabulated.

Table 4.8 Rate coefficients for 1,1,1-TCA as an individual and mixture

exp	Reductants	Other DNAPLs	$[CH]_{sol}$ (mM)	k_{app} [a] (day^{-1})	Modified first-order		Modified second-order			n
					k_1 (day^{-1})	r.a.e.	k_2 ($day^{-1}mM^{-1}$)	$[RC]^o$ (mM)	r.a.e.	
15	ISM	None	7.57	N.A.	0.538 (± 3.84E-2)	1.89E-2	N.A.	N.A.	N.A.	30
20		PCE, TCE	2.47	N.A.	1.53	1.59E-2	N.A.	N.A.	N.A.	9
17	Fe(II)+5%C	None	7.57	9.47E-2	N.A.	N.A.	4.08E-2 (4.08E-2)	3.96 (±1.44)	5.09E-2	27
21		PCE, TCE	2.47	0.723	N.A.	N.A.	0.182	12.0	5.35E-2	12

[a] : The corrected first-order initial rate constants was calculated from the modified second-order model

The increase in the corrected rate constants for the DNAPL mixture compared to the individual DNAPL was mainly caused by the increase in Fe(II) doses. To compare reductive capacity of both reductants, the experiment data for 1,1,1-TCA with ISM was predicted by the ML-H model. Reductive capacity for individual and DNAPL mixture were 14.9 mM and 11.8 mM, respectively. The higher reductive capacity on ISM compared to Fe(II)+5%C indicates that a greater fraction of Fe(II) in ISM was converted to an effective reductant than in Fe(II)+5%C for 1,1,1-TCA dechlorination.

Rate constants of PCE as individual and DNAPL mixture were evaluated. The modified first-order rate constants for PCE removal from the DNAPL mixture are compared to those obtained in experiments with only PCE in Table 4.9. This table includes values of rate constants, relative average absolute error (r.a.e.), and solubility. The initial concentration of Fe(II) was 225 mM. The initial concentration of PCE in experiments without other target compounds was 3.08 mM, while the initial concentration of PCE in experiments with other target compounds was 12.2 mM.

Table 4.9 Rate coefficients for degradation of PCE as individual and DNAPL mixture

exp	Reductants	Other DNAPLs	$[CH]_{sol}$ (mM)	k_1 (day^{-1})	$k_{Fe(II)}$ ($day^{-1}mM^{-1}$)	$t_{1/2}$ (days)	r.a.e.	n
1	ISM	None	0.971	1.41E-2 (±5.20E-3)	6.27E-5	97.1	6.30E-2	21
20		TCE, 1,1,1-TCA	0.474	2.75E-2 (±7.60E-3)	1.22E-4	453	1.53E-2	29
9	Fe(II)+5%C	None	0.971	9.78E-2 (±1.59E-2)	4.35E-4	15.6	6.69E-2	23
21		TCE, 1,1,1-TCA	0.474	3.77E-2 (±3.60E-3)	1.68E-4	327	7.59E-3	27

Results in Table 4.9 show that rate constants for PCE degradation by ISM in the DNAPL mixture were higher than when PCE was the only target. However, the reverse was observed in experiments with Fe(II)+5%C. There are several differences in the two sets of experiments that might explain the different results, including the initial concentration of target compound, presence of other target compounds and the value assumed for the solubility.

Rate constants for each reductant were not affected by the initial concentration of DNAPL. Data exists from previous studies that can be used to evaluate the effect of initial concentration of PCE on kinetics. It was reported previously that the dechlorination rates were not affected by changes in the initial concentrations of PCE (0.245 mM and 0.483 mM) when different iron sources (i.e. $FeCl_2$ and $FeSO_4$) were used with Fe(II)-DS/S (*71*). Furthermore, the rate constants for target compounds removed by ISM have been observed to be constant in this research when the same Fe(II) doses are used. Therefore, it is not likely that the initial concentration of PCE is the cause for the difference in rate constants between experiments with individual target compounds and the mixture.

The existence and behavior of other DNAPLs might affect dechlorination rate of each targets in DNAPL mixture compared to individual DNAPL. The increasing PCE dechlorination rates by ISM in DNAPL mixture compared to the experiment for single PCE DNAPL could suggest the enhancement of rate constants by the existence of other DNAPL. Previous research has shown that the presence of non-reactive hydrophobic hydrocarbons (i.e. benzene, toluene, and *m*-xylene) increased PCE reduction (*99*). It was

suggested that displacement of PCE from the sorption sites by the aromatic hydrocarbons enhanced dechlorination rates (*99*). This might be applicable to the condition in experiments with the DNAPL mixture when other target compounds could enhance the dechlorination rates of PCE, especially by 1,1,1-TCA. This could be due to the faster reacting compound releasing chloride ions that promote production of additional active reductants. As shown in Figure 4.12, 1,1,1-TCA was reduced very rapidly, so it could change the condition of system by changing the chemical composition both in the solution and on the surfaces of the solid reductants. As 1,1,1-TCA is dechlorinated, the concentration of chloride ion would increase in solution, and more Fe(III) could be produced by the oxidation of Fe(II). At the same time, Fe(II) that was not involved with dechlorination and existed inactive form, might react with chloride and Fe(III) and be converted into an active form of Fe(II). This production of additional reductant with similar compositions of ISM (i.e. also iron complexes of Fe(II), Fe(III), and Cl) could increase the reactivity of ISM. This might explain the observation that the rate constant in the DNAPL mixture was twice that in the individual DNAPL.

The decreasing PCE degradation rates by Fe(II)+5%C in DNAPL mixture compared to the individual DNAPL suggests that PCE dechlorination on Fe(II)+C was limited by the surface-mediated reaction. Observed first-order rate constants have been reported to decrease with increasing concentration of targets, and this was suggested as evidence for surface-mediated reactions that are being limited by saturation of reactive sites (*82,99*). Moreover, it was reported that PCE and TCE affected each other's dechlorination rates on ZVI [99]. In the presence of TCE, PCE dechlorination on ZVI

decreased by 30 %. The tabulated rate constant for PCE on Fe(II)+5%C in the presence of other chlorinated compounds decreased by 39 % compared to the rate constant for PCE by itself. Therefore, the slower rate constants for PCE in the DNAPL mixture might be caused by competition with other chlorinated compounds. It could also be caused by, the loss of reductant reactivity due to reaction with more reactive chlorinated hydrocarbons such as 1,1,1-TCA. The fact that PCE behaved differently when being dechlorination by ISM and Fe(II)+5%C in DNAPL mixtures suggests that these reductant types have different reactivity with types of targets.

Rate constants in the different experiments including the effect of solubility were compared. The rate constant for PCE in the DNAPL mixture with ISM increased by a factor of 2 compared to experiments with individual DNAPL. The solubility of PCE was estimated in the experiments with DNAPL mixture to have a value that was lower by a factor of 2. In contrast, the rate constant for PCE in the DNAPL mixture with Fe(II)+C decreased by a factor of 2.6 when the estimated solubility decreased by a factor of 2. This indicates that even though the rate constants changed in value, the rates were nearly constant, because the rates would equal the product of the rate constant and the estimated solubility (equation 4.31).

$$k_{app,1} \times [\mathrm{PCE}]_{sol,1} \approx k_{app,2} \times [\mathrm{PCE}]_{sol,2} \qquad (4.31)$$

where, k_{app} is the first-order rate constant for PCE dechlorination, $[\mathrm{PCE}]_{sol}$ is the solubility, and subscript 1 and 2 represent different total concentrations of PCE.

Therefore, solubility can be an important factor in interpreting kinetics when DNAPL is present. The products of rate constants and solubility for experiments with

individual DNAPLs and the DNAPL mixture with ISM were 1.37E-2 mM/day and 1.30E-2 mM/day, respectively. However, the product of rate constants and solubility for individual and DNAPL mixture with Fe(II)+5%C were 9.50E-2 mM/day and 1.79E-2 mM/day.

The reactivity for some targets with ISM might be enhanced by dechlorination of other targets, such as 1,1,1-TCA, which is ranked as having a higher reactivity with ISM. The order of reactivity for PCE and 1,1,1-TCA in the DNAPL mixture was the same as that for the individual DNAPLs, which was 1,1,1-TCA > PCE > TCE. On the other hand, the results for degradation of 1,1,1-TCA and PCE with Fe(II)+C in the DNAPL mixture showed different behavior from ISM. The rate of PCE dechlorination decreased in experiments with the DNAPL mixture compared to with individual DNAPL. This might be caused by having lower concentrations of active reductant, because of consumption by reaction with 1,1,1-TCA. The order of reactivity in DNAPL mixture was 1,1,1-TCA > PCE > TCE, which was the same as in the individual DNAPL experiments.

Behavior of TCE in the DNAPL mixture can be interpreted by the balance between the rates of production and removal of TCE. Little change in the concentration of TCE was observed, which could indicate that it was not being reduced or that its rate of removal equaled its rate of production. A zero reduction rate for TCE dechlorination might occur if its degradation were inhibited by competition with PCE for the same reactive sites. It has been reported that TCE is reduced by a surface-mediated reaction, because initial dechlorination rates were first-order at low concentrations (below 1.0 mM

of TCE), but became zero-order at higher concentrations (from 1.0 mM to 2 mM of TCE) (*20*). In addition, it was reported that the presence of PCE could decrease TCE sorption and dechlorination by 33 % and 30 %, respectively (*99*). This competition might reduce dechlorination rates of PCE and TCE because they were both dechlorinated relatively rapidly with Fe(II)+C.

The observation of a constant concentration of TCE in the DNAPL mixture does not preclude the possibility that TCE was being dechlorinated. The maximum yields of TCE from PCE dechlorination in experiments that began with only PCE present were about 40 % of the PCE that was removed. Therefore, some of the PCE removed in the DNAPL mixture could have been converted to TCE, and the constant TCE concentration could be due to TCE dechlorination at very low rates or by a balance between production and removal. For example, TCE could be produced approximately 4.84 mM if the production of TCE were 40 % of initial PCE DNAPL. It was shown that TCE was reduced from 12 to 4 mM when 225 mM of Fe(II) in Fe(II)+5%C was used. If 30 % of decreases of TCE dechlorination were applied, then approximately 5.6 mM of TCE is reduced in DNAPL mixture. Moreover, because of fast dechlorination of 1,1,1-TCA, the reactivity of reductant could be reduced somewhat. Therefore, the balance between production and removal could be assumed as equal. The low rates of removal could be caused by low concentrations of reductant due to the competition between chlorinated hydrocarbons.

Overall, rates of 1,1,1-TCA dechlorination on both ISM and Fe(II)+5%C were very fast compared to those of other targets (PCE and TCE). Because of this fast

dechlorination, it was assumed that 1,1,1-TCA did not compete with PCE or TCE. Even though some of reductant was consumed by 1,1,1-TCA, there was increase in the rate constant for PCE dechlorination on ISM. The enhancement of reductant reactivity was suggested to be due to the production of reactive Fe(II)-complexes that are possibly similar to ISM. These reactive complexes, are proposed to be formed from Fe(II), Fe(III) produced by the oxidation of Fe(II), and chloride ion produced by dechlorination. Formation of the reactive Fe(II) complexes would increase the amount of reductant available to dechlorinate PCE and that would increase PCE dechlorination rates.

However, PCE dechlorination rates decreased in the DNAPL mixture compared to the individual DNAPL when Fe(II)+5%C was the reductant. This might be caused by the consumption of reductant by dechlorination of 1,1,1-TCA dechlorination. It was reported that the reactivity of ISM was very weak for TCE dechlorination, and TCE dechlorination rates on Fe(II)+C was relatively fast. The relatively constant concentration of TCE could be caused by reduction of TCE at very slow rates. These results indicate that ISM and Fe(II)+5%C have different reactivity for chlorinated hydrocarbons.

CHAPTER V

SUMMARY AND CONCLUSION

Chlorinated hydrocarbons such as PCE, TCE, and 1,1,1-TCA, are one of the main sources of sub-surface contamination, especially when they are present as dense non-aqueous phase liquids (DNAPL). DNAPLs continuously dissolve to contaminate large volumes of groundwater, and the residual DNAPL is difficult to remove from soils with low permeability. This requires the effective remediation technology that removes the sources (DNAPL) in order to prevent future contamination. Iron-based degradative solidification/stabilization (Fe(II)-DS/S) can meet this requirement. Fe(II)-DS/S uses immobilization of contaminants by S/S to allow sufficient time for contaminant destruction by reductive dechlorination. Substantial research has been conducted on the ability of Fe(II)-DS/S to remove various chlorinated hydrocarbons at concentrations below their solubilities, and the results provoke the need to evaluate Fe(II)-DS/S as a method for treating DNAPL. Moreover, mixtures of solids that contain ferrous iron but not cement can act as reductants and they need to be evaluated and compared to conventional Fe(II)-DS/S for the removal of individual DNAPL and mixtures of DNAPLs. Three chlorinated hydrocarbons (PCE, TCE, and 1,1,1-TCA) were examined at concentrations above their solubilities with two reductants. One reductant was an iron solid mixture (ISM) and the other was a mixture of Fe(II) with Portland cement (Fe(II)+C).

First, an effective experimental and analytical procedure was designed in order to deal with high concentrations of chlorinated hydrocarbons. A gas-chromatographic analysis procedure was adjusted to achieve reasonably low method detection limits (MDLs) for measuring targets and their degradation products. The synthesis method for ISM was reviewed and components of ISM (Fe(II), Fe(III), and Cl) were chosen to achieve high reactivity for PCE degradation, based on results from previous research. $Ca(OH)_2$ was used for replacement of Portland cement as the method for maintaining high pH. The synthesis of the reductants occurred in an anaerobic chamber and all experimental procedures were developed to prevent contact with oxygen.

Target compounds were extracted before analysis by gas chromatography. The effectiveness of the extraction procedure was evaluated and modified to achieve high extraction efficiency for target compounds present as DNAPLs. The extraction procedure was designed to measure concentrations of targets in each phase (aqueous, non-aqueous). The addition of methanol along with hexane was necessary to achieve high extraction efficiency when solids were present. A three-point screening test was conducted to estimate the value of rate coefficients so that sampling times could be chosen to maximize the utility of data obtained during kinetic experiments. The pH in all experiments was fixed at pH 12.

Second, the effects of PCE concentrations (3.08, 6.16, 8.62, and 12.3 mM) and Fe(II) concentration in ISM (225, 424, 660, and 789 mM) on degradation kinetics were evaluated in a series of kinetic experiments. The reactivity of ISM for PCE dechlorination was close to that of Friedel's salt. The kinetics of dechlorination of PCE

present as DNAPL was observed to be zeroth-order with respect to the total PCE concentration (aqueous and non-aqueous phases) and first-order with respect to the concentration in the aqueous phase, which as approximately constant when DNAPL was present. These kinetics were described by a modified first-order model that was able to fit experimental data well. There was little effect on rate constants of total initial concentration of PCE, because the concentration of PCE in the aqueous phase remained nearly constant at the solubility. Increasing the concentration of Fe(II) in ISM increased the values of the rate constants. The half-life increased with increasing total PCE concentrations. The apparent solubility of PCE was affected by the Fe(II) doses in ISM.

The major detected intermediate of PCE degradation was TCE. The high yields of TCE with ISM indicated that ISM could have different characteristics than Fe(II)+C, because TCE was detected only in trace amounts when PCE was degraded with Fe(II)+C at low PCE concentration. DCEs (1,1-DCE and trans/cis-DCE) were also detected in trace amounts. The major non-chlorinated product was ethene, but acetylene and ethane were detected in trace amounts. The product analysis showed that ISM degraded PCE via a combination of the hydrogenolysis and β-elimination pathways. The suggested reductive pathway of PCE as DNAPL on ISM was PCE→ TCE → chloroacetylene → acetylene → ethene.

Third, experiments to evaluate the effects of types of targets (PCE, TCE, and 1,1,1-TCA) and types of reductants (ISM, ISM+C, and Fe(II)+C) on dechlorination kinetics were conducted. ISM+C is a mixture of ISM and cement. The initial concentrations of PCE (3.08 mM) and of Fe(II) in reductants (225 mM) were fixed in all

experiments. The effect of Portland cement doses (5% and 10%) was also tested. The modified first-order kinetic model was able to describe PCE dechlorination with both ISM and Fe(II)+C. The reactivity of PCE with Fe(II)+C was much higher than with ISM. The addition of cement was critical to promoting dechlorination of PCE DNAPL, but the cement doses did not affect the PCE dechlorination rates. Because of rapid dechlorination of TCE and greater production of acetylene, β-elimination appeared to be the favored pathway with Fe(II)+C.

Kinetic experiments were conducted with TCE DNAPL at an initial concentration of 12.0 mM using reductants with initial Fe(II) concentration of 225 mM. Data for TCE dechlorination with ISM were fitted best by a modified first-order kinetic model. However, data for dechlorination of TCE with Fe(II)+C were fitted best by a modified second-order model in which the concentration of reductive capacity was included in the rate equation. The reactivity of TCE DNAPL with Fe(II)+C was higher than with ISM. The results of TCE Dechlorination on ISM+C indicated that cement had adverse impact on TCE DNAPL dechlorination with ISM. The dosage of cement in Fe(II)+C did not affect TCE dechlorination. The production of more non-chlorinated products could indicate that the Fe(II) doses affected TCE dechlorination. The products analysis for TCE dechlorination showed that a trace amount of DCEs was detected, and non-chlorinated products were ethene as a major, ethane and acetylene as minor products. More acetylene production could suggest that TCE was reduced with Fe(II)+C via β-elimination as the major reductive pathway.

Experiments were conducted to evaluate degradation of 1,1,1-TCA DNAPL at 11.7 mM with three types of reductant, each containing 80 mM of Fe(II). The effects of cement and Fe(II) doses were also evaluated. Interestingly, ISM could dechlorinate 1,1,1-TCA DNAPL as well as Fe(II)+10%C. The modified first-order model interpreted data for 1,1,1-TCA dechlorination with ISM. Predictions of the modified second-order and modified Langmuir-Hinshelwood model (ML-H model) agreed well with data obtained with Fe(II)+C. The increase doses of cement and Fe(II) affected the dechlorination rates. Like TCE DANPL with ISM+C, the effect of cement in ISM showed an adverse impact on degradation of 1,1,1-TCA. The products analysis showed that ethene and ethane were major products, with trace amounts of 1,1-DCA and 2-butyne detected. The reductive pathways for 1,1,1-TCA DNAPL appear to be mainly hydrogenolysis, with some one-electron transfer and coupling.

Generally, chlorinated ethenes (PCE and TCE) were reduced faster with Fe(II)+C than with ISM. The ratio of initial reductive capacity to initial concentration of Fe(II) ($[RC]^o/[Fe(II)]^o$) confirmed that Fe(II) in Fe(II)+C had greater reductive capacity than Fe(II) in ISM. Rate coefficients for chlorinated ethane (1,1,1-TCA) showed that ISM could dechlorinate as fast as Fe(II)+10%C. The effects of cement doses (5% and 10%) for chlorinated ethenes could be ignored with Fe(II)+C. However, increasing cement doses in Fe(II)+C increased rates of 1,1,1-TCA dechlorination. The addition of cement to ISM to form ISM+C reduced its reactivity for TCE and 1,1,1-TCA compared to ISM. Especially, it was noted that ISM had lower reactivity for TCE than for the other target compounds (PCE and 1,1,1-TCA).

Finally, experiments were conducted with a mixture of DNAPLs (PCE, TCE, and 1,1,1-TCA) and two reductants (ISM and Fe(II)+5%C). The measured effective solubility was used to interpret kinetics in experiments with the DNAPL mixture. The order of dechlorination rates for compounds in the DNAPL mixture followed the order of reactivity for them as individual DNAPLs with both reductants (1,1,1-TCA > PCE > TCE). The concentration of TCE was nearly constant and this could be due to it not being degraded or being degraded as rapidly as it were produced from PCE degradation.

ISM and Fe(II)+C showed different reactivity for dechlorination of chlorinated hydrocarbons. The ratio of $[RC]^o/[Fe(II)]^o$ indicated that Fe(II) in Fe(II)+C was more involved in dechlorination than Fe(II) in ISM. Dechlorination of chlorinated ethenes with Fe(II)+C was mainly via β-elimination, and ISM was via a combination of hydrogenolysis and β-elimination. Dechlorination of a chlorinated ethane (1,1,1-TCA) with ISM indicates that ISM dechlorinated 1,1,1-TCA via hydrogenolysis.

LITERATURE CITED

(1) Doherty, R. E. A history of the production and use of carbon tetrachloride, tetrachloroethylene, trichloroethylene and 1,1,1-trichloroethane in the United States: part 1 - historical background; carbon tetrachloride and tetrachloroethylene, *Environ. Forensics* **2000**, *1*, 69-81.

(2) Doherty, R. E. A history of the production and use of carbon tetrachloride, tetrachloroethylene, trichloroethylene and 1,1,1-trichloroethane in the United States: part 2 - trichloroethylene and 1,1,1-trichloroethane, *Environ. Forensics* **2000**, *1*, 83-93.

(3) Fay, R. M.; Mumtaz, M. M. Development of a priority list of chemical mixtures occurring at 1188 hazardous waste sites, using the HazDat database, *Food Chem. Toxicol.* **1996**, *34*, 1163-1165.

(4) Albanese, R. A.; Banks, H. T.; Evans, M. V.; Potter, L. K. Physiologically based pharmacokinetic models for the transport of trichloroetylene in adipose tissue, *B. Math. Biol.* **2002**, *64*, 97-131.

(5) McClure, P. *Interaction Profile for: 1,1,1-Trichloroethane, 1,1-Dichloroethane, Trichloroethylene, and Tetrachloroethylene* U.S. Department of Health and Human Services, Public Health Service, Agency for Toxic Substances and Disease Registry 2004.

(6) Lampron, K. J.; Chiu, P. C.; Cha, D. K. Reductive dehalogenation of chlorinated ethenes with elemental iron: the role of microorganisms, *Water Res.* **2001**, *35*, 3077-3084.

(7) Brahma, P. P.; Harmon, T. C. The effect of multicomponent diffusion on NAPL dissolution from spherical ternary mixtures, *J. Contam. Hydrol.* **2003**, *67*, 43-60.

(8) Bradford, S. A.; Rathfelder, K. M.; Lang, J.; Abriola, L. M. Entrapment and dissolution of DNAPLs in heterogeneous porous media, *J. Contam. Hydrol.* **2003**, *67*, 133-157.

(9) Fennelly, J. P.; Roberts, A. L. Reaction of 1,1,1-trichloroethane with zero-valent metals and bimetallic reductants, *Environ. Sci. Technol.* **1998**, *32*, 1980-1988.

(10) Lagrega, M. D.; Buckingham, P. L.; Evans, J. C.; Environmental Resources Management *Hazardous Waste Management*; McGraw-Hill: New York, 2001.

(11) Gillham, R. W.; Ohannesin, S. F. Enhanced degradation of halogenated aliphatics by zero-valent iron, *Ground Water* **1994**, *32*, 958-967.

(12) Schlicker, O.; Ebert, M.; Fruth, M.; Weidner, M.; Wust, W.; Dahmke, A. Degradation of TCE with iron: the role of competing chromate and nitrate reduction, *Ground Water* **2000**, *38*, 403-409.

(13) Kober, R.; Schlicker, O.; Ebert, M.; Dahmke, A. Degradation of chlorinated ethylenes by Fe-0: inhibition processes and mineral precipitation, *Environ. Geol.* **2002**, *41*, 644-652.

(14) U.S.EPA *Evaluation of Technologies for In-Situ Cleanup of DNAPL Contaminated Sites*, EPA/600/R-94/120, Office of Research and Development, Robert S. Kerr Environmental Research Laboratory, Washington, DC, 1994.

(15) Batchelor, B.; Hapka, A. M.; G.J., I.; Jensen, R. H.; McDevitt, M. F.; Schultz, D.; Whang, J. M. *Method for Remediating Contaminated Soils* U.S. Patent 5,789,649 U.S. Patent Office, Washington, DC, 1998.

(16) Batchelor, B.; Hapka, A. M.; G.J., I.; Jensen, R. H.; McDevitt, M. F.; Schultz, D.; Whang, J. M. *Method for Remediating Contaminated Soils* US Patent 6,492,572 B2 U.S. Patent Office, Washington, DC, 2002.

(17) Hwang, I.; Batchelor, B. Reductive dechlorination of tetrachloroethylene in soils by Fe(II)-based degradative solidification/stabilization, *Environ. Sci. Technol.* **2001**, *35*, 3792-3797.

(18) Hwang, I.; Batchelor, B. Reductive dechlorination of tetrachloroethylene by Fe(II) in cement slurries, *Environ. Sci. Technol.* **2000**, *34*, 5017-5022.

(19) Hwang, I.; Batchelor, B. Reductive dechlorination of chlorinated methanes in cement slurries containing Fe(II), *Chemosphere* **2002**, *48*, 1019-1027.

(20) Hwang, I.; Park, H. J.; Kang, W. H.; Park, J. Y. Reactivity of Fe(II)/cement systems in dechlorinating chlorinated ethylenes, *J. Hazard. Mater.* **2005**, *118*, 103-111.

(21) Jung, B. Ph.D. Dissertation, Department of Civil Engineering, Texas A&M University, College Station, TX, 2005.

(22) Lee, W.; Batchelor, B. Abiotic reductive dechlorination of chlorinated ethylenes by iron-bearing soil minerals: 1. pyrite and magnetite, *Environ. Sci. Technol.* **2002**, *36*, 5147-5154.

(23) Lee, W.; Batchelor, B. Abiotic, reductive dechlorination of chlorinated ethylenes by iron-bearing soil minerals: 2. green rust, *Environ. Sci. Technol.* **2002**, *36*, 5348-5354.

(24) Lee, W. J.; Batchelor, B. Abiotic reductive dechlorination of chlorinated ethylenes by iron-bearing phyllosilicates, *Chemosphere* **2004**, *56*, 999-1009.

(25) Ko, S. B. Ph.D. Dissertation, Department of Civil Engineering, Texas A&M University, College Station, TX, 2005.

(26) Erbs, M.; Hansen, H. C. B.; Olsen, C. E. Reductive dechlorination of carbon tetrachloride using iron(II) iron(III) hydroxide sulfate (green rust), *Environ. Sci. Technol.* **1999**, *33*, 307-311.

(27) Lee, W.; Batchelor, B. Abiotic reductive dechlorination of chlorinated ethylenes by soil, *Chemosphere* **2004**, *55*, 705-713.

(28) U.S.EPA "Evaluation of the likelihood of DNAPL presence at NPL sites: national results", EPA/540/R-95/073, Office of Solid Waste and Emergency Responce, 1993.

(29) Fountain, J. C. "Technologies for dense nonaqueous phase liquid source zone remediation", TE-98-02, Ground-Water Remediation Technologies Analysis Center, 1998.

(30) Stegemann, J. A.; Caldwell, R. J.; Shi, C. Variability of field solidified waste, *J. Hazard. Mater.* **1997**, *52*, 335-348.

(31) Conner, J. R. *Chemical fixation and solidification of hazardous wastes*; Van Nostrand, Reinhold: New York, 1990.

(32) Kohn, T.; Roberts, A. L. The effect of silica on the degradation of organohalides in granular iron columns, *J. Contam. Hydrol.* **2006**, *83*, 70-88.

(33) O'Loughlin, E. J.; Kelly, S. D.; kemner, K. M.; Csencsits, R.; Cook, R. E. Reduction of Ag(I), Au(III), Cu(II), and Hg(II) by Fe(II)/Fe(III) hydroxysulfate green rust, *Chemosphere* **2003**, *53*, 437-446.

(34) Double, D. D. New developments in understanding the chemistry of cement hydration, *Phil. Trans. R. Soc. Lond.* **1983**, *A 310*, 53-66.

(35) Lothenbach, B.; Winnefeld, F. Themodynamic modeling of the hydration of Portland cement, *Cement Concrete Res.* **2006**, *36*, 209-226.

(36) Taylor, H. F. W. *Cement Chemistry*; Academic Press: New York, 1990.

(37) Csizmadia, J.; Balazs, G.; Tamas, F. D. Chloride ion binding capacity of aluminoferrites, *Cement Concrete Res.* **2001**, *31*, 577-588.

(38) Matschei, T.; Lothenbach, B.; Glasser, F. P. The AFm phase in Portland cement, *Cement Concrete Res.* **2007**, *37*, 118-130.

(39) Glasser, F. P.; Kindness, A.; Stronach, S. A. Stability and solubility relationships in AFm phases; part I. chloride, sulfate and hydroxide, *Cement Concrete Res.* **1999**, *29*, 861-866.

(40) Emanuelson, A.; Hansen, S. Distribution of iron among ferrite hydrates, *Cement Concrete Res.* **1997**, *27*, 1167-1177.

(41) Carrado, K. A.; Kostapapas, A.; Suib, S. L. Layered double hydroxides (LDHs), *Solid State Ionics* **1988**, *26*, 77-86.

(42) Gehin, A.; Ruby, C.; Abdelmoula, M.; Benali, O.; Ghanbaja, J.; Refait, P.; Genin, J.-M. R. Synthesis of Fe(II-III) hydroxysulphate green rust by coprecipitation, *Solid State Sci.* **2002**, *4*, 61-66.

(43) Sagoe-Crentsil, K. K.; Glasser, F. P. "Green rust," iron solubility and the role of chloride in the corrosion of steel at high pH, *Cement Concrete Res.* **1993**, *23*, 785-791.

(44) L.Raki; J.J.Beaudoin; L.Mitchell Layered double hydroxide-like materials: nanocomposites for use in concrete, *Cement Concrete Res.* **2004**, *34*, 1717-1724.

(45) Bravo-Suarez, J. J.; Paez-Mozo, E. A.; Oyama, S. T. Models for the estimation of thermodynamic properties of layered double hydroxides: application to the study of their anion exchange characterisitcs, *Quim. Nova.* **2004**, *27*, 574-581.

(46) Refait, P.; Charton, A.; Genin, J.-M. R. Identification, composition, thermodynamic and structural properties of a pyroaurite-like iron(II)-iron(III) hydroxy-oxalate green rust, *Eur. J. Sol. State Inor.* **1998**, *35*, 655-666.

(47) Genin, J.-M. R.; Ruby, C. Anion and cation distributions in Fe(II-III) hydroxysalt green rusts from XRD and Mossbauer analysis (carbonate, chloride, sulphate, ...); the "fougerite" mineral, *Solid State Sci.* **2004**, *6*, 705-718.

(48) Delagrave, A.; Marchand, J.; Ollivier, J.-P.; Julien, S.; Hazrati, K. Chloride binding capacity of various hydrated cement paste systems, *Advn. Cem. Bas. Mat.* **1997**, *6*, 28-35.

(49) Suryavanshi, A. K.; Scantlebury, J. D.; Lyon, S. B. Mechanism of Friedel's salt formation in cements rich in tri-calcium aluminate, *Cement Concrete Res.* **1996**, *26*, 717-727.

(50) Birnin-Yauri, U. A.; Glasser, F. P. Friedel's salt, Ca2Al(OH)6(Cl,OH)2H2O: its solid solutions and their role in chloride binding, *Cement Concrete Res.* **1998**, *28*, 1713-1723.

(51) Fortune, J. M.; Coey, J. M. D. Hydration products of calcium aluminoferrite, *Cement Concrete Res.* **1983**, *13*, 696-702.

(52) Liang, T.; Nanru, Y. Hydration products of clacium aluminoferrite in the presence of gypsum, *Cement Concrete Res.* **1994**, *24*, 150-158.

(53) Glasser, F. P. Mineralogical aspects of cement in radioactive waste disposal, *Mineral. Mag.* **Oct. 2001**, *65*, 621-633.

(54) Refait, P.; Benali, O.; Abdelmoula, M.; Genin, J.-M. R. Formation of 'ferric green rust' and/or ferrihydrite by fast oxidation of iron (II-III) hydroxychloride green rust, *Corros. Sci.* **2003**, *45*, 2435-2449.

(55) Refait, P.; Gehin, A.; Abdelmoula, M.; Genin, J.-M. R. Coprecipitation thermodynamics of iron (II-III) hydroxysulphate green rust from Fe(II) and Fe(III) salts, *Corros. Sci.* **2003**, *45*, 659-676.

(56) Genin, J.-M. R.; Refait, P.; Bourrie, G.; Abdelmoula, M.; Trolard, F. Structure and stability of the Fe(II)-Fe(III) green rust "fougerite" mineral and its potential for reducing pollutants in soil solutions, *Appl. Geochem.* **2001**, *16*, 559-570.

(57) Genin, J. M. R.; Bourrie, G.; Trolard, F.; Abdelmoula, M.; Jaffrezic, A.; Refait, P.; Maitre, V.; Humbert, B.; Herbillon, A. Thermodynamic equilibria in aqueous suspensions of synthetic and natural Fe(II)-Fe(III) green rusts: occurrences of the mineral in Hydromorphic soils, *Environ. Sci. Technol.* **1998**, *32*, 1058-1068.

(58) Ruby, C.; Gehin, A.; R.Aissa; Genin, J.-M. R. Mass-balance and Eh-pH diagrams of FeII-III green rust in aqueous sulphated solution, *Corros. Sci.* **2006**, *48*, 3824-3837.

(59) Refait, P. H.; Abdelmoula, M.; Genin, J. M. R. Mechanisms of formation and structure of green rust one in aqueous corrosion of iron in the presence of chloride ions, *Corros. Sci.* **1998**, *40*, 1547-1560.

(60) Refait, P.; Genin, J.-M. R. The mechanisms of oxidation of ferrous hydroxychloride beta-Fe2(OH)3Cl in aqueous solution: the formation of akaganeite vs goethite, *Corros. Sci.* **1996**, *39*, 539-553.

(61) O'Loughlin, E. J.; Kemner, K. M.; Burris, D. R. Effects of Ag, Au, and Cu on the reductive dechlorination of carbon tetrachloride by green rust, *Environ. Sci. Technol.* **2003**, *37*, 2905-2912.

(62) Myneni, S. C. B.; Tokunaga, T. K.; Jr., G. E. B. Abiotic selenium redox transformations in the presence of Fe(II,III) oxides, *Science* **1997**, *278*, 1106-1109.

(63) Loyaux-Lawniczak, S.; refait, P.; Ehrhardt, J.-J.; Lecomte, P.; Genin, J.-M. R. Trapping of Cr by formation of ferrihydrite during the reduction of chromate ions by Fe(II)-Fe(III) hydroxysalt green rust, *Environ. Sci. Technol.* **2000**, *34*, 438-443.

(64) Hansen, H. C. B.; Koch, C. B.; Krogh, H. N.; Borggaard, O. K.; Sorensen, J. Abiotic nitrate reduction to ammonium: key role of green rust, *Environ. Sci. Technol.* **1996**, *30*, 2053-2056.

(65) Son, S. Ph.D. Dissertation, Department of Civil Engineering, Texas A&M University, College Station, TX, 2002.

(66) Choi, J. Y. Ph.D. Dissertation, Department of Civil Engineering, Texas A&M University, College Station, TX, 2005.

(67) Ritter, K.; Odziemkowski, M. S.; Gillham, R. W. An in situ study of the role of surface films on granular iron in the permeable iron wall technology, *J. Contam. Hydrol.* **2002**, *55*, 87-111.

(68) O'Loughlin, E. J.; Kelly, S. D.; Cook, R. E.; Csencsits, R.; Kemner, K. M. Reduction of uranium(VI) by mixed iron(II)/iron(III) hydroxide (green rust): formation of UO2 nanoparticles, *Environ. Sci. Technol.* **2003**, *37*, 721-727.

(69) Schwarzenbach, R. P.; Gschwend, P. M.; Imboden, D. M. *Environmental Organic Chemistry*; John Wiley & Sons, Inc.: New York, 1993.

(70) Vogel, T. M.; Criddle, C. S.; McCarty, P. L. Transformation of halogenated aliphatic compounds, *Environ. Sci. Technol.* **1987**, *21*, 722-736.

(71) Hwang, I. Ph.D. Dissertation, Department of Civil Engineering, Texas A&M University, College Station, TX, 2000.

(72) Jeffers, P. M.; Ward, L. M.; Woytowitch, L. M.; Wolfe, N. L. Homogeneous hydrolysis rate constants for selected chlorinated methanes, ethanes, ethenes, and propanes, *Environ. Sci. Technol.* **1989**, *23*, 965-969.

(73) Cooper, W. J.; Mehran, M.; Riusech, D. J.; Joens, J. A. Abiotic transformations of halogenated organics. 1. elimination reaction of 1,1,2,2-tetrachloroethane and formation of 1,1,2-trichloroethene, *Environ. Sci. Technol.* **1987**, *21*, 1112-1114.

(74) Liu, Z.; Betterton, E. A.; Arnold, R. G. Electrolytic reduction of low molecular weight chlorinated aliphatic compounds: structural and thermodynamic effects on process kinetics, *Environ. Sci. Technol.* **2000**, *34*, 804-811.

(75) Cervini-Silva, J. Linear free-energy relationship analysis of the fate of chlorinated 1- and 2-carbon compounds by redox-manipulated smectite clay minerals, *Environ. Toxicol. Chem.* **2003**, *22*, 2298-2305.

(76) Jeffers, P. M.; Wolfe, N. L. Homogeneous hydrolysis rate constants - part II: additions, corrections and halogen effects, *Environ. Toxicol. Chem.* **1996**, *15*, 1066-1070.

(77) Wolfe, N. L.; Jeffers, P. M. "Transformations of halogenated hydrocarbons: hydrolysis and redox processes", EPA/600/M-89/032, Environmental Reseach Laboratory, Athens, GA., 1990.

(78) Kohn, T.; Kane, S. R.; Fairbrother, D. H.; Roberts, A. L. Investigation of the inhibitory effect of silica on the degradation of 1,1,1-trichloroethane by granular iron, *Environ. Sci. Technol.* **2003**, *37*, 5806-5812.

(79) Cervini-Silva, J.; Kostka, J. E.; Larson, R. A.; Stucki, J. W.; Wu, J. Dehydrochlorination of 1,1,1-trichloroethane and pentachloroethane by microbially reduced ferruginous smectite, *Environ. Toxicol. Chem.* **2003**, *22*, 1046-1050.

(80) Roberts, A. L.; Jeffers, P. M.; Wolfe, N. L.; Gschwend, P. M. Structure-reactivity relationship in dehydrohalogenation reactions of polychlorinated and polybrominated alkanes, *Crit. Rev. Env. Sci. Tec.* **1993**, *23*, 1-39.

(81) Roberts, A. L.; Totten, L. A.; Arnold, W. A.; Burries, D. R.; Campbell, T. J. Reductive elimination of chlorinated ethylenes by zero-valent metals, *Environ. Sci. Technol.* **1996**, *30*, 2654-2659.

(82) Arnold, W. A.; Roberts, A. L. Pathways and kinetics of chlorinated ethylene and chlorinated acetylene reaction with Fe(0) particles, *Environ. Sci. Technol.* **2000**, *34*, 1794-1805.

(83) Lesage, S.; Brown, S.; Milliar, K. A different mechanism for the reductive dechlorination of chlorinated ethenes: kinetic and spectroscopic evidence, *Environ. Sci. Technol.* **1998**, *32*, 2264-2272.

(84) Arnold, W. A.; Winget, P.; Cramer, C. J. Reductive dechlorination of 1,1,2,2-tetrachloroethane, *Environ. Sci. Technol.* **2002**, *36*, 3536-3541.

(85) Song, H.; Carraway, E. R. Reduction of chlorinated ethanes by nanosized zero-valent iron: kinetics, pathways, and effects of reaction conditions, *Environ. Sci. Technol.* **2005**, *39*, 6237-6245.

(86) O'Loughlin, E. J.; Burris, D. R. Reduction of halogenated ethanes by green rust, *Environ. Toxicol. Chem.* **2004**, *23*, 41-48.

(87) *Agilent Techlonogies*; http://www.chem.agilent.com/cag/cabu/pdf/c585.pdf, (Accessed Jan 2007).

(88) Gibbs, C. R. Characterization and application of ferrozine iron reagent as a ferrous iron indicator, *Anal. Chem.* **1976**, *48*, 1197-1201.

(89) Ball, W. P.; Xia, G.; Durfee, D. P.; Wilson, R. D.; Brown, M. J.; Mackay, D. M. Hot methanol extraction for the analysis of volatile organic chemicals in subsurface core samples from Dover Air Force Base, Delaware, *Ground Water Monit. R.* **1997**, *17*, 104-121.

(90) Chudek, J. A.; Hunter, G.; Jone, M. R.; Scrimgeour, S. N.; Hewlett, P. C.; Kudryavtsev, A. B. Aluminium-27 solid state NMR spectroscopic studies of chloride binding in Portland cement and blends, *J. Mater. Sci.* **2000**, *35*, 4275-4288.

(91) Pecher, K.; Haderlein, S. B.; Schwarzenbach, R. P. Reduction of polyhalogenated methanes by surface-bound Fe(II) in aqueous suspensions of iron oxides, *Environ. Sci. Technol.* **2002**, *36*, 1734-1741.

(92) Wust, W. F.; Kober, R.; Schlicker, O.; Dahmke, A. Combined zero- and first-order kinetic model of the degradation of TCE and cis-DCE with commercial iron, *Environ. Sci. Technol.* **1999**, *33*, 4304-4309.

(93) Birchall, J. D.; Howard, A. J.; Bailey, J. E. On the hydration of portland cement, *Proc. R. Soc. Lon. Ser.-A.* **1978**, *360*, 445-453.

(94) Klausen, J.; vikesland, P. J.; Kohn, T.; Burris, D. R.; Ball, W. P.; Roberts, A. L. Longevity of granular iron in groundwater treatment processes: solution composition effects on reduction of organohalides and nitroaromatic compounds, *Environ. Sci. Technol.* **2003**, *37*, 1208-1218.

(95) Elsner, M.; Schwarzenbach, R. P.; Haderlein, S. B. Reactivity of Fe(II)-bearing minerals toward reductive transformation of organic contaminants, *Environ. Sci. Technol.* **2004**, *38*, 799-807.

(96) Liu, Y.; Majetich, S. A.; Tilton, R. D.; Sholl, D. S.; Lowry, G. V. TCE dechlorination rates, pathways, and efficiency of nanoscale iron particles with different properties, *Environ. Sci. Technol.* **2005**, *39*, 1338-1345.

(97) Cervini-Silva, J.; Larson, R. A.; Wu, J.; Stucki, J. W. Transformation of chlorinated aliphatic compounds by ferruginous smectite, *Environ. Sci. Technol.* **2001**, *35*, 805-809.

(98) Ponder, S. M.; Darab, J. G.; Bucher, J.; Caulder, D.; Craig, I.; Davis, L.; Edelstein, N.; Lukens, W.; Nitsche, H.; Rao, L.; Shuh, D. K.; Mallouk, T. E. Surface chemistry and electrochemistry of supported zerovalent iron nanoparticles in the remediation of aqueous metal contaminants, *Chem. Mater.* **2001**, *13*, 479-486.

(99) Dries, J.; Bastiaens, L.; Springael, D.; Agathos, S. N.; Diels, L. Competition for sorption and degradation of chlorinated ethenes in batch zero-valent iron systems, *Environ. Sci. Technol.* **2004**, *38*, 2879-2884.

(100) Maithreepala, R. A.; Doong, R.-A. Enhanced dechlorination of chlorinated methanes and ethenes by chloride green rust in the presence of copper(II), *Environ. Sci. Technol.* **2005**, *39*, 4082-4090.

(101) Chudek, J. A.; Hunter, G.; Jone, M. R.; Scrimgeour, S. N.; Hewlett, P. C.; Kudryavtsev, A. B. Aluminium-27 solid state NMR spectroscopic studies of chloride binding in Portland cement and blends, *J. Mater. Sci.* **2000**, *35*, 4275-4288.

(102) Wust, W. F.; Kober, R.; Schlicker, O.; Dahmke, A. Combined zero- and first-order kinetic model of the degradation of TCE and cis-DCE with commercial iron, *Environ. Sci. Technol.* **1999**, *33*, 4304-4309.

(103) Klausen, J.; vikesland, P. J.; Kohn, T.; Burris, D. R.; Ball, W. P.; Roberts, A. L. Longevity of granular iron in groundwater treatment processes: solution composition effects on reduction of organohalides and nitroaromatic compounds, *Environ. Sci. Technol.* **2003**, *37*, 1208-1218.

(104) Birchall, J. D.; Howard, A. J.; Bailey, J. E. On the hydration of portland cement, *Proc. R. Soc. Lon. Ser.-A.* **1978**, *360*, 445-453.

(105) Liu, Z.; Betterton, E. A.; Arnold, R. G. Electrolytic reduction of low molecular weight chlorinated aliphatic compounds: structural and thermodynamic effects on process kinetics, *Environ. Sci. Technol.* **2000**, *34*, 804-811.

(106) Ponder, S. M.; Darab, J. G.; Bucher, J.; Caulder, D.; Craig, I.; Davis, L.; Edelstein, N.; Lukens, W.; Nitsche, H.; Rao, L.; Shuh, D. K.; Mallouk, T. E. Surface chemistry and electrochemistry of supported zerovalent iron nanoparticles in the remediation of aqueous metal contaminants, *Chem. Mater.* **2001**, *13*, 479-486.

(107) Liu, Y.; Majetich, S. A.; Tilton, R. D.; Sholl, D. S.; Lowry, G. V. TCE dechlorination rates, pathways, and efficiency of nanoscale iron particles with different properties, *Environ. Sci. Technol.* **2005**, *39*, 1338-1345.

(108) Scherer, M. M.; Balko, B. A.; Gallagher, D. A.; Tratnyek, P. G. Correlation analysis of rate constants for dechlorination by zero-valent iron, *Environ. Sci. Technol.* **1998**, *32*, 3026-3033.

(109) Dries, J.; Bastiaens, L.; Springael, D.; Agathos, S. N.; Diels, L. Competition for sorption and degradation of chlorinated ethenes in batch zero-valent iron systems, *Environ. Sci. Technol.* **2004**, *38*, 2879-2884.

(110) Schafer, D.; Kober, R.; Dahmke, A. Competing TCE and cis-DCE degradation kinetics by zero-valent iron-experimental results and numerical simulation, *J. Contam. Hydrol.* **2003**, *65*, 183-202.

APPENDIX A

A-1. COMPUTER PROGRAM (MATLAB®) TO PREDICT DECHLORINATION OF CHLORINATED HYDROCARBONS USING THE MODIFIED FIRST ORDER MODEL

```
% This coding is for a non-linear regression using nlinfit and ODE function to calculate
initial concentration and rate constant.
clear;
data=load('data_3PCE_789ISM.txt');  % Call experimental data for 3.08 mM PCE
dechlorination by 789 mM ISM
t=data(:,1);   % Sampling time
c=data(:,2);  % Total PCE concentrations at each sampling time
e=data(:,3);  % Errors at each sampling time, which are standard deviation of triplicates
errorbar(t, c, e, 'o')   % Command to draw data and error bar
hold on
beta0 = input('guess=');  % Initial guesses
global Ca0;
[beta,r,j]=nlinfit(t, c, @ode_First, beta0);   % A non-linear regression which use ODE
function to solve differential equation
con=nlparci(beta,r,j);   % Confidence intervals for each variable at  α=0.05
k=beta(1)   % Predicted first-order rate constant
Ca0=beta(2)  % Predicted initial PCE concentration
error=abs(r)   % Absolute values of errors at each sampling time
con=con'
tspan=[0:0.01:55];
   [tout,cout]=ode45(@matbalance_ode_First, tspan, Ca0, [], beta);  % Estimate PCE
concentrations at each time by using ODE function which solve differential equation
plot (tspan, cout);  %Drawing prediction line
```

```
hold off
```

```
% This coding is OCE function to solve differential equations

Function cesta=ode_First(beta,t)

global Ca0;
k=beta(1);
Ca0=beta(2);

if(size(t,1)==1)
   tspan=[0;t];
   [tout,cout]=ode45(@matbalance_ode_First, tspan, Ca0, [], beta);
   cesta=cout(size(cout,1),1)
else
    if(t(1)==0)
       tspan=t;
       [tout, cout]=ode45(@matbalance_ode_First, tspan, Ca0, [], beta);
       cesta=cout;
    else
       tspan=[0;t];
       [tout, cout]=ode45(@matbalance_ode_First, tspan, Ca0, [], beta);
       cesta=cout(2:size(cout,1));
    end
end
```

```
% This coding is material balances using modified first order kinetic model

Function dcdt=matbalance_ode_First(t,c,beta)

csol=0.640;   % Solubility for 3.08 mM PCE reduced by 789mM ISM
k=beta(1);
Ca0=beta(2);

I_above=find(c>=csol);  % Data of total PCE concentration when NAPL existed
I_below=find(c<csol);    % Data of total PCE concentraiton when no NAPLs

dc(I_above)=k*csol;   % Differential equation when NAPL existed
dc(I_below)=k*c(I_below);  % Differential equation when no NAPL

dcabove=-dc(I_above);
dcbelow=-dc(I_below);
dcdt=[dcabove' dcbelow'];
```

A-2. COMPUTER PROGRAM (MATLAB®) TO PREDICT DECHLORINATION OF CHLORINATED HYDROCARBONS USING THE MODIFIED SECOND-ORDER MODEL

```
% This coding is for a non-linear regression using nlinfit and ODE function to calculate
second-order rate constant, initial concentration, and initial reductive capacity.
clear;
data=load('data_12TCE_225Fe+5C.txt');  % Call experimental data for 12.0 mM TCE
reduction by 225 mM Fe+5%C
t=data(:,1);   % Sampling time
c=data(:,2);  % Total TCE concentration at each sampling time
e=data(:,3);  % Errors at each sampling time, which are standard deviation of triplicate
errorbar(t, c, e, 'o')
hold on

beta0 = input('guess=');  % Initial guesses
global Ca0;
[beta,r,j]=nlinfit(t, c, @ode_second, beta0);   % A non-linear regression which use ODE
function to solve differential equation
con=nlparci(beta,r,j);   % Confidence intervals for four variables at  α=0.05
k2=beta(1)   % Predicted second-order rate constant
Crc0=beta(2)      % Predicted initial reductive capacity
Ca0=beta(3)  % Predicted initial TCE concentration
error=abs(r)   % Absolute values of errors at each sampling time
con=con'
```

```
tspan=[0:0.01:120];
   [tout,cout]=ode45(@matbalance_ode_second, tspan, Ca0, [], beta);  % Estimate TCE
concentrations at each time by using ODE function which solve differential equation
plot (tspan, cout);  %Drawing prediction line
hold off
```

```
% This coding is OCE function to solve differential equations
function cesta=ode_second(beta,t)
global Ca0;
k2=beta(1)   % Predicted second-order rate constant
Crc0=beta(2)      % Predicted initial reductive capacity
Ca0=beta(3)  % Predicted initial TCE concentration

if(size(t,1)==1)
   tspan=[0;t];
   [tout,cout]=ode45(@matbalance_ode_second, tspan, Ca0, [], beta);
   cesta=cout(size(cout,1),1)
else
    if(t(1)==0)
       tspan=t;
       [tout, cout]=ode45(@matbalance_ode_second, tspan, Ca0, [], beta);
       cesta=cout;
    else
       tspan=[0;t];
       [tout, cout]=ode45(@matbalance_ode_second, tspan, Ca0, [], beta);
       cesta=cout(2:size(cout,1));
    end
end
```

```
% This coding is material balances using modified second-order model

function dcdt=matbalance_ode_second(t,c,beta)

csol=7.45; % solubility of TCE
k2=beta(1)   % Predicted second-order rate constant
Crc0=beta(2)      % Predicted initial reductive capacity
Ca0=beta(3)  % Predicted initial TCE concentration

I_above=find(c>=csol);  % Data of total TCE concentration when NAPL existed
I_below=find(c<csol);    % Data of total TCE concentraiton when no NAPLs

dc(I_above)= k2 *(Crc0-(Ca0-c(I_above)))*csol;    % Differential equation when NAPL
existed
dc(I_below)= kLH *(Crc0-(Ca0-c(I_below)))*c(I_below);   % Differential equation when
no NAPL

dcabove=-dc(I_above);
dcbelow=-dc(I_below);
dcdt=[dcabove' dcbelow']';
```

A-3. COMPUTER PROGRAM (MATLAB®) TO PREDICT DECHLORINATION OF CHLORINATED HYDROCARBONS USING THE MODIFIED LANGMUIR-HINSHELWOOD MODEL

```
% This coding is for a non-linear regression using nlinfit and ODE function to calculate
initial concentration, Langmuir-Hinshelwood rate constant, sorption coefficient, and
initial concentration of reductive capacity.
clear;
data=load('data_TCA_80Fe+10C.txt');  % Call experimental data for 11.7 mM 1,1,1-
TCA reduction by 80 mM Fe+10%C
t=data(:,1);   % Sampling time
c=data(:,2);  % Total 1,1,1-TCA concentration at each sampling time
e=data(:,3);  % Errors at each sampling time, which are standard deviation of triplicate
errorbar(t, c, e, 'o')   % Command to draw data and error bar
hold on

beta0 = input('guess=');  % Initial values
global Ca0;
[beta,r,j]=nlinfit(t, c, @ode_LH, beta0);   % A non-linear regression which use ODE
function to solve differential equation
con=nlparci(beta,r,j);   % Confidence intervals for four variables at  α=0.05
k_LH=beta(1)   % Predicted Langmuir-Hishelwood rate constant
K=beta(2)      % Predicted sorption coefficient
Ca0=beta(3)  % Predicted initial 1,1,1-TCA concentration
Crc0=beta(4)   % Predicted initial concentration of reductive capacity
error=abs(r)   % Absolute values of errors at each sampling time
con=con'
```

```
tspan=[0:0.1:700];
   [tout,cout]=ode45(@matbalance_ode_LH, tspan, Ca0, [], beta);  % Estimate 1,1,1-
TCA concentrations at each time by using ODE function which solve differential
equation
plot (tspan, cout);  %Drawing prediction line
hold off
```

```
% This coding is OCE function to solve differential equations
function cesta=ode_LH(beta,t)
global Ca0;
k_LH=beta(1);   % Predicted Langmuir-Hishelwood rate constant
K=beta(2);      % Predicted sorption coefficient
Ca0=beta(3);  % Predicted initial 1,1,1-TCA concentration
Crc0=beta(4);   % Predicted initial concentration of reductive capacity
if(size(t,1)==1)
   tspan=[0;t];
   [tout,cout]=ode45(@matbalance_ode_LH, tspan, Ca0, [], beta);
   cesta=cout(size(cout,1),1)
else
    if(t(1)==0)
       tspan=t;
       [tout, cout]=ode45(@matbalance_ode_LH, tspan, Ca0, [], beta);
       cesta=cout;
    else
       tspan=[0;t];
       [tout, cout]=ode45(@matbalance_ode_LH, tspan, Ca0, [], beta);
       cesta=cout(2:size(cout,1));
    end
end
```

```
% This coding is material balances using modified L-H kinetic model

function dcdt=matbalance_ode_LH(t,c,beta)

csol=7.57; % solubility of 1,1,1-TCA
k_LH=beta(1);   % Predicted Langmuir-Hishelwood rate constant
K=beta(2);      % Predicted sorption coefficient
Ca0=beta(3);  % Predicted initial 1,1,1-TCA concentration
Crc0=beta(4);   % Predicted initial concentration of reductive capacity

I_above=find(c>=csol);  % Data of total 1,1,1-TCA concentration when NAPL existed
I_below=find(c<csol);    % Data of total 1,1,1-TCA concentraiton when no NAPLs

dc(I_above)= k_LH *(Crc0-(Ca0-c(I_above)))*csol/(1/K+csol);    % Differential equation
when NAPL existed
dc(I_below)= k_LH *(Crc0-(Ca0-c(I_below)))*c(I_below)/(1/K+c(I_below));   %
Differential equation when no NAPL

dcabove=-dc(I_above);
dcbelow=-dc(I_below);
dcdt=[dcabove' dcbelow'];
```

APPENDIX B

THE RELATIONSHIP BETWEEN SOLUBILITY OF PCE AND FE(II) IN ISM

Table B-1. The solubility values varied with Fe(II) in ISM in condition of $[PCE]^{o}_{total}$=3.08 mM at pH 12

	$[FE(II)]_{ISM}$ (mM)			
	225	424	660	789
Solubility (mM)	0.971	0.847	0.719	0.640

APPENDIX C

EFFECTS OF TYPES OF VARIOUS REDUCTANTS AND THE RELATIONSHIP OF AQUEOUS EQUILIBRIUM CONCENTRATION VERSUS THE FERROUS-IRON-NORMALIZED RATE CONSTANTS.

Table C-1. Ferrous-normalized rate coefficients on various reductants

Types of Reductants	Aqueous equilibrium conc. (mM)	$k_{Fe(II)}$ (day^{-1} mM^{-1})
Fe(II)-PCX	0.242	1.10E-2
MSCXFe	0.242	3.80E-3
Fe(II)Fe(III)Cl_GR12	0.242	1.50E-3
Fe(II)Fe(III)Cl	0.242	8.20E-4
Friedel's salts	0.242	1.30E-4
789 mM of Fe(II) in ISM	0.640	1.49E-4
660 mM of Fe(II) in ISM	0.719	1.35E-4
424 mM of Fe(II) in ISM	0.847	1.05E-4
225 mM of Fe(II) in ISM	0.971	6.27E-5

APPENDIX D

TABULATED DATA

Conc. is average value and error is standard deviation of three points.

Table D-1 The effects of Fe(II) in ISM for 3.08 mM PCE dechlorination

exp.1			exp.2			exp.3			exp.4		
time (days)	conc. (mM)	error	time (days)	conc. (mM)	error	time (days)	conc. (mM)	error	time (days)	conc. (mM)	error
0.17	2.8966	0.0754	0.17	2.8807	0.0650	0.17	2.9492	0.0639	0.17	2.7003	0.0250
13.0	2.5531	0.1004	7.00**	2.3001	0.0073	4.0	2.2320	0.0814	3.0	2.2209	0.0440
26.0	2.2938	0.1074	13.0**	2.0190	0.0165	9.0	1.8918	0.0168	7.0	1.9531	0.0582
36.0	1.8425	0.2534	21.0	1.9363	0.0393	13.0	1.7292	0.0252	10.0	1.6291	0.0322
55.0	1.9003	0.0460	27.0	1.7250	0.0065	17.0	1.4002	0.0439	13.0	1.5092	0.0232
70.0	1.6219	0.0706	34.0	1.4204	0.0262	24.0	1.0179	0.0942	16.0	1.3265	0.0266
127	1.0787	0.0599	39.0**	1.3426	0.0156	28.0	0.8576	0.0102	20.0	0.9724	0.0115
			49.0	0.9304	0.0425	34.0**	0.5677	0.0490	24.0	0.7381	0.0075
			54.0	0.5681	0.0182	37.0	0.4864	0.0391	28.0	0.5388	0.0324
			63.0	0.4119	0.0360	42.0	0.3254	0.0159	33.0**	0.2827	0.0657
			76.0	0.1930	0.0157	52.0*	0.0973		47.0**	0.0875	0.0134

** : At this sampling times, conc. is average for two points and error is absolute value of subtraction between average and measured value

* : At this sampling times, the value of one points is used

Table D-2 The effects of PCE DNAPL concentration on 789 mM Fe(II) in ISM

exp.5			exp.6			exp.7		
time (days)	conc. (mM)	error	time (days)	conc. (mM)	error	time (days)	conc. (mM)	error
0.21	6.1011	0.1503	0.21	8.4636	0.3927	0.80	11.568	0.5973
5.88	4.8628	0.1298	8.0	6.8334	0.6984	9.90	10.319	0.5631
9.80	4.0908	0.0490	14.9	6.4682	0.2472	21.9	9.6118	0.6836
14.9	3.8745	0.3096	25.0	5.5765	0.6092	33.9	8.5397	0.1022
19.9	3.3229	0.1216	32.0	5.2430	0.0137	48.0	7.6158	0.2721
26.9	2.7803	0.0839	39.0	4.7560	0.1189	62.0	7.0739	0.2082
34.0	2.5602	0.0392	53.0	3.7421	0.1090	76.0	5.2271	0.2333
41.0	1.7329	0.1085	67.0	2.4691	0.2863	90.0	4.5933	0.3729
55.0	1.0380	0.1673	76.0	1.8788	0.2179			
66.0	0.3656	0.0734	88.0	1.3266	0.1538			

Table D-3 The effects of reductant types on 3.08 PCE DNAPL

exp.8			exp.9			exp.10		
time (days)	conc. (mM)	error	time (days)	conc. (mM)	error	time (days)	conc. (mM)	error
0.21	2.9756	0.0297	0.90	2.8853	0.0756	0.90	2.8761	0.0385
5.90	2.2601	0.0744	5.0**	2.4157	0.1465	6.0	2.3054	0.1546
13.0	1.5683	0.0138	8.0	2.2963	0.2341	13.9	1.9210	0.0137
16.0	1.3617	0.0791	12.0	1.6778	0.1140	21.0	0.9733	0.0445
20.0	0.9876	0.0593	20.0	1.2323	0.1698	28.0	0.3221	0.0185
23.0	0.7322	0.0050	25.0	0.6909	0.0264	32.0	0.1103	0.0060
27.0	0.5665	0.0319	28.0	0.3811	0.0321	35.0	0.0511	0.0090
34.0	0.3539	0.0033	35.0	0.0970	0.0264	39.0	0.0290	0.0083
41.0	0.1987	0.0081						
50.0	0.1138	0.0089						

** : At this sampling times, conc. is average for two points and error is absolute value of subtraction between average and measured value

Table D-4 The effects of reductant types on 12.0 mM of TCE DNAPL

exp.11			exp.12			exp.13			exp.14		
time (days)	conc. (mM)	error	time (days)	conc. (mM)	error	time (days)	conc. (mM)	error	time (days)	conc. (mM)	error
0.17	11.632	0.0990	0.19	11.494	0.0710	0.27	11.5080	0.1180	0.23	10.7850	0.1580
1.70	11.705	0.0930	1.90	11.254	0.7100	6.0	10.6980	0.0640	3.87	10.4020	0.1000
8.70	11.161	0.0220	4.80	11.550	0.0450	12.8	9.7310	0.1200	8.0	9.8010	0.1300
13.9	10.966	0.0710	12.9	11.191	0.1870	21.9**	7.8060	0.0640	12.8	9.2900	0.1328
29.9	10.668	0.0290	26.9	10.730	0.1180	26.9	7.5030	0.1090	18.0	8.2870	0.0120
40.8	10.593	0.2010	42.0	10.663	0.0730	41.0	6.0980	0.2160	32.8	7.1110	0.2500
75.0	9.4270	0.3900	57.0	10.287	0.1360	54.0	5.3460	0.0670	46.8	5.9620	0.0790
93.0	9.3470	0.2140	70.0**	9.5420	0.0380	69.0	4.7770	0.2670	67.9	4.8910	0.1150
112	9.2770	0.1318	120**	9.5690	0.2360	84.0	4.1760	0.0400	84.8**	4.2540	0.1160
						104	4.1430	0.1730	103	4.2160	0.2370

** : At this sampling times, conc. is average for two points and error is absolute value of subtraction between average and measured value

Table D-5 The effects of cement on ISM to dechlorinate 11.7 mM of 1,1,1-TCA DNAPL

exp.15			exp.16		
time (hours)	conc. (mM)	error	time (hours)	conc. (mM)	error
4.0	10.3800	0.1340	4.0	10.916	0.0650
7.50	9.6730	0.0659	8.50	10.215	0.0980
11.0	9.0290	0.0981	14.5	9.5340	0.0460
14.5	8.5110	0.1700	25.0**	8.3290	0.0560
20.0	7.5980	0.1365	42.0	7.2460	0.0540
25.5	6.9520	0.1205	67.5	5.7120	0.0700
31.0	6.0650	0.1745	92.5	4.5410	0.0670
44.0	4.5630	0.2367	120	3.4070	0.0220
72.5	2.2270	0.0252	161	2.2030	0.0310
145	0.0930	0.0120	210	1.2370	0.0190

** : At this sampling times, conc. is average for two points and error is absolute value of subtraction between average and measured value

Table D-6 The effects of cement and Fe(II) doses in Fe(II)+C on 11.7 mM1,1,1-TCA DNAPL

exp.17			exp.18			exp.19		
time (hours)	conc. (mM)	error	time (hours)	conc. (mM)	error	time (hours)	conc. (mM)	error
3.0	9.7920	0.2089	4.50	7.8990	0.0166	4.0	9.7980	0.1372
9.0	8.4730	0.1030	17.8	5.1070	0.0970	33.0	6.7861	0.6365
21.0	7.9490	0.1133	31.5	3.2720	0.1110	68.5	5.4900	0.1113
33.0	7.4680	0.0236	48.8	2.0640	0.0930	104**	4.6760	0.0266
45.0	7.2950	0.2340	57.0	2.0050	0.0610	129	4.3790	0.1445
70.5	6.8970	0.1258	75.5	1.2220	0.0160	151**	4.3249	0.1869
119	6.7610	0.1814	113	0.8210	0.0360	185	4.0547	0.1931
191	6.1350	0.1153	146	0.3740	0.0200	214**	3.9882	0.5175
359	4.8570	0.1153	184	0.1080	0.0180	421**	3.2344	0.3477

** : At this sampling times, conc. is average for two points and error is absolute value of subtraction between average and measured value

Table D-7 Dechlorination of DNAPL mixture on ISM

exp.20						
	1,1,1-TCA		PCE		TCE	
time (days)	conc. (mM)	error	conc. (mM)	error	conc. (mM)	error
0.17	8.8090	0.0750	11.633	0.0920	11.220	0.0590
0.83	3.3330	0.0830	11.696	0.0690	11.068	0.1071
1.81	0.6130	0.0640	11.650	0.2730	11.003	0.0790
4.83			12.012	0.1340	11.339	0.0420
13.8			11.952	0.2370	11.296	0.2480
34.8			11.176	0.3310	11.181	0.2840
54.8			11.426	0.1430	11.282	0.2360
74.9**			10.885	0.1140	11.525	0.1236
99.8			10.446	0.0760	10.833	0.2610
125			10.124	0.1110	10.920	0.7486

** : At this sampling times, conc. is average for two points and error is absolute value of subtraction between average and measured value

Table D-8 Dechlorination of DNAPL mixture on Fe(II)+C

	exp.21					
	1,1,1-TCA		PCE		TCE	
time (days)	conc. (mM)	error	conc. (mM)	error	conc. (mM)	error
0.19	9.5380	0.1000	11.685	0.0850	10.850	0.0650
1.92	3.3790	0.1100	11.600	0.0480	10.768	0.0650
2.92	2.1910	0.0630	11.800	0.0920	10.952	0.0920
5.13	0.3930	0.0440	11.353	0.0560	11.021	0.0380
20..0			11.425	0.0480	11.181	0.0960
41.0			11.029	0.3230	11.209	0.2130
62.9			10.518	0.2020	12.137	0.1480
89.9**			10.040	0.0210	11.188	0.2700
115**			9.528	0.1518	11.207	0.1402
144**			9.132	0.2190	11.484	0.2125

** : At this sampling times, conc. is average for two points and error is absolute value of subtraction between average and measured value

VITA

Name: Si Hyun Do

Permanent Address: 30-3, Samsung-Dong, Kangnam-Gu, Seoul, South Korea, 135-092

Email Address: sihyun2@neo.tamu.edu, or sihyun.environ@gmail.com

Education: B.S., Chemical Engineering, Soong Sil University, 1999

M.S., Chemical Engineering, Han Yang Univeristy, 2001

Ph.D., Civil Engineering, Texas A&M University, 2007